Galactic Angular Momentum

XXXth IAU General Assembly, Focus Meeting 6

Vienna, 20–22 August 2018

Edited by Danail Obreschkow, Patricia Tissera, Chanda Jog and Claude Carignan

Chief editor for articles published in Focus in Astronomy: Teresa Lago (IAU General Secretary)

National Organising Committee

Gerhard Hensler (University of Vienna, chair), Norbert Przybilla (University of Innsbruck, deputy chair), João Alves (University of Vienna, local deputy chair), Werner Zeilinger (University of Vienna, local deputy chair), Pascale Ehrenfreund (DLR Bonn), Manuel Güdel (University of Vienna), Mag. Anneliese Haika (WAA Wien), Arnold Hanslmeier (University of Graz), Franz Kerschbaum (University of Vienna), Christian Köberl (University of Vienna), Theresa Lüftinger (University of Vienna), Helmut Rucker (Commission for Astronomy of the Austrian Academy of Sciences (Graz), Sabine Schindler (University of Innsbruck), Astrid Veronig (University of Graz), Bodo Ziegler (University of Vienna)

Local Organising Committee

Gerhard Hensler (chair), João Alves, Bernhard Baumschlager, Julia Bog, Sudeshna Boro Saikia, Ines Brott, Odysseas Dionatos, Manuel Güdel, Anneliese Haika, Jeannette Höfinger, Margarethe Jurenitsch, Collin Johnstone, Franz Kerschbaum, Kristina Kislyakova, Ulrike Kuchner, Matthias Kühtreiber, Artur Löcker, Theresa Lüftinger, Nikolaus Ortner, Falk Pastner, Thomas Posch, Christian Reimers, Tanja Rindler-Daller, Gerald Schneider, Thomas Schobesberger, Ruth-Sophie Taubner, Patrick Steyrleithner, Stefan Wallner, Alexandra Wassipaul, Günther Wuchterl, Werner Zeilinger, Bodo Ziegler

Scientific Organising Committee

Danail Obreschkow (chair, co-editor), Françoise Combes (co-chair, conference summary), Aaron Romanowsky (co-chair), Rachel Somerville (co-chair), Roger Davies (co-chair), Claude Carignan (co-editor), Arianna Di Cintio (poster summary), Chanda Jog (co-editor), Patricia Tissera (co-editor), Karl Glazebrook, Mark Swinbank, Eric Emsellem, Sebastian F. Sanchez, Romeel Davé, Charlotte Christensen, Yipeng Jing

Invited Speakers

James E. Peebles, Susana Pedrosa, James Bullock, Matthew Colless, Kareem El-Badry, Rhea-Silvia Remus, Filippo Fraternali, Claudia Lagos, Lia Athanassoula, Jean Brodie, Susan Kassin, Michele Cappellari, Jayaram Chengalur, Jenny Greene, Kanak Saha, Sarah Sweet, Shy Genel, Aura Obreja, Xiaohu Yang, Sarah Blyth

Additional Speakers

Caroline Foster, Rachel Somerville, Chandrashekar Murugeshan, Martha Tabor, Claudia Pulsoni, Hoseung Choi, Lorenzo Posti, Francesca Rizzo, Daniel DeFelippis, Charlotte Welker, Michael Fall, Anelise Audibert

Poster Presenters

Valentina Abril Melgarejo, Sung-Ho An, Aleksandra Antipova, Joan Font (for John Beckman), Sebastian Bustamante, Bernardo Cervantes Sodi, Horacio Dottori, Joan Font, Shy Genel, Jesus A. Gomez-Lopez, Katherine Harborne, Ivan Kacala, Eunbin Kim, Keiichi Kodaira, Baerbel Koribalski, Andrea Lapi, Jie Li, Katharina Lutz, Brisa Mancillas-Vaquera, Kyoko Onishi, Sol Rosito, Luis Enrique Prez Montao, Nicolas Peschken, Antonio J. Porras, Christoph Saulder, Felix Schulze, Yun-Kyeong Sheen, Shravan Shetty, Olga Silchenko, Matthias Steinmetz, Jolanta Zjupa

The image of the spiral galaxy M88 used on the front cover was taken by Adam Block.

Index

Astronomy in Focus, Volume 1
XXXth IAU General Assembly, August 2018
Teresa Lago, ed.

DOI: 10.5281/zenodo.1481602

Focus Meeting: Galactic Angular Momentum

Danail Obreschkow[1,2]

[1]International Centre for Radio Astronomy Research (ICRAR), M468,
University of Western Australia, WA 6009, Australia
[2]ARC Centre of Excellence for All Sky Astrophysics in 3 Dimensions (ASTRO 3D)
email: danail.obreschkow@icrar.org

Abstract. The 6th Focus Meeting (FM6) at the XXXth IAU GA 2018 aimed at overviewing the rise in angular momentum (AM) science seen in the last 10 years and debating new emerging views on galaxy evolution. The foundational works on galaxy formation of the 1970s and 80s clearly exposed the fundamental role of AM, suspected since the time of Kant. However, quantitative progress on galactic AM remained hampered by observational and theoretical obstacles. Only in the last 10 years, numerical simulations began to produce galactic disks with realistic AM. Simultaneously, the fast rise of Integral Field Spectroscopy (IFS) and millimetre/radio interferometry have opened the door for systematic AM measurements, across representative samples and cosmic volumes. The FM bridged between cutting-edge observational programs and leading simulations in order to review, debate and resolve core issues on AM science, ranging from galactic substructure (e.g. gas fraction, turbulence, clumps) to global properties (e.g. size evolution, morphologies) and cosmology (spin alignment, cosmic origin of AM). The co-chairs and SOC members strived to assemble a representative selection of leading scientists in the field, while adhering to principles of equal opportunity and inclusivity.

Keywords. Galaxies: general – Galaxies: formation – Galaxies: evolution – Galaxies: galaxies: fundamental parameters – Galaxies: halos – Galaxies: bulges – Cosmology: theory.

---

1. Rationale: state of affairs motivating this meeting

In the standard model of galaxy formation, cold dark matter (CDM) haloes grow from primordial density fluctuations while acquiring AM through tidal torques. Galactic disks then condense at the halo centres by radiative dissipation of energy. The cooling baryons naturally exchange AM with their haloes, but the mass-size relation of local star-forming galaxies suggests that, on average, the specific AM of the baryons must remain approximately conserved. Explaining this apparent conservation has been a long-standing problem for theory: until recently (early 2010), hydro-gravitational simulations (using both particle-based and grid-based techniques) systematically failed at reproducing disks as large and thin as normal late-type galaxies, such as the Milky Way. The simulated galaxies were deficient in AM, making them too small and too bulgy – a problem so severe that it became known as the 'AM catastrophe'. Overcoming this catastrophe via increased computing power and refined feedback physics has been one of the major recent success stories of galaxy simulations. However, there is still debate about exactly how this is achieved: is outflowing gas torqued so that re-accreted gas has higher AM, is low AM material preferentially removed from galaxies, or do the winds prevent loss of AM by making inflows smoother?

A certain result from the AM catastrophe is that AM is one of the most critical quantities for explaining galaxy morphologies, opening a new bridge between theory and observation. The recent fast rise of IFS has enabled simultaneous measurements of the composition and Doppler velocity at every position in a 2D galaxy image, hence enabling

a pixel-by-pixel integration of the AM. Such measurements of AM in early-type galaxies (ATLAS^{3D} survey, 2011) led to the surprising discovery that most of these seemingly featureless objects exhibit a rotational structure akin to that of normal spiral galaxies, thus containing more AM than previously suspected. The fewer actual 'slow-rotators' host up to ten times less AM at a fixed mass. AM thus offers a more fundamental, albeit harder to measure, classification of galaxy types than the classical Hubble sequence. This conclusion was cemented by recent AM measurements in spiral galaxies, again suggesting that the Hubble morphology sequence might be substituted for a more physical classification by AM. The precise form of this new AM-based classification scheme remains nonetheless a source of much argument. Many recent hydro-gravitational simulations (e.g. Illustris, EAGLE, Horizon, Magneticum, MAGICC, CLUES, NIHAO) contribute to this discussion, as do most major kinematic observing programs. Prominent examples include optical IFS/IFS-like surveys (e.g. ATLAS^{3D}, CALIFA, MaNGA, SLUGGS, PN.S, KROSS, SAMI Survey), interferometric radio surveys (e.g. THINGS on the VLA) and many other kinematic observations on modern and future instruments (e.g. KMOS, MUSE, SINFONI, HECTOR, ALMA, NOEMA, JWST, SKA and precursors).

The strong correlations between morphology and AM of local galaxies raises the question as to whether the cosmic evolution of morphologies is paralleled, or even driven, by the evolution of AM. Observationally, the Hubble Space Telescope's (HST) exquisite spatial resolution showed that star-forming galaxies at redshift $z > 1$ had very different structures to local grand-design spirals: The rapidly star-forming early galaxies showed a predominance of 'clumpy' and 'irregular' morphologies caused by super-giant (300 to 1000 pc) star-forming complexes. The physical origin of these clumpy morphologies and the processes that drive the large star formation rates are currently heavily debated. High-z IFS observations surprised with the finding that most of the clumpy star-forming galaxies have a regular, rotating disk structure. Interestingly, the emission line velocity dispersions appear to be about five times larger than in mass-matched local disks, which presents a major puzzle, because high velocity dispersions are predicted to stabilise the disks, preventing them from fragmenting into star-forming clumps. While high gas fractions could explain instabilities in spite of high dispersion, deep IFS studies (on Keck-OSIRIS, Gemini-GMOS) in rare nearby clumpy disks suggest that low AM is the dominant driver of instabilities. This motivates the arguable conjecture that the cosmic evolution of AM plays indeed a major role in the morphological transformation of the star-forming population – a hypothesis that was debated at this FM.

Answers to key questions regarding the cosmic evolution of AM are about to emerge from new high-z IFS observations on 8m-class telescopes (e.g. KMOS and MUSE on the VLT), as well as from an array of cosmological hydro-gravitational simulations (see above). Meanwhile multi-wavelength surveys are about to pile up evidence for strong correlations between AM and various baryonic processes (e.g. star formation rates, the transition from atomic to molecular gas and the growth of black holes). Moreover, ongoing and near-future surveys (see above) are about to expand AM science to smaller and larger scales: for the first time, enough spatially resolved velocity maps are available to systematically study the spatial distribution of the baryon AM in galaxies, which offers a nuanced test of different evolution models. On large scales, the number and spatial completeness of galaxies mapped using IFS are about to become sufficient to test the weak correlations between AM and cosmic large scale structure predicted by simulations.

In summary, observational and computational studies of AM have induced major progress in galaxy evolution theory over the last decade. The rich and fast evolving diversity of AM-related topics and the need for bringing observers and theoreticians together were the primary drivers for this FM at the XXXth IAU GA 2018.

2. Contributions: proceedings, talks, posters

2.1. *Proceedings*

All our proceedings are published and indexed online on Zenodo. A subset of forty pages of substantial reviews and summaries are additionally printed in Focus in Astronomy by Cambridge University Press.

Proceedings of oral presentations published on Zenodo and in Focus in Astronomy

- Danail Obreschkow, "Focus Meeting: Galactic Angular Momentum".
- Françoise Combes, "Angular Momentum – Conference Summary".
- P. J. E. Peebles, "On the History and Present Situation".
- Claudia del P. Lagos, "Angular Momentum Evolution of Galaxies: the Perspective of Hydrodynamical Simulations".
- Matthew Colless, "Emerging Angular Momentum Physics from Kinematic Surveys".
- Susana Pedrosa, "The Fundamental Physics of Angular Momentum Evolution in a ΛCDM Scenario".
- Filippo Fraternali and Gabriele Pezzulli, "Angular Momentum Accretion onto Disc Galaxies".

Proceedings of oral presentations published online on Zenodo

- Daniel DeFelippis, et al., "Baryonic Angular Momentum in Simulated Disks: The CGM".
- Kareem El-Badry, "The Interplay between Galactic Angular Momentum and Morphology".
- Michael Fall & Aaron Romanowsky, "New Perspectives on Galactic Angular Momentum, Galaxy Formation, and the Hubble Sequence".
- Shy Genel, "A Lagrangian View on the Relation between Galaxy and Halo Angular Momentum".
- Chandrashekar Murugeshan, et al., "Does Angular Momentum Regulate the Atomic Gas Content in H I-deficient Spirals?".
- Aura Obreja, "Galaxy Simulations after the Angular Momentum Catastrophe".
- Lorenzo Posti, "Angular Momentum-Mass Law for Discs in the Nearby Universe".
- Claudia Pulsoni, et al., "The extended Planetary Nebula Spectrograph (ePN.S) Early Type Galaxy Survey: the Kinematic Diversity of Stellar Halos".
- Rhea-Silvia Remus, et al., "Connecting Angular Momentum, Mass and Morphology: Insights from the Magneticum Simulations".
- Francesca Rizzo, "S0 Galaxies Are Faded Spirals: Clues from their Angular Momentum Content".
- Kanak Saha, "Angular Momentum Transport in Lopsided Galaxies".
- Sarah M. Sweet, et al., "Spatially Resolved Galaxy Angular Momentum".
- Charlotte Welker, "Stellar Kinematics in the Cosmic Web: Lessons from the SAMI Survey and the Horizon-AGN Simulation".

2.2. *Oral presentations*

All oral presentations are available online at http://gam18.icrar.org. The abstracts of all oral presentations, other than summaries and addresses, are available online at https://astronomy2018.univie.ac.at/abstractsFM06.

Each proceeding listed in §2.1 corresponds to an oral presentation. The titles of the additional oral presentations are:

- Jenny Greene, "The role of AM in central and satellite ETGs".
- Xiaohu Yang, "Observing various alignment signals of galaxies ".
- James Bullock, "From halos to disks: the physics of AM profiles".
- Rhea-Silvia Remus, "Connecting AM, mass and morphology: insights from the Magneticum simulations".
- Michele Cappellari, "Surprises in kinematic observations of ETGs".
- Jean Brodie (presented by presented by R.-S. Remus, "Understanding the assembly histories of ETGs from the kinematics of stars and globular clusters".
- Jayaram Chengalur, "Expanding AM measurements to dwarf galaxies".
- Sarah Blyth, "Future high-redshift observations of H I kinematics".
- Lia Athanassoula, "AM and the evolution of disc galaxies".
- Susan Kassin, "The Assembly of Disk Galaxies: From Keck to JWST".
- Caroline Foster, "Spinning galaxies into shape".
- Rachel Somerville, "On the relationship between galaxy and halo size and spin".
- Martha Tabor, "Untangling galaxy components: the AM of bulges and disks in the MaNGA survey".
- Hoseung Choi, "Spin evolution of Horizon-AGN ETGs".
- Anelise Audibert, "Morphology and kinematics of the cold gas inside the central kiloparsec of nearby AGN with ALMA".
- Arianna Di Cintio, "Poster overview session".

2.3. *Posters*

The titles and abstracts of all posters are available online at https://astronomy2018.univie.ac.at/PosterAbstracts/posterFM06

Posters were presented by Valentina Abril Melgarejo, Sung-Ho An, Aleksandra Antipova, Joan Font (for John Beckman), Sebastian Bustamante, Bernardo Cervantes Sodi, Horacio Dottori, Joan Font, Shy Genel, Jesus A. Gomez-Lopez, Katherine Harborne, Ivan Kacala, Eunbin Kim, Keiichi Kodaira, Baerbel Koribalski, Andrea Lapi, Jie Li, Katharina Lutz, Brisa Mancillas-Vaquera, Kyoko Onishi, Sol Rosito, Luis Enrique Prez Montao, Nicolas Peschken, Antonio J. Porras, Christoph Saulder, Felix Schulze, Yun-Kyeong Sheen, Shravan Shetty, Olga Silchenko, Matthias Steinmetz and Jolanta Zjupa.

3. People: organisers, presenters, attendees

The Scientific Organising Committee (SOC) consisted of 16 members assembled from 12 countries and 5 continents, including senior astronomers as well as earlier career researchers. Collectively, the SOC members led and won the original proposal to host this FM at the XXXth IAU GA, put forward the list of invited speakers, selected the contributed talks and posters, chaired most of the sessions during the meeting and edited the proceedings. The organisation of the local logistics of the entire General Assembly

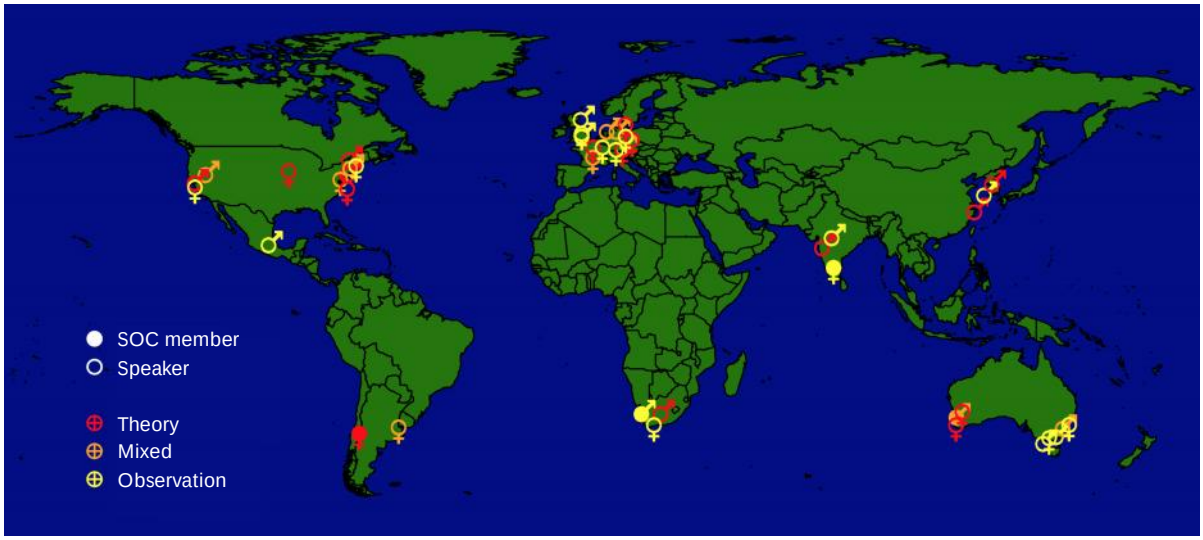

Figure 1. The geographical distribution of the SOC members and selected speakers, as well as their expertise, was fairly balanced, apart from a natural European clustering.

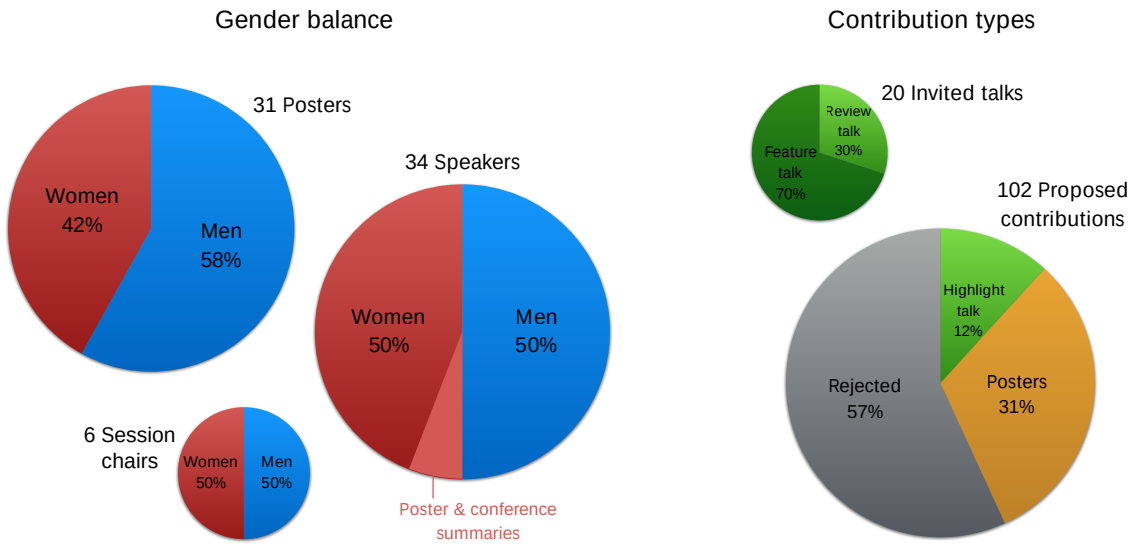

Figure 2. LEFT: An almost 50-50 gender balance was achieved for presenters and session chairs during the meeting. RIGHT: In addition to 20 invited talks, 102 proposal for additional talks and posters were received. Of those submissions, 31 were assigned a poster and 14 a short talk.

was handled by a dedicated LOC, headed by Gerhard Hensler, in conjunction with the IAU secretary and a national organising committee.

The SOC invited 20 high-level speakers for 20-min "review talks" and 14-min "feature talks" and selected 14 submitted proposals for 9-min "highlight talks". These talks were paralleled by a poster exhibition featuring the 31 highest-ranked additional submissions, out of 102 submissions in total (see Figure 2, right). According to NASA ADS, 10 of the 15 highest cited researchers on "Galactic AM" (and similar) of the last 20 years were present among the speakers and SOC members, making this meeting representative of the state-of-the-art.

Figures 1 and 2 (left) show a balanced mix of speakers in terms of gender and geographical distribution, bar a natural over-density in Europe, the site of many world-leading academic institutions and the location of the meeting. Figure 1 also reveals a fairly balanced mix of theoretical and observational expertise among the SOC members and

speakers. Furthermore, the list of presenters included a wide range of seniority, spanning from early-career researchers, even first-time presenters, to very senior astronomers, most notably Prof James Peebles, one of the most influential theoretical cosmologists of the last 50 years and a key player in early AM science. Many PhD students and several Master students were selected for poster presentations.

In total, 374 participants of the General Assembly signed up for this meeting, but other participants were free to walk in. We estimate that 400–500 people attended parts of the meeting, with an average of 150 present at any one time.

4. Acknowledgements

On behalf of the whole SOC, I sincerely thank all our speakers and poster presenters for the high standard of their contributions. Many invited speakers, especially those presenting a review, made a respectable effort to paint a holistic picture of recent results and persisting questions. These presentations, which extended well beyond the presenters' personal research, were particularly important and deserve a special acknowledgement. I extend this gratitude to all those, whose proposal was not selected for a presentation. Undoubtedly, most rejected submissions would have been on par with the high standard of the meeting and would have enriched the scientific discussion. Those submissions helped us gauge the collective interest of our attendees and optimise the program. I also wish to thank the estimated 400–500 people who attended (parts of) this meeting and who contributed through challenging and interesting questions.

On behalf of all attendees and SOC members, I would like to send a warm thank you to the local organisers in Vienna, especially to Gerhard Hensler and his team, to the excellent technical crew at the convention centre, and to the overall coordination by the IAU, in particular to the then General Secretary Piero Benvenuti and his successor Teresa Lago, who is the chief editor of the proceedings published in Focus in Astronomy.

As the chair of the SOC, I would like to express my fullest gratitude to all SOC members for their enormous help from the early vision (mid 2016) to successful completion (late 2018) of this meeting – a two-year long process, which I would walk again with this driven team of brilliant scientists and reliable organisers.

Astronomy in Focus, Volume 1
XXXth IAU General Assembly, August 2018
Teresa Lago & Danail Obreschkow, ed.

DOI: 10.5281/zenodo.1481291

Angular Momentum – Conference Summary

Francoise Combes[1]

[1]Observatoire de Paris, LERMA, College de France, CNRS, PSL Univ., Sorbonne Univ., F-75014, Paris, France
email: francoise.combes@obspm.fr

Abstract. Angular momentum (AM) is a key parameter to understand galaxy formation and evolution. AM originates in tidal torques between proto-structures at turn around, and from this the specific AM is expected to scale as a power-law of slope 2/3 with mass. However, subsequent evolution re-shuffles this through matter accretion from filaments, mergers, star formation and feedback, secular evolution and AM exchange between baryons and dark matter. Outer parts of galaxies are essential to study since they retain most of the AM and the diagnostics of the evolution. Galaxy IFU surveys have recently provided a wealth of kinematical information in the local universe. In the future, we can expect more statistics in the outer parts, and evolution at high z, including atomic gas with SKA.

Keywords. galaxies: bulges – galaxies: dwarf – galaxies: evolution – galaxies: formation – galaxies: general – galaxies: halos

---

This focus meeting has emphazised the high importance of angular momentum, to understand the formation and evolution of galaxies. It is now used extensively, given the progress of IFU instruments and large galaxy surveys.

Given these recent developments, it is difficult to imagine the debate that was occurring only 60 years ago, about the origin of the angular momentum of galaxies. The theory was first proposed by C. von Weizsäcker that galaxies were originating in large eddies of cosmic turbulence. This theory was followed by many people like G. Gamow, V. Rubin, his student or J. Oort.

Jim Peebles convinced Jan Oort that turbulence was irrelevant, that gravity and tidal torques could create the right amount of angular momentum (AM). For that he computed the torques with N-body simulations (N=90) and showed that the un-dimensional value of the AM $\lambda = \frac{J|E|^{1/2}}{GM^{5/2}} \sim 0.1$, in agreement from analytical estimations.

Since then, dark matter has been introduced, the problem is more complex, since we observe only the angular momentum of the baryons, which has to be related to the dark matter one. How are these acquired, how do they exchange?

The first cosmological simulations with baryons and dark matter, pointed out a serious problem, called the AM catastrophy: the baryons were losing their angular momentum through dynamical friction in mergers in favor of the dark matter, and were accumulating in very small disks at the bottom of the potential wells. Thanks to the feedback, and also the increase in spatial resolution of the simulations (lowering the effects of friction), the AM catastrophy is now limited (e.g. Obreja, Pedrosa and others, this meeting).

1. The "Fall" relation

In their pioneering study, Fall & Efstathiou (1980) take into account baryons and dark matter, which was only made of old stars at this epoch. Fall (1983) considers several scenarios of AM, mass or energy conservation, and concludes that the best scenario fitting the observations is that of baryonic mass M and AM conserved, while energy

is dissipated. In this case, the specific angular momentum, i.e. j= J/M is a power-law function of mass, with slope 2/3. Several parallel lines can be traced, with the same slope in the logj-logM diagram, the highest one is for very late disk galaxies (Sc), while the early-type galaxies (ETG) fall below, due to their high velocity dispersion and low rotation (low V/σ). When only dark matter halos are concerned, the Virial relation combined with the hypothesis that all halos at any mass are formed out of a constant volumic density, leads to the power-law relation with slope 2/3.

Thirty years later Romanowsky & Fall (2012), and Fall & Romanowsky (2013) follow up using the much better determined AM and the much larger statistics provided by modern galaxy surveys. They show that the specific j can be used as a new classification scheme for galaxies, since all the Hubble sequence can be retrieved through parallel lines of 2/3 slopes in the logj-logM baryonic diagram. Many other versions of this diagram and classification were published (Obreschkow & Glazebrook, 2014; Cortese et al., 2016; Posti et al., 2018; Sweet et al., 2018).

All these studies led to consider a third parameter in the AM scaling relation: the relation can be viewed in a 3-dimension space, where the third axis is the bulge to total mass ratio B/T (Fall & Romanowsky 2018, also Obreschkow & Glazebrook 2014). The scaling relation M-j-B/T can then be retrieved from the well known Tully-Fisher relation for spirals, and fundamental plane for early-type galaxies. together with a structure relation (for instance the Freeman's relation $M \propto R^2$ for high-surface brightness spirals).

2. ΛCDM hydro numerical simulations

In the recent years, there has been a burst of simulation papers, interested in following angular momentum, as described by Susana Pedrosa in her review (Pedrosa & Tissera 2015, Genel et al. 2015, Teklu et al. 2015, Obreja et al. 2016, 2018, Lagos et al.2018). Although the most realistic simulations, including star formation and feedback, have solved the AM catastrophy (through the effect of feedback and higher spatial resolution), they have revealed that the scaling relations of specific AM (j) versus baryonic mass are flatter than those observed. The various galaxies follow parallel lines in the logj-logM baryonic diagram, with the B/T parameter increasing towards the bottom right, but the slope of the lines are nearly 1/3.

Although the stellar feedback helps to solve the AM catastrophy, it also excessively thickens galaxy disks. Simulations still predict too massive bulges, and feedback is not sufficient to produce the large number of observed bulgeless galaxies.

James Bullock remarked that very different results (especially in density and temperature) can be obtained in general in cosmological simulations when using different codes, different algorithms (Eulerian, Lagrangian), different resolutions, different recipes for star formation and feedback. However, the results on angular momentum, either of stars (j_*) or gas (j_{gas}) are converging!

Due to dissipation, gaseous filaments are much thinner than dark matter filaments. This means that even before matter enters into galaxies, the specific AM of baryons is 3 times higher than the specific AM of dark matter. This changes the initial conditions in general adopted in semi-analytical models, where baryons and dark matter are assumed to have gained the same specific j through tidal torques. The virial radius R_V changes a lot with time, it increases by a factor ~ 3 from z=1 to z=0. Since $j \propto \lambda R_V$, it is still possible that the size of baryonic disks are the same at the end. The final j will depend on the AM of the gas accreted in the mean time.

The size ratio between the stellar and dark matter components decreases with time for

low M, this was not reproduced before by the semi-analytical models. Now abundance matching is considering sizes, as Rachel Somerville showed in her talk.

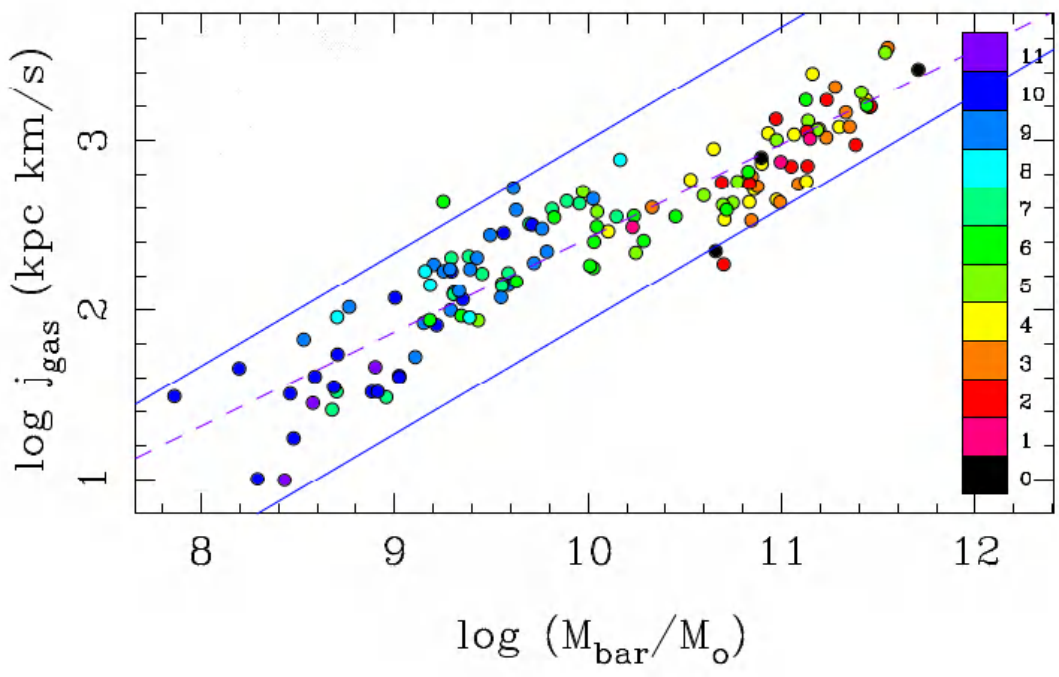

Figure 1. The specific gas angular momentum $j_{gas} \propto R_d\ V_{[}flat$, versus the baryonic mass M_{bar}= M_* +M(HI), from the 175 spiral galaxies of the SPARC sample of Lelli et al. (2016). The atomic gas is rotating maximally (negligible velocity dispersion), and the diagram should follow the upper envelope with a slope 2/3. In fact, the best fit has a slope of 0.55. The colour indicates the galaxy type, 0 being a lenticular, then Sa, Sab .. 9 is Sm, 10 Im and 11 BCD.

3. Why such a scaling relation?

The observation of the logj_* - logM_* scaling relations in parallel lines with a slope 2/3 is not straightforward to interpret. The first predictions were done with the total matter, and can be applied essentialy to the dark matter, but it is not obvious why the stars would follow the same relation.

Posti et al. (2018a,b) have proposed some biased collapse scenario, to explain why the baryons do not retain all their initial angular momentum. However, the scenario must be rather contrived. Indeed, to derive from the dark matter relation $j_{DM} = J_{DM}/ M_{DM} \propto M_{DM}^{2/3}$, the equivalent relation for stars, $j_* \propto f_j\ f_*^{-2/3}\ M_*^{2/3}$, we must assume that the product $f_j\ f_*^{-2/3}$ = cst, with $f_j = j_*/j_{DM}$ and $f_* = M_*/M_{DM}$. This last ratio is the well known fraction of stellar mass in a galaxy, which is much below the universal baryon fraction f_b=17%. From abundance matching, this function peaks for halos of the Milky Way mass, and then falls steeply on each side by 2 orders of magnitude (e.g. Behroozi et al. 2010). To interpret the AM observations, we should explain why the f_j ratio has the same behaviour, more exactly $f_j \propto f_*^{2/3}$. the biased collapse scenario proposed by Posti et al. (2018b) requires that the outer parts of halos, rich in AM, fail to accrete on the galaxy to form stars. This requirement looks like a conspiracy!

May be the specific AM of baryons does not always follow the scaling relation with slope 2/3. When dwarfs dominated by dark matter and gas are considered, the slope is more near 0.5, as shown in Figure 1.

4. Exchanges of AM – Secular evolution

During galaxy evolution, angular momentum is not frozen either in the baryons or dark matter, but their fraction may vary. AM can be exchanged through spiral arms within the disk, which produces radial migration. Some density breaks in the radial distribution of stars can be attributed to these processes (Athanassoula 2014, Peschken et al. 2017). Bars exchange AM with the dark halo, enhancing the formation of bars, which are waves of negative angular momentum. Bars can also be destroyed through torquing the gas, which is driven to the center.

It is interesting to follow AM along cosmic filaments. Galaxies have special orientations with respect to filaments: spirals have their spin parallel to them, while ellipticals, coming from mergers of spirals, have their spin perpendicular to them. The fraction of fast rotators (at least faster than the average) is increasing with the distance to the filaments. Galaxy surveys begin to be able to check all these predictions. (Welker et al. 2014, Xiaohu Yang et al. 2018)

5. Large complexity in AM evolution

Shy Genel described a long long equation, supposed to control the evolution of the angular momentum, and follow its evolution along a galaxy life, with matter accretion and major mergers. All parameters have to be taken into account, such as the stars formed in situ, or ex-situ, the gas forming stars, and what happens during the feedback, the new star formation from the gas lost, the gas accretion, the minor mergers, the radial migration, the AM exchange with DM. All this is far from the AM prediction from torques at turn-around, and the scaling relation of $j \propto M^{2/3}$.

How can we explain this miracle?

First the envelope at high j applies to pure disks, with 100% efficiency to retain AM. This is relatively obvious if material is almost in circular orbits: this plays the role of an attractor (see the talk from Francesca Rizzo, and Rizzo et al. 2018). Then you depart progressively from this attractor, as soon as you form bulges, spheroids, heating the stellar component, without the possibility of gas cooling.

6. Apparent contradictions

AM is a proxy for morphological types, as Fall & Romanowsky (2013) proposed. It is also well known that morphological types are segregated by the densiy of environment (Dressler et al., 1980). Spirals are dominating in the field, while their abundance decreases at high galaxy density in favor of lenticulars and ellipticals. Michele Capellari (2016) in his review article proposes to apply this segregation with density to fast and slow rotators, to replace the spiral/elliptical classification. And indeed, slow rotators are found at density peaks in clusters and groups.

But in her talk, Jenny Greene claimed that there is no evidence of environment effect on the AM of early-type galaxies (Greene et al., 2018). This is obtained from many surveys (MASSIVE, SAMI, MANGA), and the AM depends only on mass.

Another issue when considering AM, is to know whether studies are extending enough in radius. As described beautifully by Matthew Colless, we are witnessing a golden age for kinematical studies of galaxies, with integral field units (IFU) large surveys (Atlas3D, SAMI, CALIFA, MANGA etc..). However, large numbers (thousands) of galaxies are observed only to Re, and hundreds to 2Re. In general you need HI surveys to reach the flat portion of rotation curves, richer in AM.

In the optical, the kinematics of Globular Clusters (GC) show that the spin and ellipticity increase in S0, while they drop in Ellipticals with radius, as described with the SLUGGS survey by Jean Brodie (Brodie & Romanowsky 2016). With Planetary Nebulae (PNe) Pulsoni et al. (2018) go much further in radius, to 15-20 Re, where all the AM and signatures of the galaxy formation subsist. There is a large diversity of situations for ETG. Some slow rotators begin to rotate in the outer parts, and among fast rotators, 70% slowly rotate in the outer parts.

The transition radius between in-situ and ex-situ material is $\propto 1/\mathrm{M}_*$: i.e. there is more ex-situ material in massive galaxies, formed through mergers. This is perfectly compatible with Illustris simulations (Rodriguez-Gomez et al. 2016).

Lagos et al. (2018) have measured in detail through simulations how galaxies gain and lose AM by matter accretion and mergers. Dry mergers reduce specific j by 30%, while wet mergers inscrease j by 10%.

7. Atomic gas and dwarfs

As shown in Obreschkow et al. (2016) and in Murugeshan's talk, the angular momentum has a large influence in the stability of spiral galaxies and their HI gas fraction. The stability criterion can be written as $\mathrm{q} = \mathrm{j}\ \sigma_v/\mathrm{GM} \propto \mathrm{M}^{-1/3}$, and the HI gas fraction f_{atm} is AM-regulated and also $\propto \mathrm{M}^{-1/3}$. A related study by Romeo & Mogotsi (2018) on stability and AM regulation includes the thickness of the stellar disk T_*, i.e. $\mathrm{Q}_* \sim \sigma_v\ \mathrm{T}_*$.

In Chengalur's talk, another discrepancy between simulations and observations was revealed for dwarf galaxies: the specific AM of baryons j_b increases below a baryonic mass of $10^{9.1}\mathrm{M}_\odot$, with respect to the $\mathrm{M}^{2/3}$ expected scaling relation (Kurapati et al. 2018). For these dwarfs, disks become thicker due to star formation feedback, and to the shallow potential well. There is no dependency on large-scale environment, so this is not due to possible accretion. Another explanation is that such dwarfs are dominated by dark matter, therefore their observed rotational velocity is much higher with respect to their visible mass (M_{bar}) than for spiral of larger masses.

In FIRE simulations, dwarfs have very low rotational support: the large SF feedback gives them a rounder shape (El-Badry et al. 2018), and their specific j falls below the $\mathrm{M}^{2/3}$ scaling relation.

8. Perspectives

May be all diagnostics of galaxy evolution are retained in the outer parts: accretion, ex-situ star formation, etc. In that case PNe are the best tracers of AM and evolution. It is of prime importance to acquire more statistics, for instance in the Hector IFS survey, 10^5 galaxies will be obtained. Also other parameters must be followed, metallicity, stellar populations (see Kassin's talk).

With ELT and JWST, it will be possible to track the evolution with redshift. We know already that galaxies become clumpy at $z > 2$ and have much lower j_*. While it is predicted that $\mathrm{j}_* \sim (1+\mathrm{z})^{-1/2}$ (Obreschkow et al. 2015), F. Fraternali in his talk found no evolution with z. [*Remark by the co-editor, Danail Obreschkow: It seems important to bear in mind that the approximation* $j \propto (1+z)^{-1/2}$ *for dark haloes of fixed mass only applies to the matter-dominated era* ($z \gtrsim 1$). *Explicitly, neglecting the weak evolution of* j *expected from the cosmic evolution of the virial over-density* $\Delta_{\rm vir}$, *we find* $\langle j/M^{2/3}\rangle \propto E^{-1/3}(z) = (\Omega_m(1+z)^3+\Omega_\Lambda)^{-1/6}$, *which asymptotes to* $\Omega_m^{-1/6}(1+z)^{-1/2}$ *for* $z\to\infty$, *but Taylor-expands to* $(1+z)^{-\Omega_m/2} \approx (1+z)^{-0.15}$ *around* $z=0$.]

It is also paramount to study external accretion of gas, which contains a lot of AM, is at the origin of warps, etc. HI maps are badly needed at intermediate and high z; in the future SKA will provide a large number of these gas maps.

References

Athanassoula, E.: 2014, *MNRAS*, 438, L81
Behroozi, P. S., Conroy, C., Wechsler, R. H.: 2010, *ApJ*, 717, 379
Brodie, J., Romanowsky, A. J.: 2016, *IAUS*, 317, 190
Bullock, J. S., Boylan-Kolchin, M.: 2017, *ARA&A*, 55, 343
Capellari , M.: 2016, *ARA&A*, 54, 597
Cortese, L., Fogarty, L. M. R., Bekki, K. et al.: 2016 *MNRAS*, 463, 170
Dressler, A.: 1980 *ApJ*, 236, 351
El-Badry, K., Quataert, E., Wetzel, A. et al.: 2018, *MNRAS*, 473, 1930
Fall, S. M., Efstathiou, G.: 1980, *MNRAS*, 193, 189
Fall, S. M.: 1983, *IAUS*, 100, 391
Fall, S. M., Romanowsky, A. J.: 2013, *ApJ*, 769, L26
Fall, S. M., Romanowsky, A. J.: 2018, *ApJ*, in press, arXiv180802525
Genel, S., Fall, S. M., Hernquist, L. et al.: 2015, *ApJ*, 804, 40L
Greene, J. E., Leauthaud, A., Emsellem, E. et al.: 2018, *ApJ*, 852, 36
Kurapati, S., Chengalur, J. N., Pustilnik, S., Kamphuis, P.: 2018, *MNRAS*, 479, 228
Lagos, C., Stevens, A. R. H., Bower, R. G. et al.: 2018, *MNRAS*, 473, 4956
Lelli, F., McGaugh, S. S., Schombert, J. M.: 2016, *AJ*, 152, 157
Obreja, A., Stinson, G. S., Dutton, A. A. et al.: 2016, *MNRAS*, 459, 467
Obreja, A., Dutton, A. A., Maccio, A. V. et al.: 2018, *MNRAS*, in press, arXiv180406635
Obreschkow, D., Glazebrook, K.: 2014, *ApJ*, 784, 26
Obreschkow, D., Glazebrook, K., Bassett, R. et al.: 2015, *ApJ*, 815, 97
Obreschkow, D., Glazebrook, K., Kilborn, V., Lutz, K.: 2016 *ApJ*, 824, L26
Pedrosa, S. E., Tissera, P. B.: 2015, *A&A*, 584, A43
Peschken, N., Athanassoula, E., Rodionov, S. A.: 2017, *MNRAS*, 468, 994
Posti, L., Fraternali, F., Di Teodoro, E. M., Pezzulli, G.: 2018a, *A&A*, 612, L6
Posti, L., Pezzulli, G., Fraternali, F., Di Teodoro, E. M.: 2018b, *MNRAS*, 475, 232
Pulsoni, C., Gerhard, O., Arnaboldi, M. et al.: 2018, *A&A*, in press, arXiv171205833
Rizzo, F., Fraternali, F., Iorio, G.: 2018, *MNRAS*, 476, 2137
Rodriguez-Gomez, V., Pillepich, A., Sales, L. V. et al.: 2016, *MNRAS*, 458, 2371
Romanowsky, A. J., Fall, S.M: 2012, *ApJS*, 203, 17
Romeo, A. B., Mogotsi, K. M.: 2018, *MNRAS*, 480, L23
Somerville, R. S., Behroozi, P., Pandya, V. et al.: 2018, *MNRAS*, 473, 2714
Sweet, S. M., Fisher, D., Glazebrook, K. et al.: 2018, *ApJ*, 860, 37
Teklu, A. F., Remus, R.-S., Dolag, K. et al.: 2015, *ApJ*, 812, 29
Welker, C., Devriendt, J., Dubois, Y.; Pichon, C., Peirani, S.: 2014, *MNRAS*, 445, L46
Yang, X., Zhang, Y., Wang, H. et al.: 2018, *ApJ*, 860, 30

Astronomy in Focus, Volume 1
XXXth IAU General Assembly, August 2018
Teresa Lago, Patricia Tissera & Danail Obreschkow, ed.

DOI: 10.5281/zenodo.1481378

On the History and Present Situation

P. J. E. Peebles

Princeton University,
Princeton New Jersey, 08544, USA
email: pjep@princeton.edu

Abstract. A common thought in the 1950s was that galaxies rotate because they are remnants of primeval currents, as in turbulence. But this idea is quite unacceptable in an expanding universe described by general relativity theory. Since we are no smarter now than in the 1950s the lesson I draw is that we do well on occasion to pause to consider whether we might be missing something. An example is the pure disk galaxies that are so common nearby and so rare in simulations. We have something to learn from this.

Keywords. galaxies: bulges, galaxies: formation, cosmology: theory.

Carl Friedrich von Weizsäcker (1951) argued for the likely importance of turbulence in protoplanetary disks, and he proposed that turbulence may also play a role in galaxy formation: "I do not propose a theory of the origin of this initial turbulence" but "it is a consistent theory to think of the galaxies (or perhaps the clusters of galaxies) as the largest eddies of a cosmic turbulence that existed a couple of billion years ago." Von Weizsäcker's student Sebastian von Hoerner had a distinguished career in radio astronomy and SETI. In a paper while still at the University of Göttingen, von Hoerner (1953) considered how matter might be distributed in a galaxy that grew out of a turbulent eddy. He concluded that (in my translation) "Since we have obtained qualitatively consistent statements on the surface density run in spiral nebulae in three completely different ways, we will consider this result as an argument for the applicability of the assumed turbulence theory."

George Gamow was an intuitive genius but not always careful with details. He felt the present mean mass density is far too low for the gravitational assembly of galaxies. He and Teller had proposed that this meant galaxies formed at high redshift, when the density would have been more important. But Gamow (1954) argued that "The only escape from this difficulty is to assume the existence of very large original density fluctuations in the primordial gas ... in a turbulent state. Besides, in order to permit large variations of density, this turbulence must have been supersonic." Gamow's student Vera Rubin had a distinguished career in astronomy, with particular attention to the informative role of rotation curves of galaxies. In her PhD thesis she introduced and applied statistical measures of the galaxy distribution; she pioneered an important line of research. Rubin (1954) concluded that her statistical measures are "physically reasonable if the galaxies have condensed from a turbulent gaseous medium."

The relation between student and teacher can be complicated. We can only wonder how enthusiastic these two students were about their evidence for primeval turbulence.

In an important review Jan Henrik Oort (1958) showed that the empirical support for cosmology was scant but by no means trivial. Oort argued that "Most galaxies deviate greatly from the spherical shape and have a considerable angular momentum. The total angular momentum must have been present in the primeval clump of material from which

the galaxy has contracted." Turbulence is not mentioned, but I count Oort's picture as a variant of the concept of primeval currents.

Leonid Ozernoi was a leading figure in exploration of the primeval turbulence picture in the early 1970s. We agreed that primeval turbulence calls for irrotational flow, $\nabla \times \vec{v} = 0$. This is because currents with nonzero divergence would produce density fluctuations that (with a reasonable mass density) would grow by gravitational attraction, the usual gravitational instability picture. Suppose the primeval irrotational flow has comoving coherence length y, or physical length $a(t)y$ at expansion time t, where $a(t)$ is the expansion parameter. How the flow behaves depends on the ratio

$$R(t) = \frac{v(t)t}{a(t)y}, \text{ where } R(t) \propto a(t) \text{ if } p = \rho/3, \ R(t) \propto a(t)^{-1/2} \text{ if } p = 0. \tag{1}$$

At redshift $z > z_{\rm eq} = 5000$ the universe was dominated by radiation and $R(t)$ would have been growing. If $R(t)$ approached unity flows moving in different directions would have encountered each other and been forced to change direction. That is, turbulence would have formed and decayed to viscosity. But this is far too early for galaxy formation. At $z < z_{\rm eq}$ the ratio $R(t)$ decreases, so if turbulence had not developed by then it would not develop. I concluded (Peebles 1971a) that the primeval turbulence theory is not viable. Ozernoi (1972) disagreed (by long distance, he was in the USSR). Interest in primeval turbulence continued through the 1970s, but attention was turning to the role of gravity.

At the conference where von Weizsäcker (1951) spoke about primeval turbulence Fred Hoyle (1951) proposed that gravitational transfer of angular momentum caused galaxies to rotate. He evidently was unaware that Gustaf Strömberg (1934) had expressed similar thoughts some two decades earlier. (I am grateful to Matthias Steinmetz for alerting me to Strömberg directly after my IAU lecture.) As Hoyle put it, a young protogalaxy would have been an irregular blob that could be torqued by the gravitational field gradients of neighboring blobs, transferring angular momentum. His estimate of the effect suggested this is a credible explanation of why galaxies rotate.

The NASA archive ADS lists no citations to Hoyle's paper for the next two decades, and no citations to Strömberg (1934) until 1995. The rate of research in cosmology through most of the $20^{\rm th}$ century was modest. Another example is the exchange with Werner Heisenberg after Hoyle's talk:
Heisenberg: "How can an irregular thing like a cloud have originated otherwise than as a consequence of turbulent motion?"
Hoyle: "A cloud can form in a more or less uniform medium through gravitational instability."
Heisenberg: "This possibility exists, but wouldn't you say that if we believe in the expanding universe (I know that some of us do not but that is another matter), then we should also assume that there is an enormous energy in this primary cosmic gas which expands? Now, if there is this enormous kinetic energy of the gaseous masses, I suppose there must be turbulence, because the turbulent motion is the normal motion of the gas, whereas laminar flow is extremely exceptional."

In the late 1960s I was taken by the idea that galaxies, and their clumpy spatial distribution, grew by the gravitational instability of the expanding universe. I had to explain why galaxies rotate. I did not know Hoyle's 1951 argument then, but worked along similar lines in my computation of the gravitational angular momentum transfer. The analytic estimate in Peebles (1969) amounts to

$$\lambda \equiv \frac{L|E|^{1/2}}{GM^{5/2}} \sim 0.08. \tag{2}$$

Here L is the angular momentum of the newly assembled protogalaxy, M is its mass, and E is its gravitational binding energy. (This combines eqs. [35] and [36] in Peebles 1969. I introduced λ in Peebles 1971b.)

Oort (1970) argued that I had seriously overestimated the gravitational transfer of angular momentum, and concluded that galaxies "must have been endowed with their angular momentum from the beginning." That led me to compute the angular momentum transfer in numerical N-body simulations. They indicated $\lambda = 0.07^{+0.1}_{-0.03}$. These simulations had $N = 90$ to 150 particles. This is ludicrous by today's standard, but that was a different age. In this paper I ventured to add that since λ is a pure number set by the scale-invariant physics of gravity and a pressureless ideal gas one might expect λ to be of order unity. What other value might it have?

I don't know which of my arguments was the more persuasive, but after publication of this paper Oort sought me out to explain, not at length but quite clearly, that he withdrew his objection to my result. It was an edifying example for this callow youth.

Efstathiou and Jones (1979) found $\lambda = 0.07 \pm 0.03$ in simulations with $N = 1000$ particles. That number also is tiny by today's standards, but far better than I did, and I suppose large enough to make the case: gravity in an expanding Einstein-de Sitter universe produces angular momentum in the neighborhood of $\lambda \sim 0.1$

The next advance was the proposal, independently by White and Rees (1978) and Gunn, Lee, Lerche, *et al.* (1978), that the luminous parts of galaxies formed by dissipative settling of baryonic gas and plasma in subluminal massive halos. (Gunn *et al.* had in mind halos of nonbaryonic matter, later known as WIMPS. White and Rees felt that remnants of early stellar generations are more likely forms of subluminal matter, but that nonbaryonic dark matter would do.) Neither paper mentions rotation of galaxies.

Strömberg(1934) and Fall (1979) pointed out that dissipative settling could spin up a young galaxy. Fall could be more explicit: it could bring $\lambda \sim 0.1$ up to the value $\lambda \sim 1$ suitable for the disk of a spiral galaxy. Fall and Efstathiou (1980) elaborated on this point. Let v_c be the speed of rotation of a newly gravitationally assembled protogalaxy, and let $v_r \sim (GM/R)^{1/2}$ be its internal speed of support, mainly random. The angular momentum parameter is, roughly, $\lambda \sim v_c/v_r$. Suppose that after assembly the bulk of the mass dissipatively settled by the factor α. The rotation speed would scale up as $v_c \propto \alpha$, and the speed of pressure support would increase as $v_r \propto \alpha^{1/2}$. So we see that the protogalaxy would have to have collapsed by a factor $\alpha \sim \lambda^{-2} \sim 100$ to get to rotational support. That seems excessive. Surely the protogalaxy would instead fragment into something like an elliptical galaxy. But if instead the diffuse baryons settled in a subluminal massive halo with density run $\rho \propto r^{-2}$, and the diffuse baryon mass were subdominant, then spin-up would require settling by the factor $\alpha \sim \lambda^{-1} \sim 10$. This factor of ten is about what Eggen, Lynden-Bell, and Sandage (1962) found could account for the metal-poor high-velocity stars in the Milky Way. It's a valuable sanity check.

By 1980 gravitational transfer of angular momentum had become the standard and accepted explanation of why galaxies rotate. That was followed by the development of increasingly detailed numerical simulations of how baryons and dark matter gather by gravity and non-gravitational stresses in all their complexities to produce what are now impressively good approximations to real galaxies. I don't imagine much attention is given to λ anymore; the simulations take care of it.

If primeval turbulence is so manifestly wrong, as I argue, why was the idea so commonly accepted in the 1950s and 1960s? There was phenomenology: spiral galaxies call to mind turbulent eddies. The expanding universe was familiar, but not so carefully considered, or so well trusted, as to make the idea of primeval turbulence seem suspicious. Recall

Heisenberg's remarks. And we must bear in mind that ideas can be self-reenforcing: people analyzed primeval turbulence because others had.

I began with the thought of pausing on occasion to consider whether, as for primeval turbulence, we are overlooking something. I offer the paper by Kormendy, Drory, Bender, and Cornell (2010), with the title *Bulgeless Giant Galaxies Challenge Our Picture of Galaxy Formation by Hierarchical Clustering.* I suggest that those who do not often admire the wonderfully detailed images of nearby galaxies to be seen on the web contemplate NGC 1300. (The reader is referred to the high-resolution HST image.) I don't see a classical bulge; the central region looks like a whirlpool. Would an HST image reveal its funnel? or maybe a star cluster? Also worth contemplating is the image of M 101 in Figure 3 in Peebles (2014), adapted from Kormendy *et al.* (2010). It has a central star cluster with luminosity about a part in 10^5 of the galaxy. The galaxy spiral arms are seen all the way in to this relatively tiny star cluster. I suppose gravity in the disk produces the spiral arms, and so expect that the central part of this galaxy cannot be dominated by mass in a classical stellar bulge.†

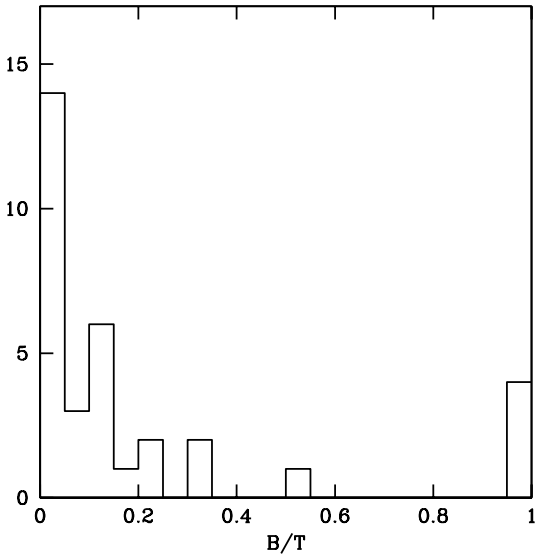

Figure 1. Distribution of bulge to total luminosities of the largest galaxies within 10 Mpc.

The variants of the pure disk phenomenon seen in NGC 1300 and M 101 seem to be common among the nearest large galaxies that can be examined in closest detail. Brent Tully's Local Universe catalog‡ lists 38 galaxies closer than 10 Mpc with K-band luminosity greater than 10^{10}. (I can't find K-band luminosities for a few, but they have large optical luminosities.) The fractions B/T of galaxy luminosities that are in classical bulges are given by Kormendy *et al.* (2010) and Fisher and Drory (2011) for 33 of these 38 galaxies. Figure 1 shows the distribution. Three ellipticals are at the far right. Near the center is the Sombrero Galaxy, also well worth a visit to the web. The galaxies M 31

† I might state my understanding that a classical bulge is supported by near isotropic stellar velocities that cause the stars to move in a near axisymmetric distribution that may rise above the disk. Stars rise above the disk in the peanut-shaped bar in the Milky Way, but I suppose this would not be termed a classical bulge. I am cautioned that a bulge luminosity derived from the excess above a pure exponental fit to the surface brightness run may be in a classical bulge, or it may be a departure from an exponential distribution of the stars moving in the disk.

‡ Available at the Extragalactic Distance Database, `http://edd.ifa.hawaii.edu`, as the catalog "Local Universe (LU)"

and M 81 are next to the left of center. The rest of these large galaxies are still further to the left, most judged to have little or no light in classical bulges.

My impression is that distributions of B/T in recent large-scale simulations peak at B/T close to 50%, quite unlike Figure 1. This is not a criticism: the authors are reporting results from painstakingly careful work. I have not detected much concern in the galaxy formation community about the failure to match Figure 1. This is sensible: galaxy model building has encountered and resolved many other problems; maybe this is just one more.

But I offer the cautionary reminder of earlier thinking about primeval turbulence. We are much better informed now, but we are reaching much further, on still quite modest empirical grounds. Star formation is observed in some detail, but it still must be schematically modeled in galaxy formation simulations. Dark matter and Einstein's cosmological constant are not even observed, apart from their gravitational effect. So although the ΛCDM theory passes demanding tests it may need improving. Thinking in cosmology has been redirected, sometimes by closer consultation of the theory, as for primeval turbulence, sometimes by observation, as in the falsification of the 1948 steady state cosmology. You can think of other examples. The pure disk phenomenon is a case of déjà vu all over again; it is certain to teach us something of value. That may be about how pure disks can be understood within the present paradigm. Or it may serve to redirect our thinking once again, toward a still better cosmology.

References

Efstathiou, G., and Jones, B. J. T. 1979, *MNRAS*, 186, 133

Eggen, O. J., Lynden-Bell, D., and Sandage, A. R. 1962, *ApJ*, 136, 748

Fall, S. M. 1979, *Nature*, 281, 200

Fall, S. M., and Efstathiou, G. 1980, *MNRAS*, 193, 189

Fisher, D. B., and Drory, N. 2011, *ApJ Lett.*, 733, L47

Gamow, G. 1954, *Proc. NAS*, 40, 480

Gunn, J. E., Lee, B. W., Lerche, I., Schramm, D. N., and Steigman, G. 1978, *ApJ*, 223, 1015

Hoyle, F. 1951, in Proceedings of a Symposium on the Motion of Gaseous Masses of Cosmical Dimensions held at Paris, August 16-19, 1949, 195

Kormendy, J., Drory, N., Bender, R., and Cornell, M. E. 2010, *ApJ*, 723, 54

Oort, J. H. 1958, Eleventh Solvay Conference. Editions Stoops, Brussels, 21 pp.

Oort, J. H. 1970, *A&Ap*, 7, 381

Ozernoi, L. M. 1972, *Soviet Astron.-AJ*, 15, 923

Peebles, P. J. E. 1969, *ApJ*, 155, 393

Peebles, P. J. E. 1971a, *A&SS*, 11, 443

Peebles, P. J. E. 1971b, *A&Ap*, 11, 377

Peebles, P. J. E. 2014, in Proceedings of the 7th International Conference on Gravitation and Cosmology, Goa, 2011, *J. Phys.: Conference Series*, 484, 012001

Rubin, V. C. 1954, *Proc. NAS*, 40, 54

Strömberg, G. 1934, *ApJ*, 79, 460

von Hoerner, S. 1953, *Zeitschrift für Astrophysik*, 32, 51

von Weizsäcker, C. F. 1951, in Proceedings of the Symposium on the Motions of Gaseous Masses of Cosmical Dimensions, Paris, August 16-19, 1949, pages 158 and 200

White, S. D. M., and Rees, M. J. 1978, *MNRAS*, 183, 341

Astronomy in Focus, Volume 1
XXXth IAU General Assembly, August 2018
Teresa Lago, Patricia Tissera & Danail Obreschkow, ed.

DOI: 10.5281/zenodo.1481532

Angular Momentum Evolution of Galaxies: the Perspective of Hydrodynamical Simulations

Claudia del P. Lagos[1,2,3]

[1]International Centre for Radio Astronomy Research (ICRAR), M468, University of Western Australia, 35 Stirling Hwy, Crawley, WA 6009, Australia

[2]ARC Centre of Excellence for All Sky Astrophysics in 3 Dimensions (ASTRO 3D)

[3]Cosmic Dawn Center (DAWN), Niels Bohr Institute, University of Copenhagen, Copenhagen, Denmark

email: claudia.lagos@icrar.org

Abstract. Until a decade ago, galaxy formation simulations were unable to simultaneously reproduce the observed angular momentum (AM) of galaxy disks and bulges. Improvements in the interstellar medium and stellar feedback modelling, together with advances in computational capabilities, have allowed the current generation of cosmological galaxy formation simulations to reproduce the diversity of AM and morphology that is observed in local galaxies. In this review I discuss where we currently stand in this area from the perspective of hydrodynamical simulations, specifically how galaxies gain their AM, and the effect galaxy mergers and gas accretion have on this process. I discuss results which suggest that a revision of the classical theory of disk formation is needed, and finish by discussing what the current challenges are.

Keywords. Galaxy: evolution - Galaxy: formation - Galaxy: fundamental parameters

1. Introduction

The formation of galaxies can be a highly non-linear process, with many physical mechanisms interacting simultaneously. Despite all that potential complexity, early studies of galaxy formation stressed the importance of three quantities to describe galaxies: mass, M, energy, E, and angular momentum (AM), J (e.g. Peebles 1969); one can alternatively define the specific AM, $j \equiv J/M$, which contains information on the scale length and rotational velocity of a system. It is therefore intuitive to expect the relation between j and M to contain fundamental information.

In recent years, Integral field spectroscopy (IFS) is opening a new window to explore galaxy kinematics and its connection to galaxy formation and evolution, with IFS based measurements of the $j_{\rm stars} - M_{\rm stars}$ relations being reported in the local (e.g. Cortese et al. 2016) and high-z Universe (Burkert et al. 2016; Swinbank et al. 2017; Harrison et al. 2017). The last decade has also been a golden one for cosmological hydrodynamical simulations, with the first large cosmological volumes, with high enough resolution to study the internal structure of galaxies being possible (Schaye et al. 2015; Dubois et al. 2016; Vogelsberger et al. 2014; Pillepich et al. 2018). These simulations have been able to overcome the catastrophic loss of AM, which refers to the problem of galaxies being too low j compared to observations (Steinmetz & Navarro 1999; Navarro & Steinmetz 2000) and over-cooling problem. This problem was solved by improving the spatial resolution, adopting j conservation numerical schemes, and including efficient feedback (e.g.Kaufmann et al. 2007; Zavala et al. 2008; Governato et al. 2010; Guedes et al. 2011; DeFelippis et al. 2017). Fig. 1 shows examples of several cosmological simulations which

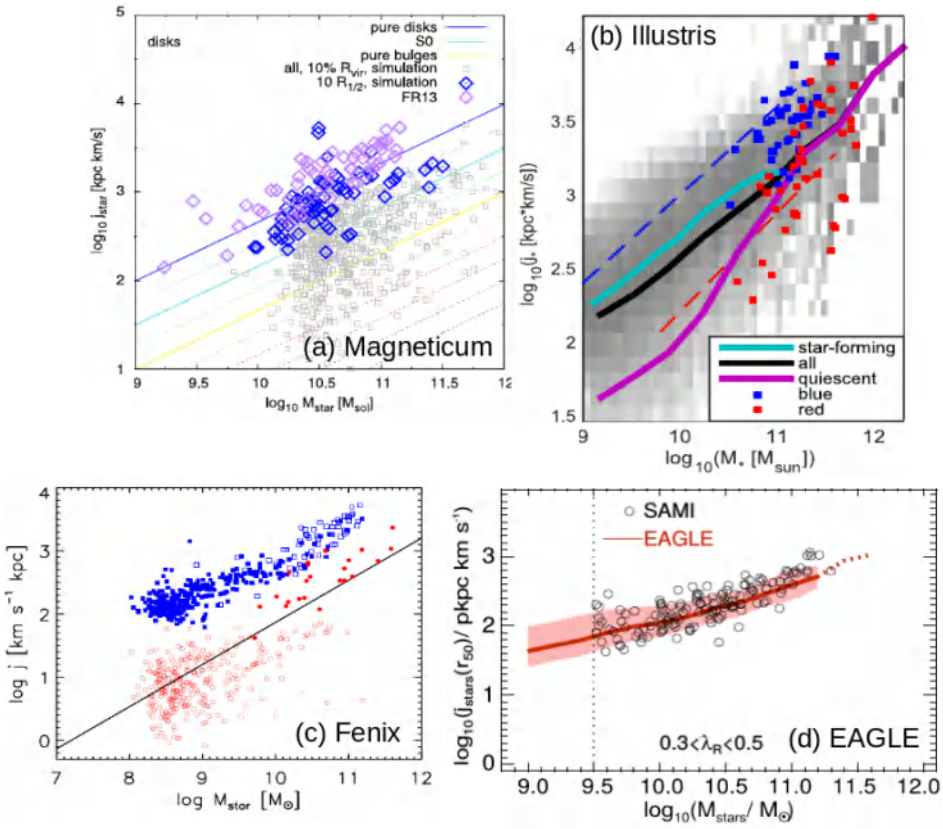

Figure 1. The $z = 0$ $j_{\rm stars} - M_{\rm stars}$ relation for several simulations: Magneticum (Teklu et al. 2015), Illustris (Genel et al. 2015), Fenix (Pedrosa & Tissera 2015) and EAGLE (Lagos et al. 2017). Panels (a), (b) and (c) show the total $j_{\rm stars}$ compared to the observational measurements of Fall & Romanowsky (2013), while panel (d) shows $j_{\rm stars}$ measured within an effective radius and compares with SAMI observations (Cortese et al. 2016).

have been shown to reproduce the observed $j_{\rm stars} - M_{\rm stars}$ relation for $z = 0$ galaxies. In addition to those above, there are several cosmological zoom-in simulations that have shown the same level of success (e.g. Wang et al. 2018; El-Badry et al. 2018).

The level of agreement of Fig. 1 gives us assurance that we can use these simulations to study how the AM of galaxies is gained/lost throughout the process of galaxy formation and evolution. The left panel of Fig. 2 shows an example of the morphologies of simulated galaxies in the $j_{\rm stars} - M_{\rm stars}$ plane at $z = 0$ in the EAGLE simulations. There is a clear correlation between a galaxy's morphology and its kinematics, as seen in observations (e.g. Cortese et al. 2016, Fall & Romanowski 2018). An important caveat, however, is that most, if not all, the simulations of Fig. 1 (and those with similar specifications) are currently unable to form very thin disks (with ellipticities $\gtrsim 0.7 - 0.8$) due to the insufficient resolution and simplistic interstellar medium (ISM) models. The latter prevent us from obtaining a realistic vertical structure of disks (see discussion in Lagos et al. 2018a).

2. How galaxies gain their angular momentum?

Lagos et al. (2017) used the EAGLE simulations (Schaye et al. 2015) to study how the stellar spin of galaxies at $z = 0$ evolved depending on their stellar population age and merger history. The stellar spin in this case was defined as a pseudo spin $\lambda'_{\rm stars} = j_{\rm stars}(r_{50})/M^{2/3}_{\rm stars}$, with $j_{\rm stars}(r_{50})$ being the stellar specific AM within one effective radius. The power-law index 2/3 comes from the predicted j-mass relation of dark matter halos (Fall 1983). The right panel of Fig. 2 shows the evolution of $\lambda'_{\rm stars}$ of $z = 0$ galaxies with different stellar ages that have had at least 1 galaxy merger. Progenitors display

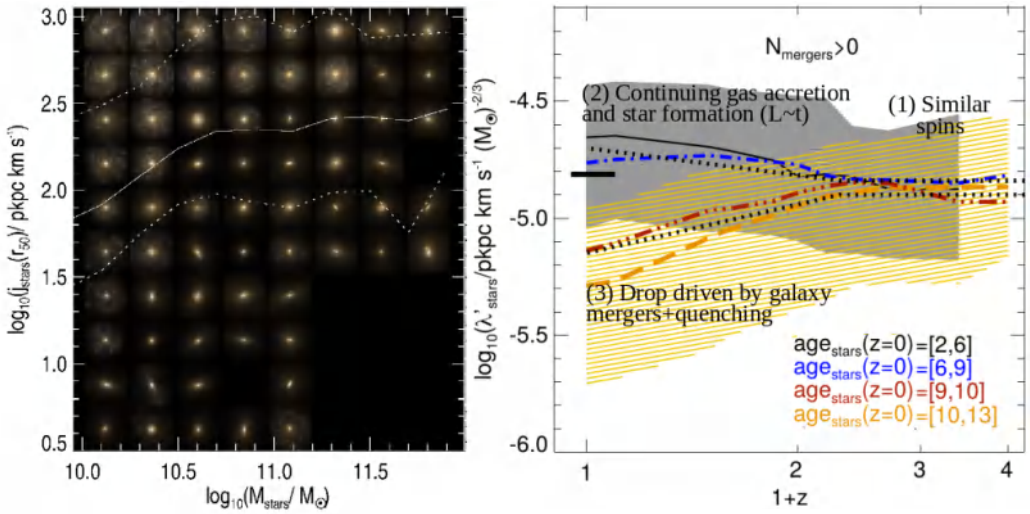

Figure 2. *Left panel:* From Lagos et al. (2018b). Synthetic gri optical images of randomly selected galaxies in the $j_{stars}(r_{50}) - M_{stars}$ plane at $z = 0$. The solid and dashed lines show the median and the $16^{th} - 84^{th}$ percentile range. *Right panel:* Adapted from Lagos et al. (2017). λ'_{stars} as a function of redshift for galaxies that by $z = 0$ have different stellar ages and that have had at least one merger with a mass ratio $\geqslant 0.1$. The shaded regions show the $16^{th} - 84^{th}$ percentile ranges for the lowest and highest age bins. At $z \gtrsim 1.2$, galaxies have similar spins, while diverging dramatically at lower redshifts. Lagos et al. (2017) identify three critical features described in the figure.

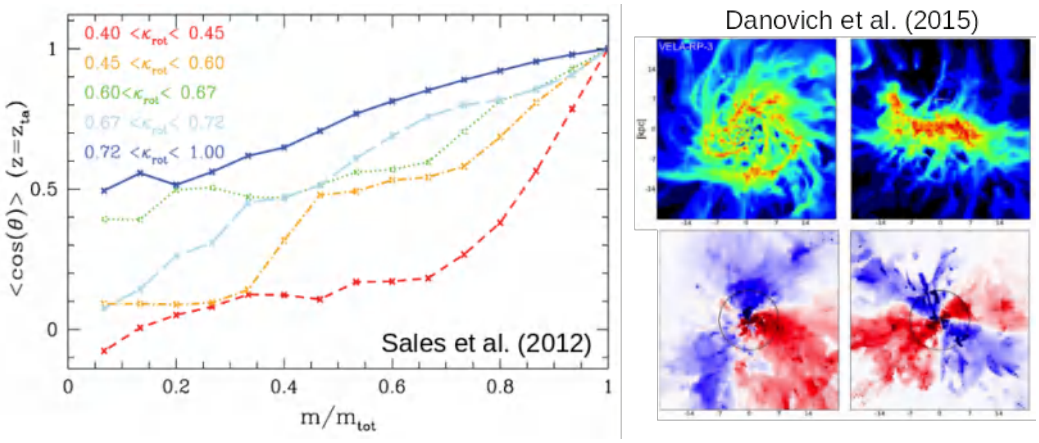

Figure 3. *Left panel:* From Sales et al. (2012). The angle between the AM vector enclosed within a given mass fraction (x-axis) and the total spin of the system, measured at the time of maximum expansion of the halo, for galaxies that by $z = 0$ have different fractions of kinetic energy invested in rotation (κ_{rot}; the higher the κ_{rot} the more rotation dominates). This figure shows that alignments between the halo and galaxy are key to facilitate the formation of disks. *Right panel:* From Danovich et al. (2015). Face-on and edge-on density (top) and normalised torque (bottom) maps of a simulated $z \approx 2$ galaxy. The figure shows that the quadrupole torque pattern expected in the idealized case of the formation of a thin disk is seen in both orientations, meaning that the galaxy is being torqued in all three axes.

indistinguishable kinematics at $z \gtrsim 1$ despite their $z = 0$ descendants being radically different ((1) in the right panel of Fig. 2). Similarly, Penoyre et al. (2017) found using Illustris that the progenitors of $z = 0$ early-type galaxies that are slow and fast rotators, had very similar properties at $z \gtrsim 1$ (see also Choi et al. 2017 for an example using the Horizon-AGN simulation). The evolution of λ'_{stars} diverges dramatically at $z \lesssim 1$, in which galaxies that by $z = 0$ have young stellar populations, grow their disks efficiently due to the continuing gas accretion and star formation ((2) in Fig. 2); galaxies that by

$z = 0$ have old stellar populations went through active spinning down, due to the effects of dry galaxy mergers and quenching ((3) in Fig. 2; discussed in more detail in § 3).

The reason why continuing gas accretion drives spinning up is because the AM of the material falling into halos is expected to increase linearly with time (as predicted by tidal torque theory; Catelan & Theuns 1996). El-Badry et al. (2018) explicitly demonstrated this using the FIRE simulations. Garrison-Kimmel et al. (2018) also using FIRE, in fact argued that the most important predictor of whether a disk will be formed by $z = 0$ is the halo gas j by the time the galaxy has formed half of its stars. These simulations thus suggest that *the later the accretion the more efficient the spinning up.*

Simulations suggest the critical transition at $z \approx 1$ is driven by a change in the main mode of gas accretion onto galaxies, from filamentary accretion to gas cooling from a hydrostatic halo (e.g. Garrison-Kimmel et al. 2018). The latter seems to be key in facilitating alignments between the accreting gas and the galaxy, while the former is by nature more stochastic. Sales et al. (2012) showed that galaxies that by $z = 0$ are more rotation-dominated formed in halos that had the inner/outer parts better aligned (see left panel in Fig. 3). Similarly, Stevens et al. (2017) showed that significant AM losses of the cooling gas to the hot halo are seen in cases where the hot halo is more misaligned with the galaxy. On the other hand, filamentary accretion at $z \gtrsim 1$ is not as efficient in spinning up galaxies mostly because gas filaments arrive from different directions (e.g. Walker et al. 2017), typically causing torques to act in all three axes of a galaxy (Danovich et al. 2015; see left panel in Fig. 3). The latter is intimately connected to high-z disks being turbulent and highly disturbed.

An important result that is robust to the details of the simulation being used, is that the circum-galactic medium (CGM) seems to have a specific AM in excess to that of the halo by factors of $3 - 5$ (Stewart et al. 2017; Stevens et al. 2017). Stevens et al. (2017) also showed that about $50 - 90\%$ of that excess j can be lost to the hot halo in the process of gas cooling and accretion onto the galaxy.

3. How galaxies loose their angular momentum?

The latest generation of hydrodynamical simulations has been able to approximately reproduce the morphological diversity of galaxies (e.g. Vogelsberger et al. 2014; Dubois et al. 2016; see left panel in Fig. 2). A long-standing question is therefore how do galaxies become elliptical with j significantly below disk galaxies of the same mass?

Zavala et al. (2016) used the EAGLE simulations to study the AM of galaxies and found a very strong correlation between the kinematic stellar bulge-to-total ratio and the net loss in AM of the stars that end up in galaxies at $z = 0$ (left panel Fig. 4), suggesting galaxy mergers to be good candidates for the physical process behind this correlation. More recently, several authors have shown (e.g. Penoyre et al. 2017; Lagos et al. 2018a,b) that the gas fraction of the merger is one of the key parameters indicating whether the merger will lead to the primary galaxy spinning up or down. Middle and right panels of Fig. 4 show the clear effect of galaxy mergers on the stellar spin parameter of galaxies in Illustris and EAGLE, respectively.

Lagos et al. (2018b) showed that other merger parameters can have a significant effect on the $j_{\rm stars}$ structure, with high orbital j and/or co-rotating mergers driving more efficient spinning up. However, gas fraction is the single strongest parameter that determines whether a galaxy spins up or down as a result of the merger, with the mass ratio modulating the effect. Active Galactic Nuclei feedback is key to prevent further gas accretion and the regrowth of galaxy disks in elliptical galaxies (e.g. Dubois et al. 2016). Early works on dry mergers (e.g. Navarro & White 1994) show that dynamical friction redistributes $j_{\rm stars}$ in a way such that most of it ends up at very large radii. However,

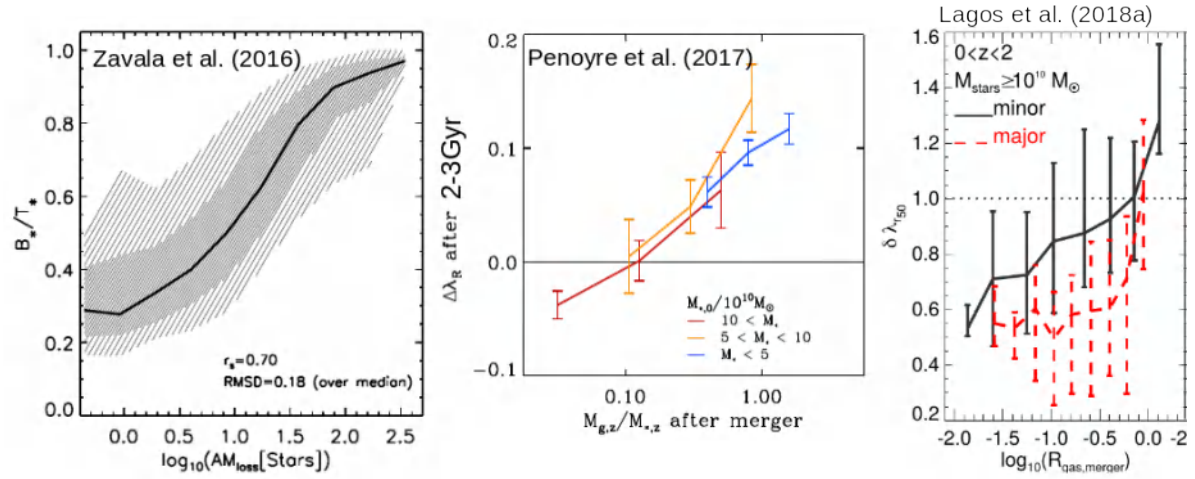

Figure 4. *Left panel:* From Zavala et al. (2016). There is a strong correlation between the bulge-to-total ratio of $z = 0$ galaxies (x-axis) and the net AM loss suffered by the galaxy stars (i.e. the difference between the maximum and $z = 0$ $j_{\rm stars}$; y-axis). *Middle panel:* From Penoyre et al. (2017). Change in stellar spin parameter in galaxies (as defined in Emsellem et al. 2007) approximately $2-3$ Gyr after a merger, as a function of the gas fraction of the secondary galaxy which merged. Galaxies can become more rotation- ($\Delta(\lambda_{\rm R}) > 0$) or dispersion-dominated ($\Delta(\lambda_{\rm R}) < 0$), depending of the gas brought up by the secondary galaxy. *Right panel:* From Lagos et al. (2018a). Fractional change in $\lambda_{\rm R}$ as a function of the total gas-to-stellar mass ratio of the merging system, for minor (mass ratios between $0.1-0.3$) and major (mass ratios $\geqslant 0.3$) mergers. Gas-poor mergers are required to significantly spin galaxies down.

when integrating over a large enough baseline, one should find $j_{\rm stars}$ converging to $j_{\rm halo}$. Using EAGLE, Lagos et al. (2018b) confirmed that to be the case: gas-poor mergers do not significantly change the *total* j of the system, but significantly re-arrange it so that the inner parts of galaxies ($r/r_{50} < 5$) become highly deficient in j compared to galaxies of the same stellar mass that went through gas-rich mergers or not mergers at all. This was also seen by Teklu et al. (2015) as very deficient $j_{\rm stars}$ profiles in early-types compared to late-types at $r/R_{\rm vir} < 0.2$. An important prediction of that process is that the cumulative $j_{\rm stars}$ radial profiles of high j galaxies are much more self-similar than those of galaxies with low j. In other words: there are few ways in which a galaxy by $z = 0$ can end up with high j, but many pathways that lead to low j (e.g. Naab et al. 2014, Garrison-Kimmel et al. 2018).

4. Discussion and future prospects

The picture that has emerged from simulations in how galaxies gain their AM is significantly more complex than the classical picture of galaxy disks forming inside out observing j conservation (e.g. Mo, Mao & White 1998). This complexity, however, is driven by processes that act in different directions and that tend to compensate quite efficiently, so that galaxies follow the classical disk formation model to within 50% (Zavala et al. 2016; Lagos et al. 2017, 2018b).

This inevitably opens the following question: to what extent are we forcing $j_{\rm stars} \sim j_{\rm halo}$ in disk galaxies through the process of tuning free-parameters in simulations? State-of-the-art simulations tend to carefully tune their parameters to reproduce some broad statistics of galaxies, such as the stellar-halo mass relation, stellar mass function, and in some cases the size-mass relation (e.g. Crain et al. 2015). A consequence of such tuning may well result in this conspiracy: the CGM's j being largely in excess of the halo's j, but then losing significant amounts of it while falling onto the galaxy, so that by $z = 0$ disk galaxies have $j_{\rm stars} \sim j_{\rm halo}$. A possible solution for this conundrum is to perform detailed,

high-resolution simulations of individual disk galaxies in a cosmological context and test widely different feedback mechanisms with the aim of understanding which conditions lead to $j_{\rm stars} \sim j_{\rm halo}$ and how independent the tuning of parameters is of the evolution of specific AM.

Another important area of research will be the improvement of the description of the vertical structure of disks, as current large cosmological hydrodynamical simulations struggle to form thin disks $\epsilon \gtrsim 0.7 - 0.8$. This is most likely due to the ISM and cooling modelling and resolution in these simulations being insufficient. Currently, simulations tend to force the gas to not cool down below $\approx 10^4$ K, which corresponds to a Jeans length of ≈ 1 kpc, much larger than the scaleheights of disks in the local Universe. This issue could be solved by including the formation of the cold ISM, which necessarily means improving the resolution of the simulations significantly.

References

Burkert A., Förster Schreiber N. M., Genzel R. et al, 2016, ApJ, 826, 214
Catelan P., Theuns T., 1996, MNRAS, 282, 436
Choi H., Yi S. K., 2017, ApJ, 837, 68
Cortese L., Fogarty L. M. R., Bekki K. et al, 2016, ArXiv:1608.00291
Crain R. A., Schaye J., Bower R. G. et al, 2015, MNRAS, 450, 1937
Danovich M., Dekel A., Hahn O. et al, 2015, MNRAS, 449, 2087
DeFelippis D., Genel S., Bryan G. L. et al, 2017, ApJ, 841, 16
Dubois Y., Peirani S., Pichon C. et al, 2016, MNRAS, 463, 3948
El-Badry K., Quataert E., Wetzel A. et al, 2018, MNRAS, 473, 1930
Emsellem E., Cappellari M., Krajnović D. et al, 2007, MNRAS, 379, 401
Garrison-Kimmel S., Hopkins P. F., Wetzel A. et al, 2018, MNRAS
Genel S., Fall S. M., Hernquist L. et al, 2015, ApJ, 804, L40
Governato F., Brook C., Mayer L. et al, 2010, Nature, 463, 203
Guedes J., Callegari S., Madau P. et al, 2011, ApJ, 742, 76
Harrison C. M., Johnson H. L., Swinbank A. M. et al, 2017, MNRAS, 467, 1965
Kaufmann T., Mayer L., Wadsley J. et al, 2007, MNRAS, 375, 53
Lagos C. d. P., Schaye J., Bahé Y. et al, 2018a, MNRAS, 476, 4327
Lagos C. d. P., Stevens A. R. H., Bower R. G. et al, 2018b, MNRAS, 473, 4956
Lagos C. d. P., Theuns T., Stevens A. R. H. et al, 2017, MNRAS, 464, 3850
Mo H. J., Mao S., White S. D. M., 1998, MNRAS, 295, 319
Naab T., Oser L., Emsellem E. et al, 2014, MNRAS, 444, 3357
Navarro J. F., Steinmetz M., 2000, ApJ, 538, 477
Navarro J. F., White S. D. M., 1994, MNRAS, 267, 401
Pedrosa S. E., Tissera P. B., 2015, A&A, 584, A43
Peebles P. J. E., 1969, ApJ, 155, 393
Penoyre Z., Moster B. P., Sijacki D. et al, 2017, MNRAS, 468, 3883
Pillepich A., Springel V., Nelson D. et al, 2018, MNRAS, 473, 4077
Sales L. V., Navarro J. F., Theuns T. et al, 2012, MNRAS, 423, 1544
Schaye J., Crain R. A., Bower R. G. et al, 2015, MNRAS, 446, 521
Steinmetz M., Navarro J. F., 1999, ApJ, 513, 555
Stevens A. R. H., Lagos C. d. P., Contreras S. et al, 2016, ArXiv:1608.04389
Stewart K. R., Maller A. H., Oñorbe J. et al, 2017, ApJ, 843, 47
Swinbank A. M., Harrison C. M., Trayford J. et al, 2017, MNRAS
Teklu A. F., Remus R.-S., Dolag K. et al, 2015, ApJ, 812, 29
Vogelsberger M., Genel S., Springel V. et al, 2014, Nature, 509, 177
Wang L., Obreschkow D., Lagos C. D. P. et al, 2018, ArXiv:1808.05564
Welker C., Dubois Y., Devriendt J. et al, 2017, MNRAS, 465, 1241
Zavala J., Okamoto T., Frenk C. S., 2008, MNRAS, 387, 364

Galactic Angular Momentum
XXXth IAU General Assembly, August 2018
Teresa Lago & Danail Obreschkow, ed.

DOI: 10.5281/zenodo.1481534

Emerging Angular Momentum Physics from Kinematic Surveys

Matthew Colless[1]

[1]Research School of Astronomy and Astrophysics, Australian National University
Canberra, ACT 2611, Australia
email: matthew.colless@anu.edu.au

Abstract. I review the insights emerging from recent large kinematic surveys of galaxies at low redshift, with particular reference to the SAMI, CALIFA and MaNGA surveys. These new observations provide a more comprehensive picture of the angular momentum properties of galaxies over wide ranges in mass, morphology and environment in the present-day universe. I focus on the distribution of angular momentum within galaxies of various types and the relationship between mass, morphology and specific angular momentum. I discuss the implications of the new results for models of galaxy assembly.

Keywords. galaxies: kinematics and dynamics, galaxies: structure, galaxies: evolution galaxies: formation, galaxies: stellar content

1. Introduction

This brief review focusses on recent integral field spectroscopy surveys of the stellar kinematics in large samples of galaxies at low redshifts. It does not cover radio HI surveys of the neutral gas in low-redshift galaxies (which are important for understanding the kinematics at large radius) nor does it extend to surveys at high redshifts (which explore the origin and evolution of galaxy kinematics). What *local* surveys of stellar kinematics can tell us about angular momentum in galaxies is its dependence on mass, morphology and other properties (if sample selection is understood) and its dependence on environment (if the sample is embedded in a fairly complete redshift survey); such dependencies can provide *indirect* evidence for the origin and evolution of angular momentum.

It is immediately apparent that all current kinematic surveys have weaknesses relating to the trade-offs demanded by instrumental constraints: firstly, between spatial resolution and spatial coverage (also between spectral resolution and spectral coverage) and, secondly, between this per-galaxy information and sample size (also sample volume and completeness). The lack of radial coverage is a serious problem for late-type disk galaxies having exponential mass profiles (i.e. having Sersic index $n \approx 1$), for which $M/M_{\rm tot} = 0.5{,}0.8$ at $R/R_e \approx 1.0{,}1.8$ and $j/j_{\rm tot} = 0.5{,}0.8$ at $R/R_e \approx 1.0{,}2.2$. But it is a much worse problem for early-type spheroidal galaxies with deVaucouleurs profiles ($n \approx 4$), for which $M/M_{\rm tot} = 0.5{,}0.8$ at $R/R_e \approx 1.0{,}3.2$ and $j/j_{\rm tot} = 0.5{,}0.8$ at $R/R_e \approx 4.4{,}>9$ (see Figure 1a). This problem is compounded by the necessary instrumental trade-off between radial coverage (field of view) and spatial resolution (spaxel scale) of integral field units (IFUs) due to constraints imposed by the limited available detector area. For example, in the SAMI sample the median major axis is $R_e = 4.4$ arcsec (10-90% range spans 1.8-9.4 arcsec) which means that the SAMI IFUs only sample out to a median radius of $1.7R_e$ (see Figure 1b).

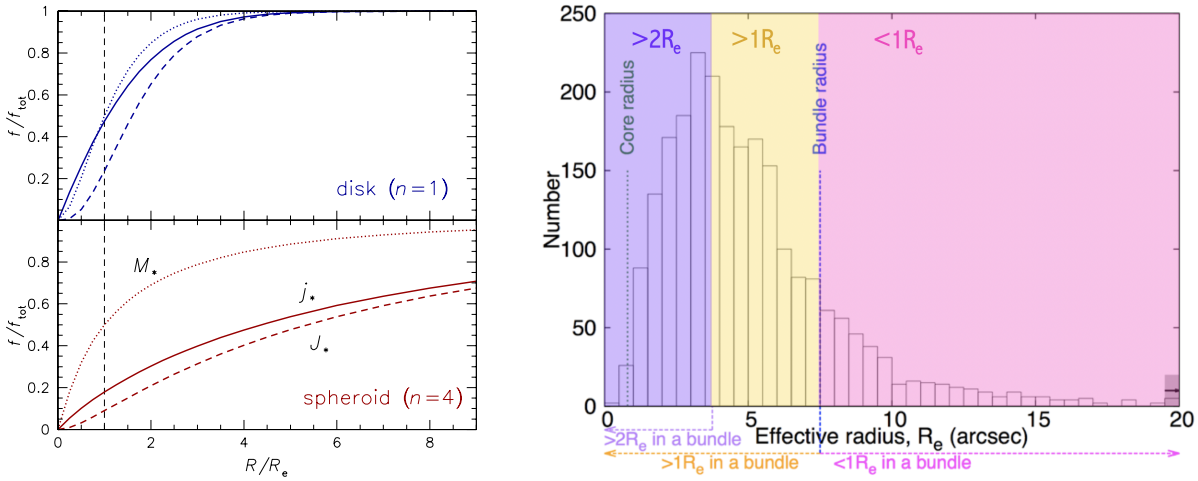

Figure 1. (a) Left panel: the fraction of mass (M), angular momentum (J), and specific angular momentum ($j = J/M$) as functions of radius (in units of the effective radius, R_e) for both an exponential disk profile (Sersic index $n = 1$; top panel) and a deVaucouleurs spheroid profile (Sersic index $n = 4$; bottom panel) [**?**, Fig.3]. (b) Right panel: the distribution of effective radius R_e (in arcsec) for the SAMI galaxy sample, showing those parts of the sample for which the integral field unit covers $<1R_e$, $>1R_e$ and $>2R_e$ [based on **?**, Fig.1].

2. Surveys

2.1. *SAMI*

SAMI is the Sydney-AAO Multi-IFU instrument on the 3.9m Anglo-Australian Telescope (AAT). It has 13 IFUs that can be positioned over a 1 degree field at the telescope's prime focus. Each hexabundle IFU has 61 × 1.6 arcsec fibres covering a 15 arcsec diameter field of view. SAMI feeds the AAOmega spectrograph, which gives spectra over 375–575nm at $R \approx 1800$ (70 km s^{-1}) and 630–740nm at $R \approx 4300$ (30 km s^{-1}). The SAMI Second Data Release (DR2) includes 1559 galaxies (about half the full sample) covering $0.004 < z < 0.113$ and $7.5 < \log(M_*/M_\odot) < 11.6$. The core data products for each galaxy are two primary spectral cubes (blue and red), three spatially binned spectral cubes, and a set of standardised aperture spectra. For each core data product there are a set of value-added data products, including aperture and resolved stellar kinematics, aperture emission line properties, and Lick indices and stellar population parameters. The data release is available online through AAO Data Central (`datacentral.org.au`).

2.2. *CALIFA*

CALIFA is the Calar Alto Legacy Integral Field survey, consisting of integral field spectroscopy for 667 galaxies obtained with PMAS/PPak on the Calar Alto 3.5m telescope. There are three different spectral setups: 375–750 nm at 0.6 nm FWHM resolution for 646 galaxies, 365–484 nm at 0.23 nm FWHM resolution for 484 galaxies, and a combination of these over 370–750 nm at 0.6 nm FWHM resolution for 446 galaxies. The CALIFA Main Sample spans $0.005 < z < 0.03$ and the colour-magnitude diagram, with a wide range of stellar masses, ionization conditions and morphological types; the CALIFA Extension Sample includes rare types of galaxies that are scarce or absent in the Main Sample.

2.3. *MaNGA*

MaNGA is the Mapping Nearby Galaxies at Apache Point Observatory survey (part of SDSS-IV). It is studying the internal kinematic structure and composition of gas and stars in 10,000 nearby galaxies. It employs 17 fibre-bundle IFUs varying in diameter from 12 arcsec (19 fibres) to 32 arcsec (127 fibers) that feed two dual-channel spectrographs

Specification	MaNGA	SAMI	CALIFA	Atlas3D
Sample Size	10,000	3,400	600	260
Selection	$M > 10^9 M_\odot$	$M > 10^{8.2} M_\odot$	$45" < D_{25} < 80"$	E/S0 $M > 10^{9.8} M_\odot$
Radial coverage	$1.5r_e$ (2/3), $2.5r_e$ (1/3)	$1\text{-}2r_e$	$>2.5r_e$	$<1r_e$
S/N at $1r_e$	15-30	10-30	~30	15
Wavelength range(Å)	3600-10300	3700-7350	3700-7500	4800-5380
Instrumental resolution	50-80 km/s	75/28 km/s	85/150 km/s	105 km/s
Input Spaxel Size	2.0″	1.6‴	2.7″	1″
Input Spaxels per object	**3x(19-127)**	3×61	3×331	1,431
Spatial FWHM	2″	2″	2.5″	1.5″
Telescope size	2.5m	**3.9m**	3.5m	4.2m

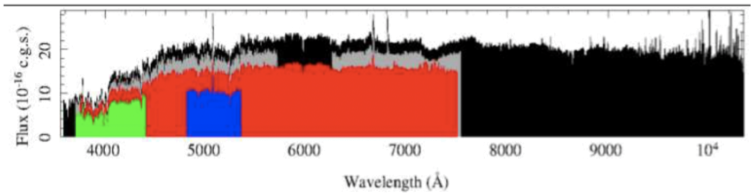

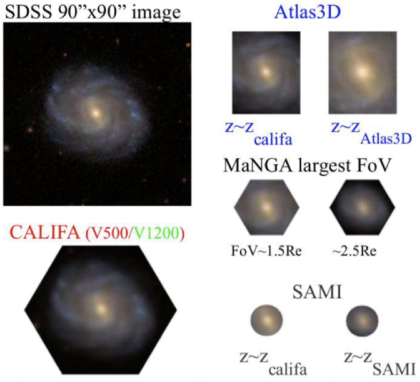

Figure 2. Upper left: table of key parameters of the MaNGA, SAMI, CALIFA and Atlas3D surveys. Lower left: the wavelength coverage of the MaNGA (black), SAMI (grey), CALIFA (red & green) and Atlas3D (blue) surveys. Right: illustration of the relative fields of view covered by the IFUs used in each survey. [Based on Sanchez *et al.* (2015), Table 1 & Figure 1.]

covering 360–1030 nm at $R \approx 2000$. The targets have $M_* > 10^9\ M_\odot$ based on SDSS-I redshifts and i-band luminosities. The MaNGA sample is designed to approximate uniform radial coverage in terms of R_e, a flat stellar mass distribution, and a wide range of environments. SDSS Data Release 14 (DR14) includes MaNGA data cubes for 2812 galaxies.

2.4. *Comparison*

Figure 2 provides a tabular and graphical summary of the parameters of these three surveys (and also the earlier Atlas3D survey), which helps to understand their various relative strengths and weaknesses, and consequently their complementarities. A few kinematic surveys of small samples offer greater radial coverage and higher velocity resolution: SLUGGS surveyed kinematics of 25 early-type galaxies to $\sim 3R_e$ from stars and to $\sim 10R_e$ using globular clusters (Bellstedt *et al.* 2018); PN.S surveyed the kinematics of 33 early-type galaxies to $\sim 10R_e$ using planetary nebulae (Pulsoni *et al.* 2018).

3. Results

3.1. *Role of angular momentum*

After mass, angular momentum is the most important driver of galaxy properties, with a key role in the formation of structure and morphology. For regular oblate rotators, angular momentum can be derived from dynamical models as well as direct estimates of projected angular momentum. Surveys can determine population variations in the total angular momentum and its distribution with radius, exploring dependencies on mass, morphology, ellipticity and other properties. These relations can provide insights on the assembly histories of galaxies for comparison with simulations.

3.2. *Angular momentum & spin profiles*

SAMI, CALIFA and MaNGA together now provide angular momentum profiles (or, alternatively, spin proxy, λ_R, as a function of R/R_e) for thousands of galaxies to $R/R_e \sim 1$ and for hundreds of galaxies to $R/R_e \sim 2$. These samples are large enough to be useful when split by mass, morphology or environment. Figure 3 shows spin profiles for galaxies from the CALIFA survey (Falcón-Barroso 2016) and the MaNGA survey (Greene *et al.* 2018); Foster *et al.* (2018) give similar results from the SAMI survey.

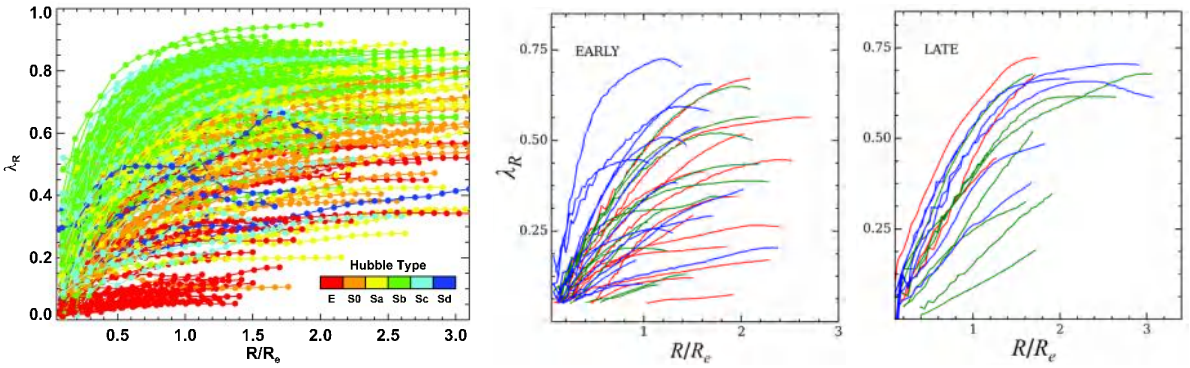

Figure 3. Left: Galaxy spin profiles from CALIFA, showing the variation with Hubble type [Falcón-Barroso (2016), Fig.2]. Right: Galaxy spin profiles from MaNGA, showing the variation with mass for early and late-type galaxies [Greene *et al.* (2018), Fig.3].

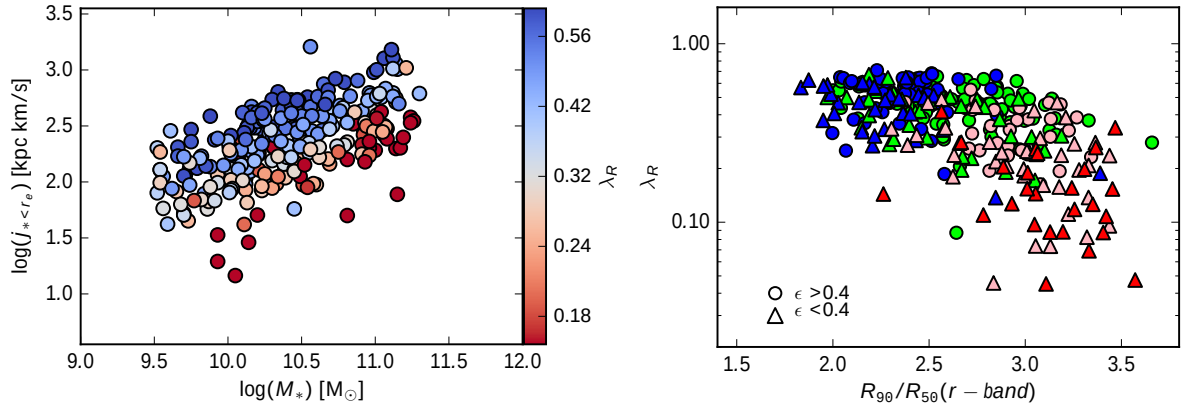

Figure 4. Left: Specific angular momentum versus stellar mass for SAMI galaxies, colour-coded by spin parameter λ_R. Right: Galaxy spin parameter versus r-band concentration for SAMI galaxies, colour-coded by morphology. [Based on Cortese *et al.* (2016), Figs 6 & 7].

3.3. *Spin, morphology & ellipticity*

Typical galaxies lie on a plane relating mass M, j and stellar distribution (quantified by, e.g., Sersic index n or photometric concentration index), with overall morphologies regulated by their mass and dynamical state (see, e.g., Cortese *et al.* 2016). The correlation shown in the left panel of Figure 4 between the offset from the mass–angular momentum (M-j) relation and spin parameter λ_R shows that at fixed M the contribution of ordered motions to dynamical support varies by more than a factor of three. The right panel of Figure 4 shows that λ_R correlates strongly with morphology and concentration index (especially if slow-rotators are removed), suggesting that late-type galaxies and early-type fast-rotators form a continuous class in terms of their kinematic properties.

The spin–ellipticity (λ_R–ϵ) diagram is a particularly revealing frame for understanding relations between kinematic and morphological properties of galaxies. This is illustrated in Figure 5, from the work of Graham *et al.* (2018) using the MaNGA survey. The left panel shows the strong correlation between the mass of a galaxy and its position in this diagram, with more massive galaxies tending to have lower spin and ellipticity. The central panel shows the areas of the diagram occupied by various morphological types: elliptical galaxies occupy the low-λ_R, low-ϵ region, while lenticular and spiral galaxies largely overlap, covering the full range of ϵ at $\lambda_R > 0.5$. The right panel shows how galaxies belonging to different kinematic classes are distributed: spirals generally lie in the region consistent with rotationally-dominated kinematics, while regular (fast-rotating) early-

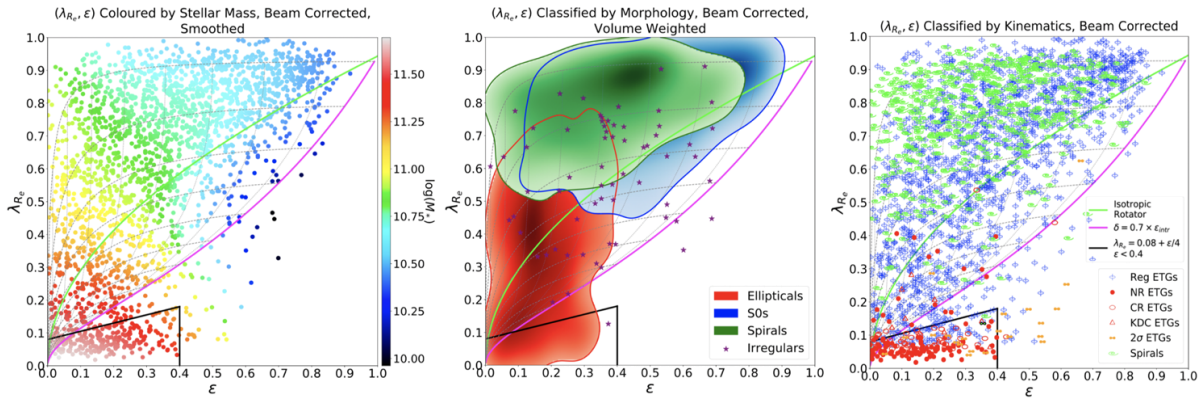

Figure 5. Distributions of galaxy properties in the spin–ellipticity (λ_R–ϵ) diagram: left—stellar mass; centre—visual morphology; right—kinematic class. [Graham *et al.* (2018), Figs 5, 8 & 9.]

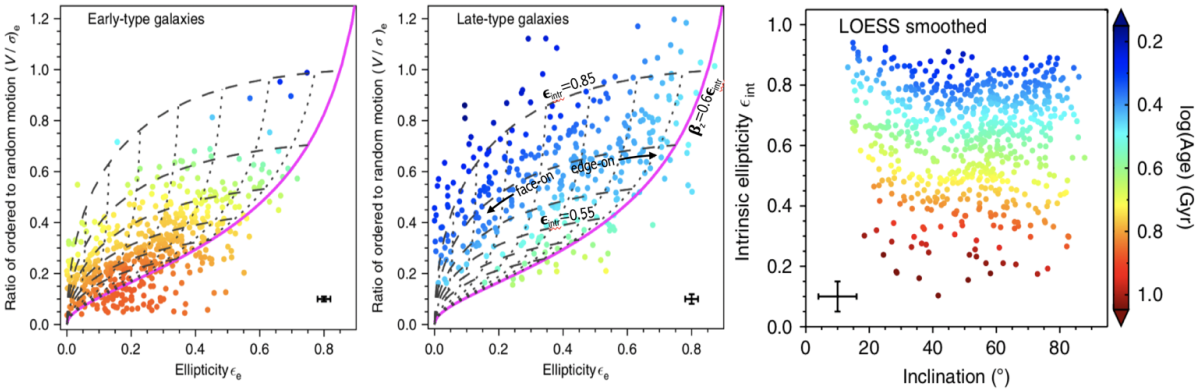

Figure 6. Left/middle panels: The ratio of ordered to random motions (V/σ) versus the apparent ellipticity for early/late-type galaxies. Right panel: assuming galaxies are oblate rotators, the derifed distribution of intrinsic ellipticity as a function of apparent inclination. [van de Sande *et al.* (2018), Figs 3 & 4.]

type galaxies occupy a wider range of λ_R at given ϵ, with lower λ_R corresponding to systems with more pressure-support; slowly-rotating ('non-rotating') early-type galaxies mainly occupy the region with $\lambda_R < 0.15$ and $0 < \epsilon < 0.4$.

There is also an strong correlation between a galaxy's spin parameter and its intrinsic ellipticity, as demonstrated using the SAMI survey by van de Sande *et al.* (2018). Figure 6 shows the distribution of the ratio of rotation velocity to velocity dispersion (V/σ) with apparent ellipticity (ϵ) for early-type and late-type galaxies, together with the inferred distribution of intrinsic ellipticity ($\epsilon_{\rm int}$). This is derived using the theoretical model predictions for rotating, oblate, axisymmetric spheroids with varying intrinsic shape and anisotropy shown by the dashed and dotted lines in the left two panels. The galaxies are colour-coded by the luminosity-weighted age of their stellar populations, and the righthand panel shows the clear trend of age with intrinsic ellipticity. As van de Sande *et al.* (2018) discuss in detail, this newly discovered relation extends beyond the general notion that disks are young and bulges are old.

3.4. *The mass–angular momentum relation*

The mass–angular momentum (M-j) relation is discussed in detail elsewhere in these proceedings. However, it is worth noting the opportunties for studying this key relation that follow from large surveys providing kinematics for many galaxies. Some prelminary results from the SAMI survey are shown in Figure 7 (D'Eugenio *et al.*, in prep.), using hundreds of galaxies with masses and angular momenta derived from self-consistent dy-

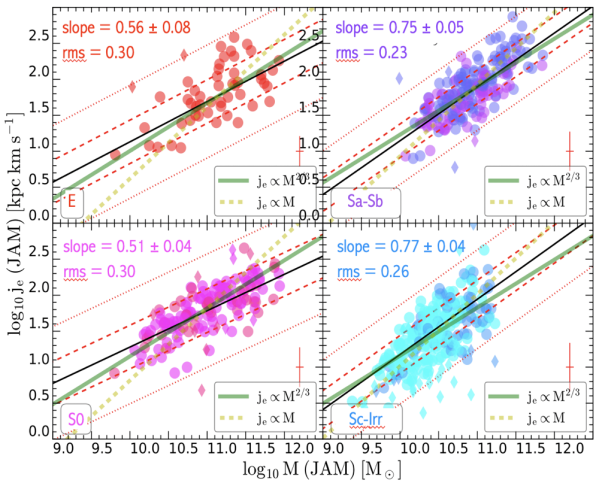

Figure 7. The relation between mass and specific angular momentum, both derived from Jeans anisotropic mass (JAM) models fitted to the SAMI kinematic data, for elliptical (E), lenticular (S0), early-spiral (Sa-Sb) and late-spiral/irregular (Sc-Irr) galaxies. [D'Eugenio *et al.*, in prep.]

namical models—in this case, Jeans anisotropic mass (JAM) models. This permits the study of the M-j relation for subsets of the population, such as different morphological types. While the results shown here are too preliminary to allow conclusions to be drawn, the opportunities are clear.

4. Summary

This is a golden age for studying galaxy angular momentum. Large kinematic surveys using integral field spectrographs are vastly increasing the amount and richness of the available information Sample sizes are now beginning to allow studies of the dependence on multiple simultaneous influences (mass/morphology/environment...) The main limitations remain instrumental trade-offs between spatial resolution and radial coverage, and challenges in spatial resolution and surface brightness at higher redshift.

References

Bellstedt, S., Forbes, D.A., Romanowsky, A. J., *et al.*, 2018, *MNRAS*, 476, 4543 [DOI: 10.1093/mnras/sty456]

Cortese, L., Fogarty, L.M.R., Bekki, K., *et al.*, 2016, *MNRAS*, 463, 170 [DOI: 10.1093/mnras/stw1891]

Falcón-Barroso, J., 2016, *Astronomical Surveys and Big Data*, ASP Conf. Series, 505, 133 [ADS: 2016ASPC..505..133F]

Foster, C., van de Sande, J., Cortese, L., *et al.*, 2018, *MNRAS*, 480, 3105 [DOI: 10.1093/mnras/sty2059]

Graham, M.T., Cappellari, M., Li, H., *et al.*, 2018, *MNRAS*, 477, 4711 [DOI: 10.1093/mnras/sty504]

Greene, J.E., Leauthaud, A., Emsellem, E., *et al.*, 2018, *ApJ*, 852, 36 [DOI: 10.3847/1538-4357/aa9bde]

Pulsoni, C., Gerhard, O., Arnaboldi, *et al.*, 2018, *A&A*, 618, 94 [DOI: 10.1051/0004-6361/201732473]

Sánchez, Sebastián F., & The CALIFA Collaboration, 2015, *Galaxies in 3D across the Universe*, IAU Symposium 309, pp85-92 [DOI: 10.1017/S1743921314009375]

van de Sande, J., Scott, N., Bland-Hawthorn, J., *et al.*, 2018, *Nature Astronomy*, 2, 483 [DOI: 10.1038/s41550-018-0436-x]

Galactic Angular Momentum, Volume 1
XXXth IAU General Assembly, August 2018
Teresa Lago, Patricia Tissera & Danail Obreschkow, ed.

DOI: 10.5281/zenodo.1481538

The Fundamental Physics of Angular Momentum Evolution in a ΛCDM Scenario

Susana Pedrosa[1 2]

[1]Institute for Astronomy and Space Science, CONICET - UBA,
Ciudad Universitaria, Buenos Aires, Argentina
email: supe@iafe.uba.ar

[2]Dept. de Física Teórica, Univ. Autónoma de Madrid
Cantoblanco, Madrid, Espana

Abstract.
Galaxy formation is a very complex process in which many different physical mechanisms intervene. Within the LCDM paradigm processes such as gas inflows and outflows, mergers and interactions contribute to the redistribution of the angular momentum content of the structures. Recent observational results have brought new insights and also triggered several theoretical studies. Some of these new contributions will be analysed here.

Keywords. galaxies: formation, galaxies: evolution

1. Introduction

Angular momentum exchange is ubiquitous in the structure assembly process. Every galaxy formation scenario assumes the exchange of angular momentum. Encrypted inside the today galactic morphology is stored the assembly history not only of the galaxy itself but also of the different regions of the DM halo. Estimations of the angular momentum content of the dark matter haloes require a connection between it and the galactic one.

In a hierarchical clustering universe the angular momentum budget of galaxies originates in primordial torques that act upon baryons and the dark matter. Fall (1983) proposed, in a seminal paper, the fundamental correlation between the angular moment (AM) content of the galactic components and the stellar mass of the galaxy. He found that both components follow a power law correlation with the stellar mass, with an exponent of ~ 0.6. The spheroidal component, although following a parallel sequence, presents an offset a factor of about 5 lower due to the lost of AM during the galaxy assembly. Theoretical models of galaxy formation (Fall & Efstathiou 1980, Mo et al. 1998) predict a linear correlation between the dark matter specific angular momentum and $M_{virial}^{2/3}$.

Within the hierarchical scenario galaxies are shaped and reshaped by several processes. For instance, supernova feedback that redistributes energy and mass through mass loaded winds is the key ingredient in the galaxy formation recipe that allows theoretical models to overcome the angular momentum catastrophe. With its inclusion more realistic galaxies could be obtained in cosmological simulations. Other processes that may ultimately determine the resulting galactic morphology are mergers, interactions and disc instabilities. For instance, mergers, in all their types, are the most accepted mechanism responsible for the formation of spheroidal galaxies.

2. Observational studies

In 2012 and 2013, Fall & Romanowsky (2013) (FR13) and Romanowsky & Fall (2012)) (FR12), revisited Fall (1983) using an improved and extended observational sample. They confirmed previous findings: all morphological types of galaxies lie along a parallel sequence with exponent $\alpha \sim 0.6$ in the stellar j - M plane. They proposed then that the j - M diagram constitutes a more physically motivated description of the galactic morphology than the typical disk to bulge classification.

Obreschkow & Glazebrook (2014), using high precision measurements of the stellar and baryonic specific AM of a THINGS sample of 16 spiral galaxies (Leroy et al. 2008), includes the β parameter (bulge fraction) in the AM description. They found a strong correlation for the plane fitting the 3D space of β, logM and log j. For a fixed β, the projection results in an exponent $\alpha \sim 1$, larger than the one found by Romanowsky & Fall (2012). They proposed that the contributions to the j-M plane of bulge and disks components were not independent.

After the FR12 and FR13 works, it followed a most interesting burst of numerical studies analysing to what extent their models fitted these observational constrains. Interestingly, despite the fact that this numerical experiments were perform with different numerical codes, different prescriptions for the subgrid physics, different resolutions, different feedback implementations, they all results in very good agreement with the new observational data. And through this process, many interesting contributions to the knowledge about the origin and evolution of the galactic AM during the assembly of the galaxy were developed. Numerical simulations constitute ideal tools for filling the gap between the observed and the inferred knowledge.

3. Numerical analysis

Genel et al. (2015) analysed the AM distribution of galaxies from the Illustris Simulation (Vogelsberger et al. 2014, Genel et al. 2014). They discriminate the $z = 0$ population based on their specific star formation rate, the flatness and the concentration, obtaining

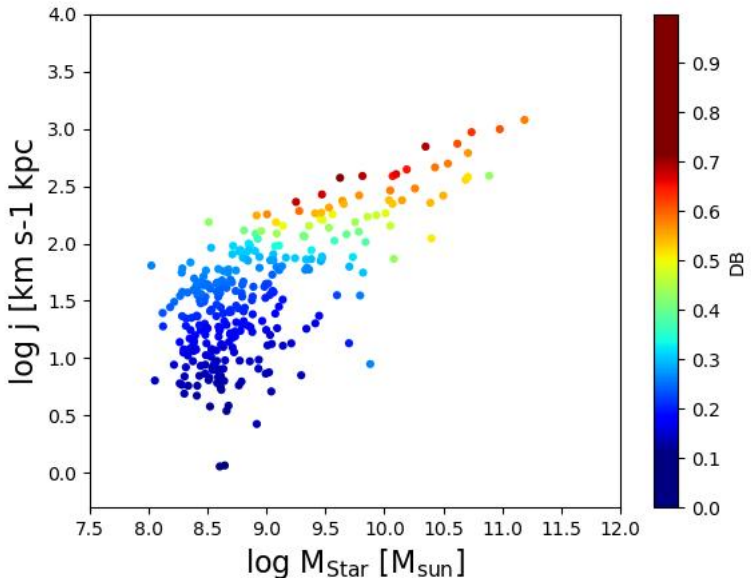

Figure 1. Relation between j and the total stellar mass for simulated galaxies with different disc-to-bulge ratios

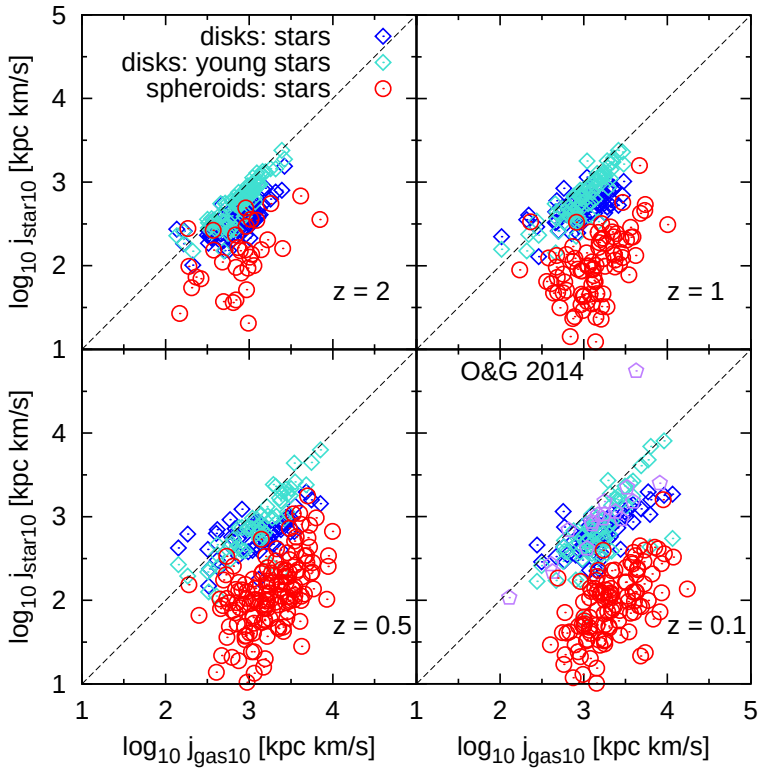

Figure 2. [Reprint from Teklu et al. (2015)] Specific angular momentum of the gas against the specific angular momentum of stars, both within 10% of the virial radius for galaxies that are classified as disks (blue diamonds) at four redshifts. For young stars only (turquoise diamonds). At z = 0.1 comparison with data from Obreschkow & Glazebrook (2014) (purple pentagons).

two parallel relations corresponding to early-and-late-type galaxies, in agreement with FR12 observations. They find that galactic winds with high mass-loading factors are crucial for getting the late-type galaxies relation that results from full conservation of the specific AM generated by cosmological tidal torques.

Using intermediate resolution cosmological simulations, Pedrosa & Tissera (2015) found the specific angular momentum of spheroidal and disk component to determine relations with the same slopes, regardless of the virial mass of their host galaxy. They found no evolution of this relation with redshift, indicating that spheroidal and disk component conserve similar relative amount of AM as they evolve, independently of virial masses. As shown in Fig.1, there is a clear correlation between the morphological type of the galaxy and its total specific AM content: higher D/T ratios are related with higher contents of specific AM. The AM of stellar bulges is consistent with elliptical galaxies indicating that bulges might be considered as mini-ellipticals, in agreement with FR12.

Teklu et al. (2015), using galaxies from the Magneticum Pathfinder Project (Dolag et al. 2015, in preparation), find that disk galaxies populate haloes with larger spin than those that host spheroidal galaxies. And disk galaxies live preferentially in haloes with central AM aligned with the AM of the whole halo. They also verify that their galaxies are located on the j-M plane in agreement with observations. Their stellar disk AM is lower than the cold gas one, in agreement with Pedrosa et al. (2015) and Obreschkow & Glazebrook (2014). They attribute this excess to the recent accretion of gas with high AM from the outer parts of the halo. This is shown in the fact that young stars (formed from this freshly accreted gas) present higher content of AM than older ones, Fig. 2.

Zavala et al. (2016), using a sample of over 2000 central galaxies extracted from the

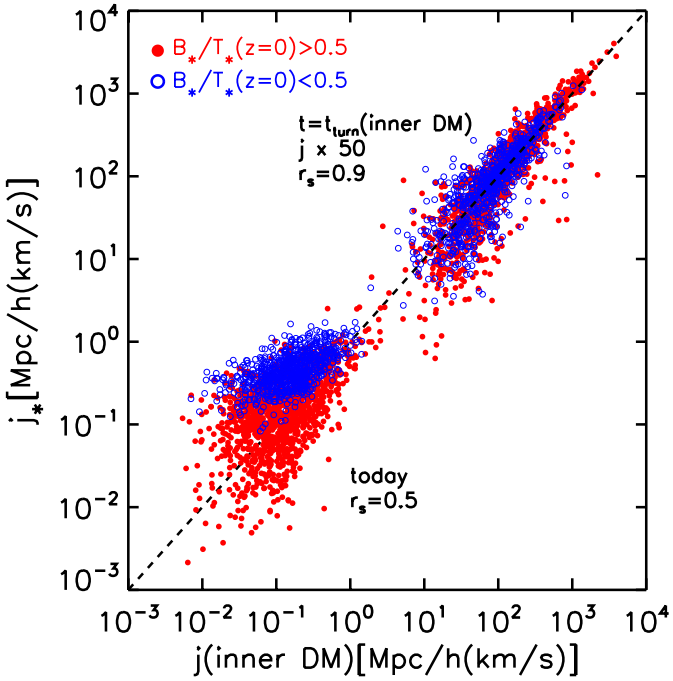

Figure 3. [Reprint from Zavala et al. (2016)] Correlation between the stellar specific angular momentum and that of the inner dark matter halo at $z = 0$ and at the time of turnaround of the inner dark matter halo (for the latter epoch, j is multiplied by 50). The sample of galaxies is divided into present-day bulge-dominated (solid red), and disc-dominated (open blue).

EAGLE simulation (Schaye et al. 2015, Crain et al. 2015) follow through time selected particles at z = 0 using a Lagrangian method. They find a correlation between the specific AM of $z = 0$ stars and that of the inner part of the DM halo. They find this link to be specially strong for stars formed before the turnaround. Spheroids, typically assembled at this epochs will then suffer loss of AM due to the merging activity of the inner halo assembly process. The cold gas, that mostly preserves the high specific AM acquired from the primordial tidal torques, forms stars after the turnaround and then build the stellar disk component. They find that the inner DM halo loses 90% of its specific AM after turnaround through transfer to dark matter clumps. While bulge dominated objects tracks the inner halo, the disk dominated ones follow the whole DM halo closely, Fig. 3. They claim that most of the stars belonging to the today ellipticals were already formed at turnaround and then got locked inside the DM clumps that will form the inner halo.

Also using a Lagrangian method, Obreja et al (2018) trace back in time structure progenitors of 25 zoom-ins simulations from the NIHAO Project (Wang et al. 2015), in order to dissect the AM budget evolution of the eight morphological components they identify (see also Dominguez Tenreiro et al (2015) . They find that thin disks typically retain 70% of its AM while thick disks only a 40%. They also find that 90% of their velocity dispersion dominated objects in the sample retain less than 10% of the central AM. Regarding the rotation dominated structures, most of the thin disks has a retention factor greater than 50% while thick disks might loose as much as 85% of its AM.

Most recently,Fall & Romanowsky (2018) presented new observational evidence that reinforce their previous assumptions. They propose a simple model, valid for all morphological type, in which the stellar AM is the linear superposition of independent contributions from disks and bulges. They obey a power scaling relation with essentially the same coefficient but differs in their normalisation. They consider that the parallel sequences in

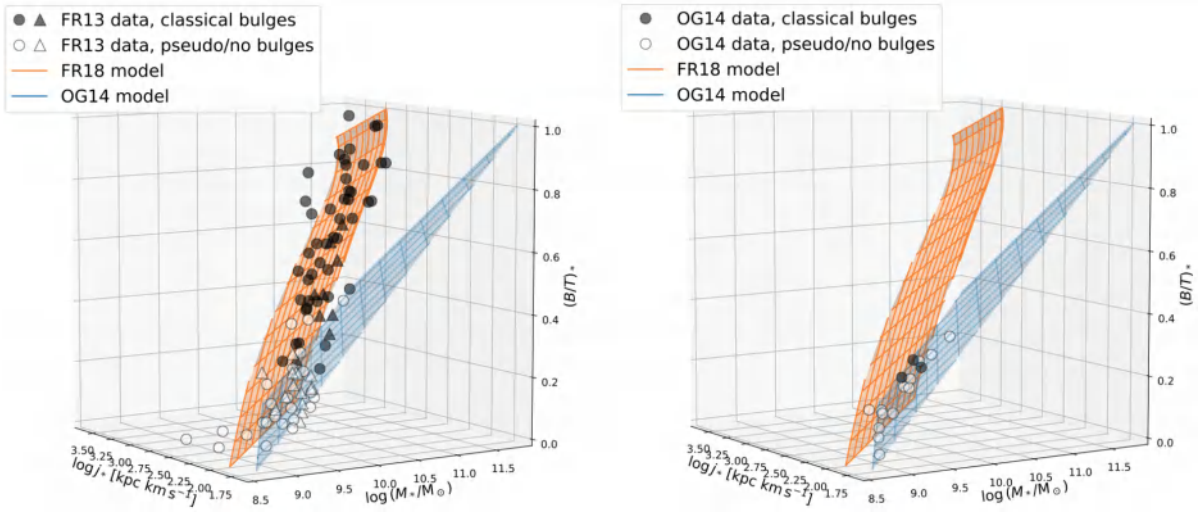

Figure 4. [Reprint from Fall & Romanowsky (2018), arXiv:1808.02525] Stellar bulge fraction beta against stellar specific angular momentum j and stellar mass M from Fall & Romanowsky (2018) (left panel) and from Obreschkow & Glazebrook (2014) (right panel). Filled symbols: galaxies with classical bulges, open symbols:pseudo bulges or no bulges. Orange surface:relation for independent disks and bulges derived in Fall & Romanowsky (2018), while the blue plane: linear regression derived by Obreschkow & Glazebrook (2014).

the j - M plane corresponding to different values of β (bulge fraction) means that disks and spheroids are formed via independent processes. Spheroidal galaxies never acquired enough AM or else they loose it in violent events, while disk-dominated systems are the result of a more quiescent processes that were not affected by mergers. One of the main feature of the new dataset studied in F&R18 is that both, photometric and kinematic data, extend to large radii, taking into account tha fact that much of the AM lies beyond the effective radius. This issue was already pointed out by Lagos et al. (2018). Using simulated galaxies from EAGLE, they find that elliptical galaxies with the higher Sersic index have most of their stellar AM budget inhabiting beyond five half mass radius. Fall & Romanowski (2018) claim that the β - j - M 3D diagram is well fitted by a plane modeled as a linear superposition of independent contribution from disks and bulges, Fig. 4.

4. Conclusions

In the last few year substantial progress has been made in our understanding of the physical processes involved in the evolution of the galactic angular momentum throughout the assembly process of the galaxy. A bigger picture has been build that allows us to grasp the morphological classification of galaxies in terms of their positions in the angular momentum - Mass plane and the processes that determine how this position will evolve. But still important questions remains to be solved. For instance, why both, disk dominated and spheroidal galaxies, follow parallel relations independently of the mass. Higher resolution simulation and improved methods for mimic observations would probably bring some answers and, of course, new questions.

References

Crain, R. et al. 2015, *MNRAS*, 450, 1937
Dominguez Tenreiro, R. et al. 2015, *ApJL*, 800, 30
Fall, S. M. in IAU Symp. 100, Internal Kinematics and Dynamics of Galaxies, ed. E. Athanassoula 1983, *IAU*, 391,
Fall, S. M., & Efstathiou, G. 1980, *MNRAS*, 193, 189
Fall, S. M., & Romanowsky, A. J. 2013, *ApJL*, 769, L26
Genel, S., Vogelsberger, M., Springel, V., et al. 2014, *MNRAS*, 445, 175
Genel, S., Fall, S. M., Hernquist, L., et al. 2015, *ApJL*, 804, L40
Lagos, C. del P., Stevens, A. R. H., Bower, R. G., et al. 2018, *MNRAS*, 473, 4956
Leroy, A. K., Walter, F., Brinks, E., et al. 2008, *AJ*, 136, 2782
Mo, H. J., Mao, S., & White, S. D. M. 1998, *MNRAS*, 295, 319
Obreja, A., Dutton, A. A., Maccio, A. V., et al. submitted arXiv:1804.06635 2018, *MNRAS*,
Obreschkow, D., & Glazebrook, K. 2014, *ApJ*, 784, 26
Romanowsky, A. J., & Fall, S. M. 2012, *ApJS*, 203, 17
Schaye J., et al. 2015, *MNRAS*, 446, 521
Teklu, A. F., Remus, R.S., Dolag, K., et al. 2015, *ApJ*, 812, 29
Vogelsberger, M., Genel, S., Springel, V., et al. 2014, *Nature*, 509, 177
Wang L., Dutton A. A., Stinson G. S., Maccio A. V., et al. 2015, *MNRAS*, 454, 83
Zavala, J., Frenk, C. S., Bower, R., et al. 2016, *MNRAS*, 460, 4466

Astronomy in Focus, Volume 1
XXXth IAU General Assembly, August 2018
Teresa Lago & Danail Obreschkow, ed.

DOI: 10.5281/zenodo.1481543

Angular Momentum Accretion onto Disc Galaxies

Filippo Fraternali[1] and Gabriele Pezzulli[2]

[1]Kapteyn Astronomical Institute, University of Groningen,
P.O. Box 800, 9700AV Groningen, The Netherlands,
email: fraternali@astro.rug.nl

[2]Department of Physics, ETH Zurich,
Wolfgang-Pauli-Strasse 27, 8093 Zurich, Switzerland
email: gabriele.pezzulli@phys.ethz.ch

Abstract. Throughout the Hubble time, gas makes its way from the intergalactic medium into galaxies fuelling their star formation and promoting their growth. One of the key properties of the accreting gas is its angular momentum, which has profound implications for the evolution of, in particular, disc galaxies. Here, we discuss how to infer the angular momentum of the accreting gas using observations of present-day galaxy discs. We first summarize evidence for *ongoing* inside-out growth of star forming discs. We then focus on the chemistry of the discs and show how the observed metallicity gradients can be explained if gas accretes onto a disc rotating with a velocity $20-30\%$ lower than the local circular speed. We also show that these gradients are incompatible with accretion occurring at the edge of the discs and flowing radially inward. Finally, we investigate gas accretion from a hot corona with a cosmological angular momentum distribution and describe how simple models of rotating coronae guarantee the inside-out growth of disc galaxies.

Keywords. Angular momentum, gas accretion, hot halo, metallicity gradient, corona

1. Introduction

At variance with massive quiescent ellipticals, which assembled most of their mass a long time ago and experienced, at some points in the past, an abrupt decline of their star formation rate, the majority of presently star forming galaxies have been undergoing, for most of the cosmic time, a rather constant or gently declining star formation history (e.g. Pacifici et al. 2016). This could in principle be explained either by a gradual consumption of a very large initial amount of cold gas, or by continuous accretion of new gas from the intergalactic medium. Both theory and observations strongly argue in favour of the second option, as i) gradual accretion is expected from the cosmological theory of structure formation (e.g. van den Bosch et al. 2014); ii) star forming galaxies have relatively short depletions times (Saintonge et al. 2011) and iii) preventing a huge initial reservoir of gas from very rapid exhaustion requires an implausibly low star formation efficiency, in stark contrast with observations (Kennicutt & Evans 2012; Fraternali & Tomassetti 2012).

Observing gas accretion into galaxies directly has proven challenging (Sancisi et al. 2008; Rubin et al. 2012). In a galaxy like the present-day Milky Way gas accretion does not seem to take place in the form of cold gas clouds at high column densities, like the classical high-velocity clouds (Wakker & van Woerden 1997) as their estimated accretion rate is too low (Putman et al. 2012) and their origin may be, at least partially, from a galactic fountain rather than a genuine accretion (Fraternali et al. 2015, Fox et al. 2016). Lower column densities have been probed in absorption but the accretion rates are more uncertain (Lehner & Howk 2011; Tumlinson et al. 2017). A possibility is that

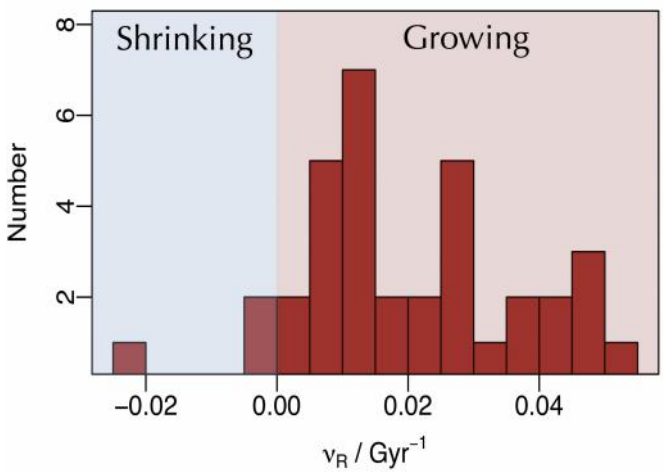

Figure 1. Distribution of the observed specific radial growth rates (ν_R) of a sample of nearby galaxies (Pezzulli et al. 2015). Note how the vast majority are growing inside out still at $z = 0$.

gas accretion takes place from the cooling of the hot gas, the galactic coronae that surround the Milky Way and similar galaxies (Miller & Bregman 2015). The cooling can be stimulated by the mixing with the disc gas through fountain condensation (Armillotta et al. 2016; Fraternali 2017). Alternatively, it may come from cold cosmological filaments directly reaching the discs (e.g. Kereš et al. 2009). To distinguish between these scenarios it is crucial to estimate the properties of the accreting gas.

A powerful tool to investigate the properties of the accreting gas is to infer them indirectly (backward approach) from observations of galaxy discs today. A simple example of this backward approach consists in the estimate of the accretion rates from the star formation histories (e.g. Fraternali & Tomassetti 2012). More elaborate estimates allow us to derive the angular momentum of the gas, the location where the accretion should take place and the properties of the medium from which the accretion originates. These topics are the focus of this proceeding.

2. Accretion of angular momentum on star forming galaxies

A very important observational fact about the evolution of currently star forming spiral galaxies, is that they have been increasing in size while increasing in mass (*inside-out growth*, e.g. Larson 1976; Dale et al. 2016). This is most likely due to the fact that the gas that has been accreted most recently is more rich in angular momentum with the respect to the one which was accreted at earlier epochs, a very well established prediction of the cosmological theory of tidal torques (Peebles 1969).

Crucially, observations indicate the radial growth – and therefore angular momentum accretion – is also a gentle process, which has been proceeding at a regular rate throughout galaxy evolution and is still ongoing today, as shown by studies of spatially resolved stellar populations (e.g. Williams et al. 2009; Gogarten et al. 2010) or recent star formation (e.g. Muñoz-Mateos at al. 2007). Pezzulli et al. (2015) have proposed a quantitative analysis of the phenomenon. They have shown that, *relative to* the well known exponential profile of the stellar mass surface density of spiral galaxies, the radial profile of the current *star formation rate surface density* shows a mild depletion in the inner regions and a slight enhancement in the outer ones, which agree both qualitatively and quantitatively with ongoing radial growth of stellar discs at a low but measurable rate. Figure 1 shows the distribution of the measured specific radial growth rate $\nu_R \equiv \dot{R}_\star / R_\star$ of the stellar scale-length $R_\star$ of the sample of nearby spiral galaxies from that study. The vast

majority of objects are currently growing, at a rate about equal to one third of their *specific star formation rate* (sSFR, or $\nu_M \equiv \dot{M}_\star/M_\star \simeq 0.1$ Gyr^{-1} at $z = 0$, e.g. Speagle et al. 2014). Furthermore, the results were shown to agree quantitatively with expectations for gradual angular momentum assembly of galaxies evolving *along* the specific angular momentum versus stellar mass (Fall) relation (Fall & Romanowsky 2013).

3. Disentangling models of accretion

We have seen that most spiral galaxies must have been (and probably are) gradually accreting angular momentum rich gas from the surrounding medium. The compelling question arises of what is the exact physical mechanism by which this happens. Two competing scenarios exist: *cold mode* accretion and *hot mode* accretion (e.g. Birnboim & Dekel 2003; Binney 2004) and different modes can dominate at different masses and redshift. In the former case, cold and angular momentum rich gas from intergalactic filaments joins the disc at large radii and then somehow drifts inwards to sustain star formation with the observed radial profile throughout the disc. We can call this *purely radial* accretion. In the second scenario, instead, the gas accreting onto the halo does not join the main body of the galaxy *directly*, but it is rather stored (together with its angular momentum) into a hot CGM (*corona*) and then only gradually condenses on to the disc as a gentle 'rain', which may be modelled, at least at first order, as mostly vertical accretion (perpendicular to the galaxy disc).

With appropriate choices of the parameters, both scenarios can give rise to the same *structural* evolution of the disc, as constrained by observations of the star and gas content of galaxies as a function of galactocentric radius and time (Pezzulli & Fraternali 2016a). The two models however differ enormously (and can thus be distinguished) in terms of *chemical* evolution. This is because vertical accretion of relatively metal-poor gas has a *metal-dilution* effect, which goes in the direction of counter-acting metal enrichment by local star formation, whereas radial accretion implies that, before arriving at the position where it is finally locked in to stars, each gas element will have already traversed other regions of the galaxy, where it will have been chemically enriched by the stars being formed there. We emphasize that i) this observational test is better performed on *gas-phase* abundances of α elements (as this choice minimizes uncertainties due to stellar radial migration and time delays in chemical enrichment) and ii) this kind of comparison between models is only meaningful *at fixed structural evolution*, as, otherwise, differences in other leading order effects (gas fraction, star formation efficiency and so on) dominate over those due to different geometry of accretion. With these specifications clarified, the discriminating power of the method is remarkable. This is illustrated in Figure 2, where the predictions are shown, for the abundance gradient of α-elements in the ISM of the Milky Way, for models with purely vertical, purely radial and mixed accretion. Details can be found in e.g. Pitts & Tayler (1989), Schönrich & Binney (2009) and Pezzulli & Fraternali (2016a). The latter work proposes an analytic and general approach to the problem, which can be readily applied to any galaxy or structural evolution model.

The clear result is that a combination of vertical and radial accretion is required to match the observed gradient (e.g. Genovali et al. 2015, marked here as a dashed line). This is actually not surprising, when angular momentum conservation is taken into account. A purely radial accretion, in fact, requires the angular momentum of the accreting gas to be transferred to some other not very well identified phase. On the other hand, purely vertical accretion is only possible if the material is accreted, at any radius, with exactly the angular momentum needed for local centrifugal balance, as any discrepancy would force the condensed gas to move radially within the disc after accretion (see also Mayor &

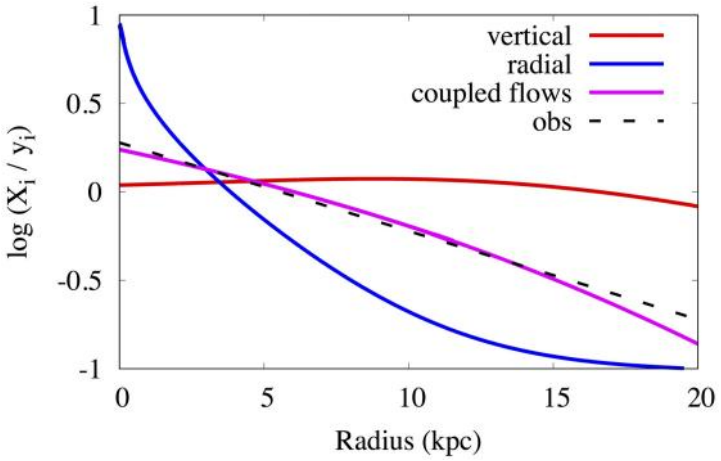

Figure 2. Abundance profiles of gas phase α-elements, as a function of the galactocentric radius, for the Milky Way at $z = 0$ predicted by disc evolution models in which the gas accretes purely vertically, purely radially or through mixed (coupled) flows. The observed profile is shown by the dashed curve. The models are calculated as described in Pezzulli & Fraternali (2016b).

Vigroux 1981; Bilitewski & Schönrich 2012). We now discuss whether a coherent physical picture can naturally give account of the findings discussed so far.

4. A consistent picture

The model which better reproduces the chemical evolution of the Milky Way (§3) requires gas accretion occurring with a specific angular momentum that is $75 \pm 5\%$ of that of the disc at each radius. This is very naturally expected for a hot mode accretion scenario (i.e. from the hot corona). Virtually every hydrodynamically consistent model of the hot CGM requires in fact the hot gas to be *not* in local centrifugal equilibrium, as the high temperatures will generally imply a significant contribution of pressure support (in addition to rotation) against gravity. Note that the same model also predicts the presence of moderate radial flows (a few $\mathrm{km\,s^{-1}}$ or less) within the disc: crucially, however, this radial flow is not due to equatorial accretion of cold flows, but it is rather the natural consequence of the rotation lag of the accreting (hot) gas and angular momentum conservation.

Two main questions arise to further test whether the model is viable in a cosmological context. First, if the disc accretes material with a local deficit of angular momentum, can the accretion still *globally* provide enough angular momentum, as required to sustain the global radial growth of the disc (§2)? Second, is the implied rotation of the corona consistent with cosmological expectation from tidal torque theory?

The answer to these questions requires building self-consistent models of the hydrodynamical equilibrium of a hot rotating corona in a galaxy scale gravitational potential and with a given angular momentum distribution. Pezzulli, Fraternali & Binney (2017) described the solution to this problem and showed that a corona with a cosmologically motivated angular momentum distribution can naturally develop, *in the proximity of the disc*, rotation velocities close to the value required to match the chemical constraints. The model also predicts that the rotation velocity of the hot gas should drop significantly when approaching the virial radius.The first prediction is in excellent agreement with the recent observations by Hodges-Kluck et al. (2016); the second will require next-generation X-ray observations to be confirmed or discarded.

Pezzulli, Fraternali & Binney (2017) also found that the specific angular momentum of

the inner corona increases rather steeply with radius and becomes larger than the *average* angular momentum of the disc at a radius $R_{\rm crit}$ slightly larger than the disc scale-length, but well within the range of direct contact between the galaxy and the hot halo. This is is sufficient to make the corona a plausible source of angular momentum growth, provided that the accretion of coronal gas is particularly efficient at relatively large radii, as predicted for instance by models of fountain-driven condensation (e.g. Marasco et al. 2012; Fraternali et al. 2013), and/or that the accretion is inhibited or counter-acted in the very central regions by star formation or AGN feedback (as suggested for instance for the Milky Way by the discovery of the Fermi bubbles; Su et al. 2010).

References

Armillotta, L., Fraternali, F. & Marinacci, F. 2016, MNRAS, 462, 4157
Bilitewski, T. & Schönrich, R. 2012, MNRAS, 426, 2266
Birnboim, Y. & Dekel, A. 2003, MNRAS, 345, 349
Binney, J. 2004, MNRAS, 347, 1093
Dale, D. A. 2016, AJ, 151, 4
Fall, S. M. & Romanowsky, A. J. 2013, ApJ, 769, 26
Fox, A. J., Lehner, N., Lockman, F. J., et al. 2016, ApJL, 816L, 11
Fraternali, F. & Tomassetti, M. 2012, MNRAS, 426, 2166
Fraternali, F., Marasco, A., Marinacci, F. & Binney, J. 2013, ApJL, 764L, 21
Fraternali, F., Marasco, A., Armillotta, L. & Marinacci, F. 2015, MNRAS, 447, L70
Fraternali, F. 2017, Gas Accretion onto Galaxies, ASSL, 430, 323
Gogarten, S. M. et al. 2010, ApJ, 712, 858
Genovali, K. et al. 2015, A&A, 580A, 17
Hodges-Kluck, E. J., Miller, M. J. & Bregman, J. N. 2016, ApJ, 822, 21
Kennicutt, R. C. & Evans, N. J. 2012 ARA&A, 50, 531
Kereš, D., Katz, N., Fardal, M., Davé, R., & Weinberg, D. H. 2009, MNRAS, 395, 160
Larson, R. B. 1976, MNRAS, 176, 31
Lehner, N., & Howk, J. C. 2011, Science, 334, 955
Marasco, A., Fraternali, F., & Binney, J. J. 2012, MNRAS, 419, 1107
Mayor, M. & Vigroux, L. 1981, A&A, 98, 1
Miller, M. J., & Bregman, J. N. 2015, ApJ, 800, 14
Muñoz-Mateos, J. C. et al. 2007, ApJ, 658, 1006
Pacifici, C., Oh, S., Oh, K., Lee, J. & Yi, S. K. 2016, ApJ, 824, 45
Peebles, P. J. E. 1969, ApJ, 155, 393
Pezzulli, G., Fraternali, F., Boissier, S. & Muñoz-Mateos, J. C. 2015, MNRAS, 451, 2324
Pezzulli G. & Fraternali F. 2016a MNRAS, 455, 2308
Pezzulli G. & Fraternali F. 2016b AN, 337, 913
Pezzulli, G., Fraternali, F. & Binney, J. 2017, MNRAS, 467, 311
Pitts, E. & Tayler, R. J. 1989, MNRAS, 240, 373
Putman, M. E., Peek, J. E. G., & Joung, M. R. 2012, ARA&A, 50, 491
Rubin, K. H. R., Prochaska, J. X., Koo, D. C., & Phillips, A. C. 2012, ApJL, 747L, 26
Saintonge A. et al. 2011, MNRAS, 415, 61
Sancisi, R., Fraternali, F., Oosterloo, T. & van der Hulst, T. 2008, A&ARv, 15, 189
Schönrich, R. & Binney, J. 2009, MNRAS, 396, 203
Speagle, J. S. et al. 2014, ApJS, 214, 15
Su, M. et al. 2010, ApJ, 724, 1044
Tumlinson, J., Peeples, M. S., & Werk, J. K. 2017, ARA&A, 55, 389
van den Bosch, F. C., Jiang, F., Hearin, A., et al. 2014, MNRAS, 445, 1713
Wakker, B. P., & van Woerden, H. 1997, ARA&A, 35, 217
Williams, B. F. et al. 2009, ApJ, 695, 15

XXXth IAU General Assembly, August 2018
Danail Obreschkow, ed.
DOI: 10.5281/zenodo.1481577

New Perspectives on Galactic Angular Momentum, Galaxy Formation, and the Hubble Sequence

S. Michael Fall[1] and Aaron J. Romanowsky[2]

[1]Space Telescope Science Institute,
3700 San Martin Drive, Baltimore, MD 21218, USA
email: fall@stsci.edu

[2]Dept. of Physics & Astronomy, San José State University,
One Washington Square, San Jose, CA 95192, USA
email: aaron.romanowsky@sjsu.edu

Abstract. This paper provides a summary of our recent work on the scaling relations between the specific angular momentum $j_\star$ and mass $M_\star$ of the stellar parts of normal galaxies of different bulge fraction $\beta_\star$. We find that the observations are consistent with a simple model based on a linear superposition of disks and bulges that follow separate scaling relations of the form $j_{\star\rm d} \propto M_{\star\rm d}^\alpha$ and $j_{\star\rm b} \propto M_{\star\rm b}^\alpha$ with $\alpha = 0.67 \pm 0.07$ but offset from each other by a factor of 8 ± 2 over the mass range $8.9 \leqslant \log(M_\star/M_\odot) \leqslant 11.8$. This model correctly predicts that galaxies follow a curved 2D surface in the 3D space of $\log j_\star$, $\log M_\star$, and $\beta_\star$.

Keywords. galaxies: elliptical and lenticular, cD — galaxies: evolution — galaxies: fundamental parameters — galaxies: kinematics and dynamics — galaxies: spiral — galaxies: structure

1. Introduction

Specific angular momentum ($j = J/M$) and mass (M) are two of the most basic properties of galaxies. We have studied the scaling relations between j and M from both observational and theoretical perspectives (Fall 1983; Romanowsky & Fall 2012; Fall & Romanowsky 2013, 2018; hereafter Papers 0, 1, 2, and 3). Here, we present some highlights from Paper 3 of this series.

2. Results

Figure 1 shows $\log j_\star$ plotted against $\log M_\star$ for the 94 galaxies in our sample (with $8.9 \leqslant \log(M_\star/M_\odot) \leqslant 11.8$). Galaxies of different bulge fraction, $\beta_\star \equiv (B/T)_\star \equiv M_{\star\rm b}/(M_{\star\rm d} + M_{\star\rm b})$, are indicated by symbols with different shapes and colors in this diagram. Here and throughout, the subscript $\star$ refers to the stellar components of galaxies, as distinct from their interstellar, circumgalactic, and dark-matter components, while the subscripts d and b refer to disks and bulges, respectively. We note from Figure 1 that galaxies with different $\beta_\star$ follow roughly parallel scaling relations of the form $j_\star \propto M_\star^\alpha$ with exponents close to $\alpha = 2/3$ ($\alpha \approx 0.6$ for disks, $\alpha \approx 0.8$ for bulges).

Figure 2 illustrates schematically the parallel $j_\star$–$M_\star$ scaling relations for galaxies of different bulge fraction β_*. This immediately suggests a connection between the locations of galaxies in the $j_\star$–$M_\star$ diagram and their morphologies. And this in turn suggests that the distribution of galaxies of different $\beta_\star$ in the $j_\star$–$M_\star$ diagram is a physically based alternative to the Hubble sequence. The analogy here is with the description of

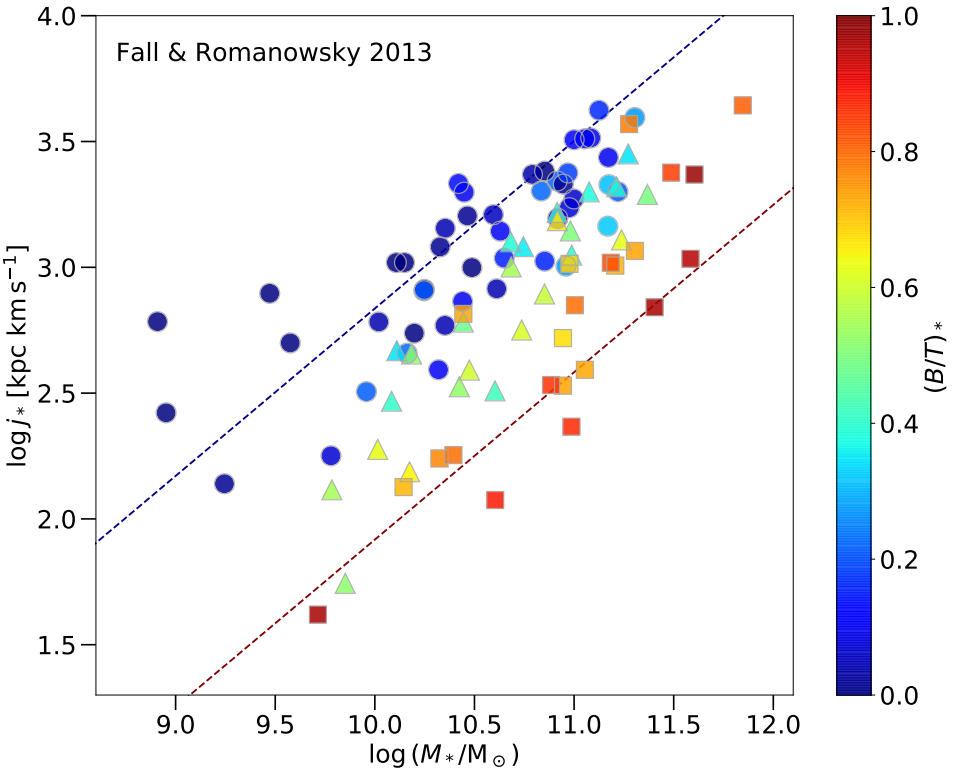

Figure 1. Stellar specific angular momentum $j_\star$ versus stellar mass $M_\star$ for galaxies of different stellar bulge fraction β (as indicated by symbol shapes and colors). The dashed lines are scaling relations for disks and bulges from 3D fitting.

elementary particles – the "eigenstates" for galaxies being disks and bulges. One wonders whether Hubble might have proposed a classification scheme for galaxies based on physical variables like j and M if he had been a physicist rather than an astronomer.

Figure 3 shows the distribution of our sample galaxies in the 3D space of ($\log j_\star$, $\log M_\star$, $\beta_\star$). Figure 1 is, of course, just the projection of this distribution onto the $\log j_\star$–$\log M_\star$ plane. We note that galaxies lie on or near the curved 2D orange surface in the 3D space. The orange surface is derived from a simple model based on a linear superposition of disks and bulges that follow separate scaling relations of the form $j_{\star\rm d} \propto M_{\star\rm d}^\alpha$ and $j_{\star\rm b} \propto M_{\star\rm b}^\alpha$ with $\alpha = 0.67 \pm 0.07$ but offset from each other by a factor of 8 ± 2.

In Paper 3, we make detailed comparisons between our $j_\star$–$M_\star$ scaling relations and those of other authors. We find excellent agreement between our results from Paper 2 and those of Obreschkow & Glazebrook (2014) and Posti et al. (2018) for disk-dominated galaxies. The $j_\star$–$M_\star$ scaling relation derived by Sweet et al. (2018) appears to suffer from an unknown systematic error (by a factor of 2) relative to the relations derived in the other three studies. We find no statistically significant indication that galaxies with classical bulges and pseudo bulges follow different relations in ($\log j_\star$, $\log M_\star$, $\beta_\star$) space.

In paper 3, we provide an updated interpretation of the $j_\star$–$M_\star$ scaling relations, following the precepts of Paper 1. In particular, we have revised slightly our earlier estimates of the fractions of angular momentum in the stellar components of galaxies relative to dark matter, $f_j \equiv j_\star/j_{\rm halo}$. We now find $f_j \sim 1.0$ for disks (slightly higher than before) and $f_j \sim 0.1$ for bulges (slightly lower than before). We also note that these fractions are

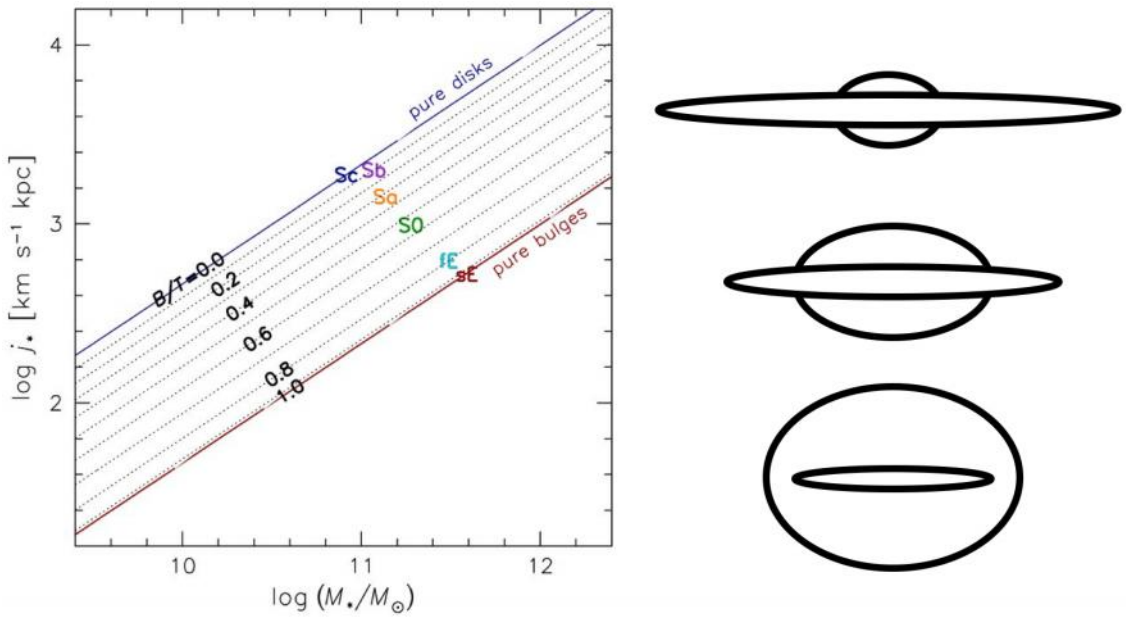

Figure 2. Physically motivated classification diagram of galaxies, with parallel $j_\star$–$M_\star$ scaling relations for fixed bulge fractions (see cartoon examples at right).

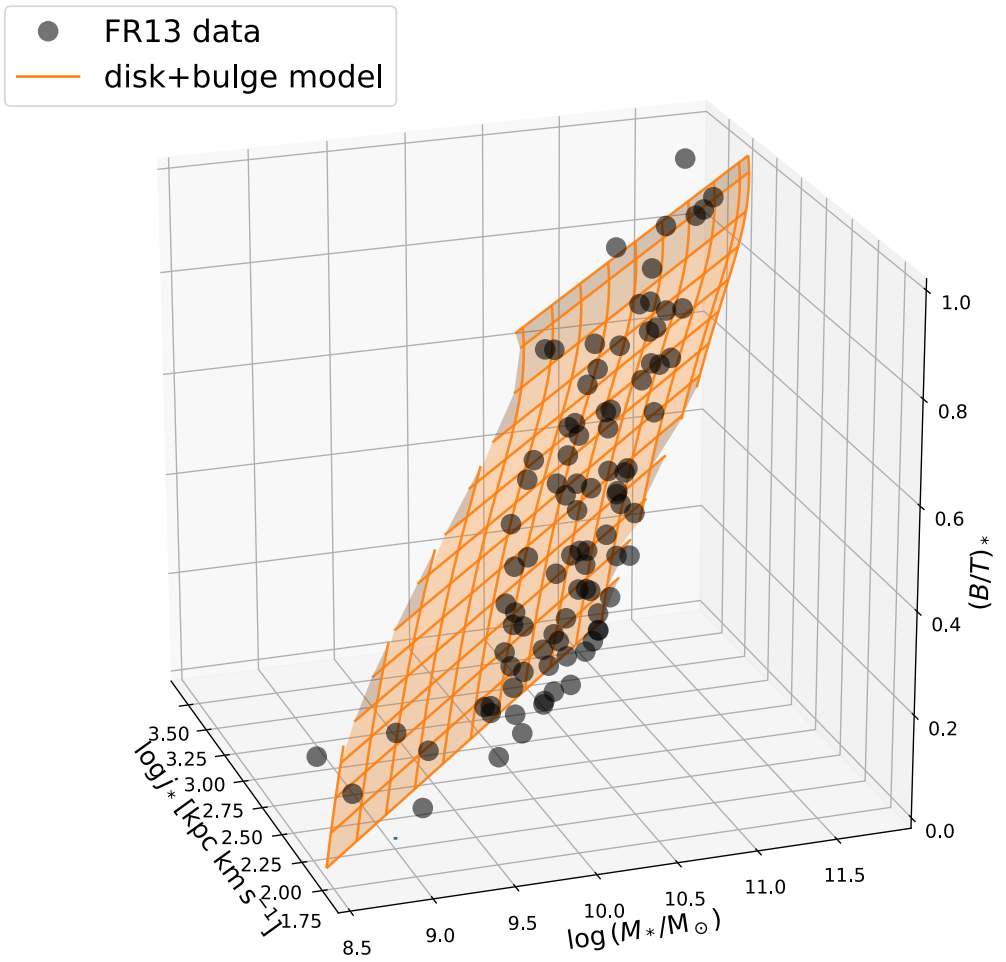

Figure 3. Bulge fraction versus specific angular momentum and mass. Points show the data, and orange surface shows our 3D relation based on independent disks and bulges.

expected to be nearly constant over the mass range $10^{9.5} M_\odot \lesssim M_\star \lesssim 10^{11.5} M_\odot$. Posti et al. (2018) suggested that f_j may decrease gradually toward lower galactic masses based on their extension of the $j_\star$–$M_\star$ relation down to $\sim 10^7 M_\odot$. Future studies should aim to determine f_j for dwarf galaxies from the *baryonic* j–M relation (including both stars and cold gas) since this may be slightly shallower than the *stellar* j–M relation, and thus consistent with $f_j \approx$ constant.

We note that the retention factor $f_j \sim 1.0$ derived from the observed $j_\star$–$M_\star$ relation for galactic disks agrees well with the value of f_j postulated in simple disk formation models (Paper 0), although the physical reasons for this agreement are still an active research topic (as discussed at this meeting by Bullock, DeFelippis, El-Badry, Genel, and others). The retention factor $f_j \sim 1.0$ also agrees well with the observed sizes of disk-dominated galaxies over the redshift range $0 \leqslant z \leqslant 3$. Using the method of abundance matching, Huang et al. (2017) showed that the relation between the sizes of galaxies and their dark-matter halos is linear and stable over this redshift range and consistent with simple disk formation models (i.e., $f_j \sim 1.0$).

3. Conclusions

1. The observed $j_\star$–$M_\star$ scaling relations for galaxies with different $\beta_\star$ constitute a physically motivated alternative to subjective classifications schemes such as the Hubble sequence.

2. At fixed $\beta_\star$, specific angular momentum and mass are related by power laws, $j_\star \propto M_\star^\alpha$, with $\alpha \approx 0.6$ for disks, $\alpha \approx 0.8$ for bulges, and $\alpha \approx 2/3$ overall.

3. For giant galaxies (with $10^{9.5} M_\odot \lesssim M_\star \lesssim 10^{11.5} M_\odot$), the angular momentum retention or sampling factors are $f_j \sim 1.0$ for disks and $f_j \sim 0.1$ for bulges.

References

Fall, S.M. 1983, in: E. Athanassoula (ed.), *IAU Symp. 100, Internal Kinematics and Dynamics of Galaxies* (Cambridge: Cambridge Univ. Press), p. 391 (Paper 0)

Fall, S.M., & Romanowsky, A.J. 2013, *ApJ* (Letters), 769, L26 (Paper 2)

Fall, S.M., & Romanowsky, A.J. 2018, ApJ, in press, arXiv:1808.02525 (Paper 3)

Huang, K.-H. et al. 2017, *ApJ*, 838, 6

Obreschkow, D., & Glazebrook, K. 2014, *ApJ*, 784, 26

Posti, L., Fraternali, F., Di Teodoro, E.M., & Pezzulli, G. 2018, *A&A*, 612, L6

Romanowsky, A.J., & Fall, S.M. 2012, *ApJS*, 203, 17 (Paper 1)

Sweet, S.M. et al. 2018, *ApJ*, 860, 37

XXXth IAU General Assembly, August 2018
Chanda Jog & Danail Obreschkow, ed.
DOI: 10.5281/zenodo.1481572

Angular Momentum-Mass Law for Discs in the Nearby Universe

Lorenzo Posti
Kapteyn Astronomical Institute, University of Groningen, P.O. Box 800, 9700 AV Groningen, the Netherlands
email: posti@astro.rug.nl

Abstract. The relation between galaxy mass and specific angular momentum is a fundamental scaling law of galaxy structure, however accurate observational determinations are made difficult by the fact that most of the specific angular momentum of a typical galaxy resides in its outer regions. I measure the stellar specific angular momenta for 154 disc galaxies at $z = 0$ (with $7 \lesssim \log M_\star/M_\odot \lesssim 11.5$) using HI rotation curves to trace stellar rotation typically beyond 5 disc scale-lengths. An accurate measurement of $j_\star$ can be derived for $\sim 60\%$ of the sample, while only lower limits can be inferred for the remaining $\sim 40\%$. I derive fits to the specific stellar angular momentum-stellar mass scaling law ($j_\star - M_\star$) both considering only 92 accurate measurements and taking into account also for 62 lower limits: I find no significant differences in these two cases. I also show how the intrinsic scatter of the $j_\star - M_\star$ relation varies as a function of the mass-to-light ratio adopted to determine the stellar masses.

Keywords. galaxies: kinematics and dynamics, galaxies: spiral, galaxies: structure

1. Introduction

Many important insights in galaxy formation and evolution can be gained by studying scaling relations of galaxy properties. Mass and specific angular momentum (i.e. angular momentum normalized by mass) are two of the most fundamental structural properties of galaxies, which are independent and subject to physical conservation laws. The scaling relation that they define, first analyzed by Fall (1983, thus hereafter *the Fall relation*), has the unique power of constraining an important aspect of galaxy formation, namely the link between the spins of galaxies and of dark matter halos (Romanowsky & Fall 2012; Shi et al. 2017; Posti et al. 2018a). However, understanding this scaling law, and hence how galaxies acquire their spin, is complicated by the fact that typically most of the angular momentum resides in the outer parts of the system, where observations are significantly more difficult. For instance, an exponential disc with a flat rotation curve has $\gtrsim 50\%$ of its specific angular momentum outside two disc scale-lengths, where spectroscopic observations are challenging. Thus, tracers of the rotation velocity of galaxies that extend further away from the centre are needed to accurately characterize the Fall relation.

Here I focus on the *stellar* Fall relation: the $j_\star - M_\star$ relation, where $M_\star$ and $j_\star$ are the stellar mass and stellar specific angular momentum respectively. Together with a stellar-to-halo mass relation, this can be used to empirically estimate the stellar-to-halo specific angular momentum relation, which is the main ingredient that sets galaxy sizes and morphologies in a galaxy formation model (e.g., Posti et al. 2018a).

2. The $j_\star - M_\star$ relation for nearby disc galaxies

I use the sample of 175 nearby disc galaxies collected by Lelli et al. (2016, hereafter SPARC) for which both accurate HI rotation curves and Spitzer photometry at 3.6μm are

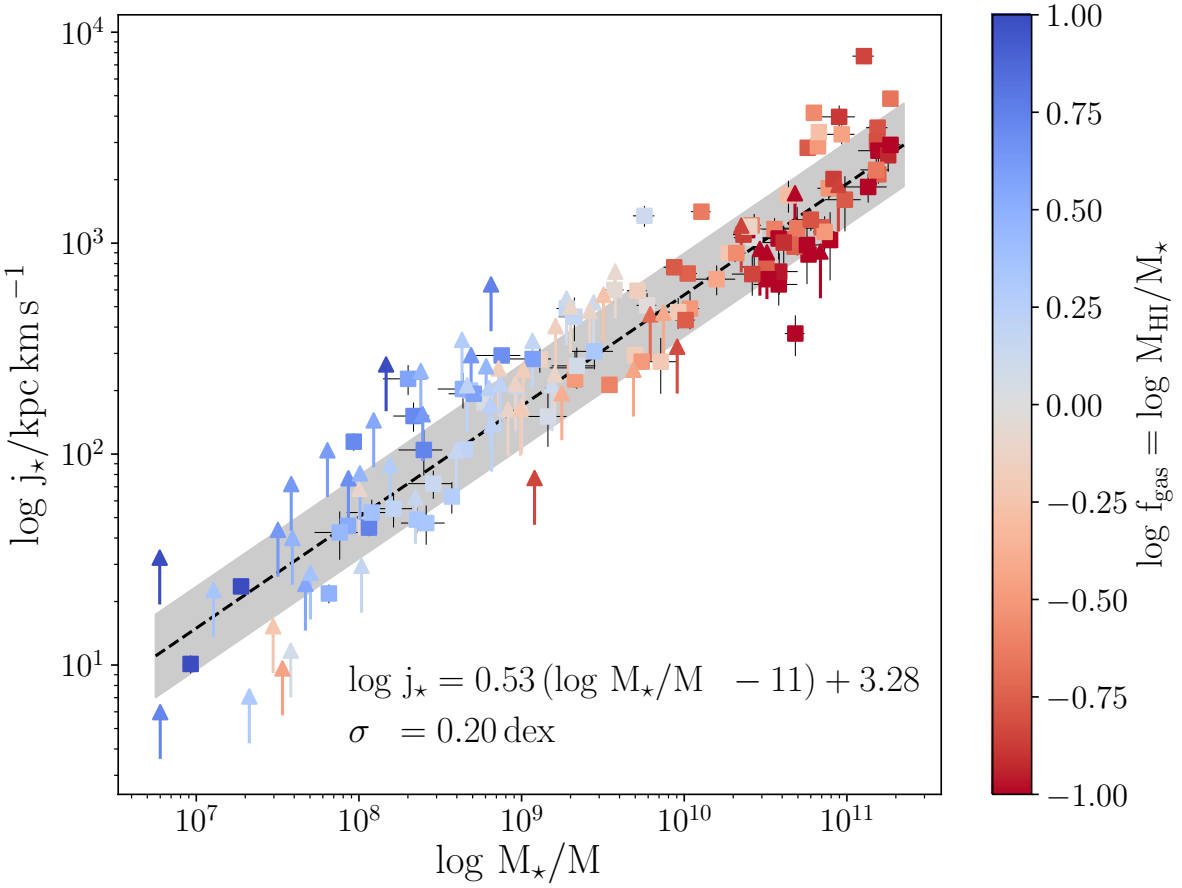

Figure 1. Stellar specific angular momentum-stellar mass relation (Fall relation) for 154 galaxies in the nearby Universe from the SPARC sample. Squares (with 1-σ uncertainties) are the accurate measurements for 92 galaxies with a converged $j_\star(< R)$ profile, while upwards arrows are lower limits for the 62 ones with non-converging profiles. The points are colour-coded by the logarithm of the gas fraction. The best-fit power-law relation, accounting also for the lower limits, is shown with a black dashed line (with the grey band representing the 1-σ intrinsic scatter).

available. Near-infrared photometry is used to trace the stellar mass surface density $\Sigma_\star$ within the galaxy, with the total stellar mass $M_\star$ being computed using constant mass-to-light ratios for the disc and the bulge component respectively $(\Upsilon_\mathrm{d}^{[3.6]}, \Upsilon_\mathrm{b}^{[3.6]}) = (0.5, 0.7)$; while the neutral hydrogen rotation curves are used to trace the stellar rotation velocity $V_\star$, after correcting for asymmetric drift (see Posti et al. 2018b, for details). I compute stellar specific angular momentum profiles as

$$j_\star(< R) = \frac{\int_0^R \mathrm{d}R'\, R'^2\, \Sigma_\star(R')\, V_\star(R')}{\int_0^R \mathrm{d}R'\, R'\, \Sigma_\star(R')} \tag{2.1}$$

and I define $j_\star$ for each galaxy as the last measured point of the $j_\star(< R)$ profile. A selection of galaxies observed at inclinations larger than 30° leaves us with 154 galaxies: this is needed since for nearly face-on systems the HI rotation curves are too uncertain. Out of these 154 objects, 92 have converged $j_\star(< R)$ profiles (i.e. they satisfy criteria (2) in Posti et al. 2018b): for these galaxies the total stellar specific angular momentum is accurately measured (better than 10%). The $j_\star(< R)$ profiles of the other 62 systems are instead still rising to the outermost measured point, thus the estimated $j_\star$ can only be considered as a lower limit of the actual stellar specific angular momentum. In Fig. 1 I

plot the accurately measured $j_\star$ as a function of $M_\star$ for the 92 galaxies as squares (with 1-σ errorbars), while upwards arrows represent the lower limits on $j_\star$ for the other 62 galaxies in the SPARC sample. The distribution of lower limits is completely compatible with that of the accurate measurements, with galaxies with more steeply rising $j_\star(< R)$ in the outermost measured points being found at lower specific angular momenta with respect to galaxies with similar stellar mass.

In Posti et al. (2018b) we presented best-fitting power-law scaling relations when only considering the 92 galaxies for which accurate $j_\star$ measurements could be obtained. Here I take into account also the other 62 lower limits and fit the $j_\star - M_\star$ relation similarly to Posti et al. (2018b). I find a perfectly compatible best-fitting model with slope $\alpha = 0.53 \pm 0.3$, normalization $\beta = 3.28 \pm 0.05$ and a slightly larger orthogonal intrinsic scatter of $\sigma_\perp = 0.2 \pm 0.02$ dex. I overplot this best-fit to the measurements and lower limits in Fig. 1.

Bulge fraction, which can be considered a proxy for galaxy morphology, is known to play an important role in the $j_\star - M_\star$ diagram, with galaxies with increasing bulge fractions having smaller $j_\star$ for a fixed $M_\star$ (see e.g. Romanowsky & Fall 2012). If for a fixed mass angular momentum traces bulge fraction, then it follows that the $j_\star - M_\star$ law for galaxies of a specific bulge fraction (i.e. of a fixed morphological type) should have the smallest intrinsic scatter. Moreover, in Posti et al. (2018b) we showed that the relation obtained only considering the discs of the 92 spiral galaxies with accurate $j_\star$ measurements has a smaller $\sigma_\perp$ with respect to the relation derived when including also their bulges. Here I systematically assess how does the orthogonal intrinsic scatter $\sigma_\perp$ of the $j_\star - M_\star$ relation varies when changing the mass-to-light ratios of the disc ($\Upsilon_{\rm d}^{[3.6]}$) and the bulge component ($\Upsilon_{\rm b}^{[3.6]}$). In Fig. 2 I show $\sigma_\perp$ as a function of $\Upsilon_{\rm d}^{[3.6]}$ and $\Upsilon_{\rm b}^{[3.6]}$, where these two vary in the range $[0.1, 1]$. Reasonable assumptions are typically those where $\Upsilon_{\rm b}^{[3.6]} \geqslant \Upsilon_{\rm d}^{[3.6]}$: for instance, stellar population models suggest $\Upsilon_{\rm b}^{[3.6]} = 1.4\Upsilon_{\rm d}^{[3.6]}$ (Schombert & McGaugh 2014). Fig. 2 shows that for reasonable choices of the mass-to-light ratios the intrinsic scatter cannot be smaller than $\sigma_\perp \sim 0.17$ dex. However, for any given $\Upsilon_{\rm d}^{[3.6]}$ I find the smallest $\sigma_\perp$ for $\Upsilon_{\rm b}^{[3.6]} \sim 0$, confirming our previous result that the $j_\star - M_\star$ relation for only the discs of spiral galaxies has the smallest intrinsic scatter (Posti et al. 2018b).

3. Conclusions

The Fall relation has become a fundamental test-bed for analytic, semi-analytic and numerical galaxy formation models. The straightness and tightness that it exhibits, over ~ 5 orders of magnitude in stellar mass for disc galaxies in the nearby Universe, demand to be reproduced by any model that aspires to be deemed as successful. While the samples accurately analyzed up to now are representative of the galaxy population, they are not complete or volume-limited. In the future we will need to measure extended angular momentum profiles for a much larger sample, and possibly complete and/or volume-limited, of both late-type and early-type galaxies. This can be done with surveys using the next generation of Integral Field Spectrographs in the optical domain and with new upcoming HI blind surveys of spatially resolved galaxies in the radio domain. This will also be helpful for modellers to constrain their formation theories without worrying about selection effects.

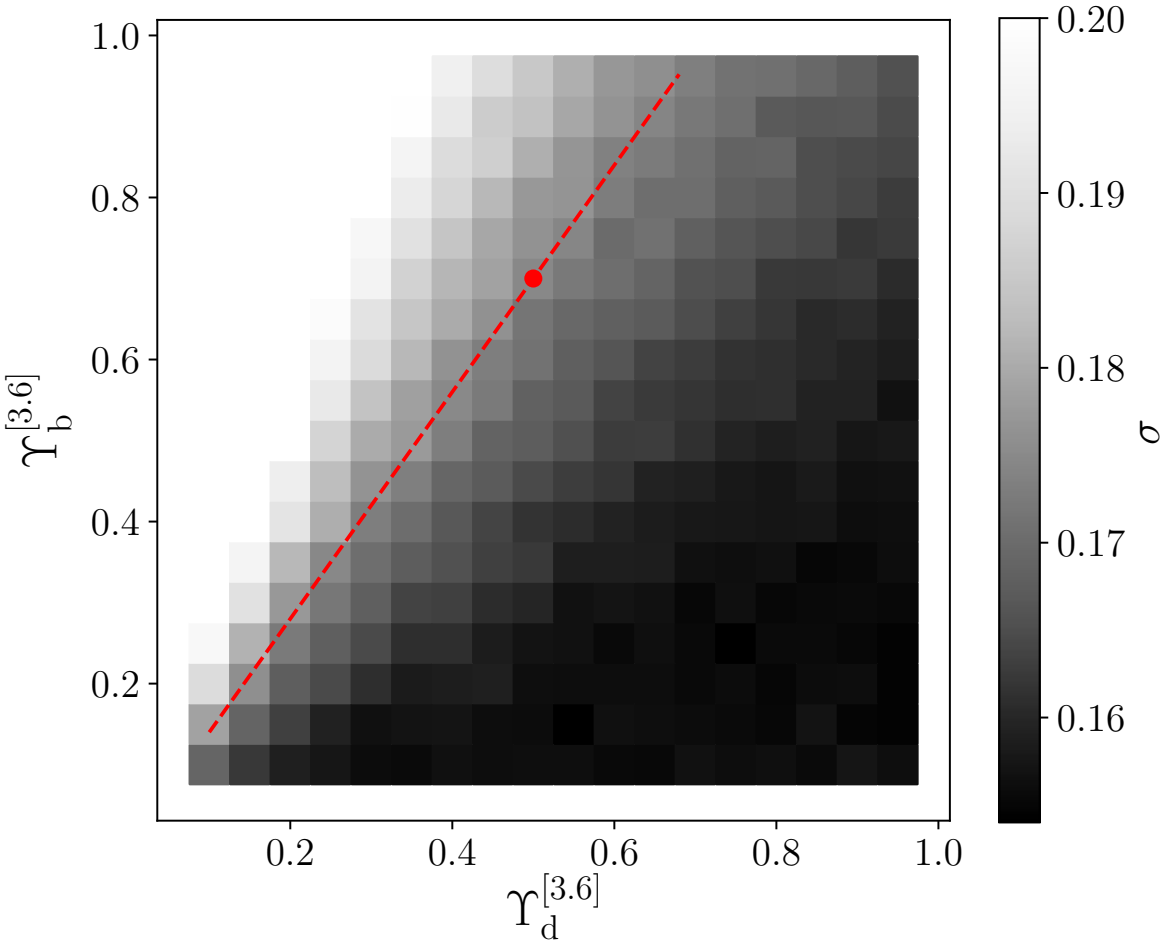

Figure 2. Orthogonal intrinsic scatter of the Fall relation, as in Fig. 1, as a function of the disc and bulge mass-to-light ratios. The red dashed line is $\Upsilon_{\rm b}^{[3.6]} = 1.4\Upsilon_{\rm d}^{[3.6]}$, the locus of values suggested by stellar population models (Schombert & McGaugh 2014), while the red dot is the fiducial value used in Fig. 1.

References

Fall S. M., 1983, IAUS, 100, 391
Lelli F., McGaugh S. S., Schombert J. M., 2016, AJ, 152, 157
Romanowsky A. J., Fall S. M., 2012, ApJS, 203, 17
Posti L., Pezzulli G., Fraternali F., Di Teodoro E. M., 2018a, MNRAS, 475, 232
Posti L., Fraternali F., Di Teodoro E. M., Pezzulli G., 2018b, A&A, 612, L6
Schombert J., McGaugh S., 2014, PASA, 31, e036
Shi J., Lapi A., Mancuso C., Wang H., Danese L., 2017, ApJ, 843, 105

XXXth IAU General Assembly, August 2018
Claude Carignan & Danail Obreschkow, ed.
DOI: 10.5281/zenodo.1481554

Baryonic Angular Momentum in Simulated Disks: The CGM

Daniel DeFelippis[1], Shy Genel[2,1], Greg Bryan[1,2]

[1]Department of Astronomy, Columbia University
550 West 120th Street, New York, NY 10027, USA
email: d.defelippis@columbia.edu

[2]Center for Computational Astrophysics, Flatiron Institute
162 Fifth Avenue, New York, NY 10010, USA

Abstract. Physical processes that occur the circumgalactic medium (CGM) are largely responsible for setting the baryonic angular momentum of simulated galaxies. However, the angular momentum of the CGM has yet to be characterized in a large cosmological simulation, which are now capable of reproducing observed angular momentum properties for large populations of galaxies. We present a first step towards understanding the angular momentum properties of the CGM statistically for galaxies in the IllustrisTNG simulation. We focus on Milky Way-mass halos at $z = 0$, but plan to extend this analysis to other masses and redshifts in future work.

Keywords. galaxies: kinematics and dynamics, galaxies: structure, hydrodynamics, methods: numerical

1. Introduction

The stellar specific angular momentum (j_*) and stellar mass (M_*) relation for disk galaxies has been well established since the 1980s observationally (Fall 1983; Fall & Romanowsky 2013), but only relatively recently have simulations been able to reproduce this relation for a large population of galaxies (e.g. Genel et al. 2015; Zavala et al. 2016). Simulations accomplish this with physically motivated feedback models that affect the dynamics of the baryons in many ways, such as by ejecting material in galactic fountains (e.g. Christensen et al. 2016), resulting in a $j_* - M_*$ relationship at $z = 0$ consistent with observations.

DeFelippis et al. (2017) investigated the effect of feedback in shaping the angular momentum of stellar disks in the Illustris simulation by performing a Lagrangian analysis of the $z = 0$ stars in Milky Way-mass galaxies. By tracing the $z = 0$ stars back through time and keeping track of their angular momentum, we found three periods during which feedback operates in different ways. First, feedback lessens angular momentum losses when gas accretes onto the dark matter halo and travels towards the galaxy (compared to a galaxy of the same mass simulated without feedback). Second, feedback causes angular momentum gains via galactic winds by successively ejecting accreted gas from the disk into the CGM. Finally, feedback halts angular momentum losses right before gas forms stars within the disk.

One of our main conclusions was that feedback within the CGM (i.e. during the first two periods defined above) is very important for setting the angular momentum of the enclosed galaxies. There have been many recent efforts to characterize the dynamics of the CGM with both observations (e.g. Turner et al. 2017) and simulations (e.g. Stevens et al. 2017), but no one has yet used a large cosmological simulation to create a comprehensive picture of the angular momentum in the CGM. We are thus motivated to do so using the Illustris and IllustrisTNG simulations.

2. Methods

Illustris (Genel et al. 2014; Vogelsberger et al. 2014a,b) and IllustrisTNG (Marinacci et al. 2018; Naiman et al. 2018; Nelson et al. 2018; Pillepich et al. 2018b; Springel et al. 2018) are large hydrodynamical simulations run in a $\approx(100\ \mathrm{Mpc})^3$ volume using the moving-mesh code AREPO (Springel 2010). In this work, we use the newer IllustrisTNG simulation, which contains models for stellar (Pillepich et al. 2018a) and AGN feedback (Weinberger et al. 2017) which match observational constraints better than the original Illustris feedback prescriptions do (see e.g. Nelson et al. 2018).

We select galaxies from IllustrisTNG in the mass range $10^{11.75} < \mathrm{M_{halo}[M_\odot]} < 10^{12.25}$ at $z = 0$ and calculate j_* of the central galaxies as follows:

$$\mathbf{j}_* = \frac{1}{M_*} \sum_{i=1}^{N} m_{*,i}(\mathbf{r}_{*,i} \times \mathbf{v}_{*,i}) \tag{2.1}$$

where $m_{*,i}$ and M_* are the mass of individual star particles and the total stellar mass respectively, the radius $\mathbf{r}_{*,i}$ is measured from the position of the most bound particle in the galaxy, and the velocity $\mathbf{v}_{*,i}$ is measured in the center of mass frame of the stars. We define a disk galaxy as one that is in the upper quartile of the j_* distribution, as a high value of j_* for a given stellar mass has been shown to be a proxy for morphological disks, both observationally (Fall & Romanowsky 2013) and in simulations (Genel et al. 2015).

For our high-j_* sample, we remove the innermost region of the halo that contains 95% of the stars and dense star-forming gas, and call the remaining gas the CGM. In order to determine the effect of temperature, we divide the CGM into hot and cold phases with a cutoff at half of the virial temperature of the halo ($\sim 10^5$ K for our mass range), and calculate j_{CGM} for those phases in the same reference frame as the calculation of j_*.

3. Results

In this section, we describe properties of our sample of high-j_* galaxies. In Figure **??**, we show the position of the high-j_* galaxies' cold and hot CGM on the specific angular momentum-mass ($j - M$) plane. Two key differences are apparent: first, the cold phase typically contains more mass and angular momentum than the hot phase, and second, there is a correlation present in the cold phase that does not appear in the hot phase. From these differences we can deduce properties of the CGM. Cold gas in the CGM is also closer to the galaxy than the hot CGM gas is, which implies that the cold phase must be rotating much more significantly than the hot phase. The correlation present in the cold phase may simply be a consequence of the large extended structures cold gas forms, which both contain a lot of angular momentum and require a lot of mass to sustain themselves.

In Figure **??**, we show the magnitudes and directions of the CGM angular momentum vectors with respect to their corresponding stellar angular momentum vectors. Unlike in Figure **??**, the two plots are very similar: the alignment angles of the hot and cold phases for this galaxy sample are usually small (median $\approx 20^\circ$) and nearly identical to each other. In other words, despite the difference in rotational velocity magnitudes between the hot and cold gas, they are nevertheless both aligned to the stars in a similar way.

In Figure **??**, we try to understand this similarity on a galaxy-by-galaxy basis by comparing the alignments of the hot and cold phases for each galaxy in our high-j_* sample and a corresponding low-j_* sample (the lower quartile of the j_* distribution) from the same halo mass bin. We see that both hot and cold phase alignments with respect to the stars for the low-j_* galaxies are nearly uniformly distributed over all possible angles

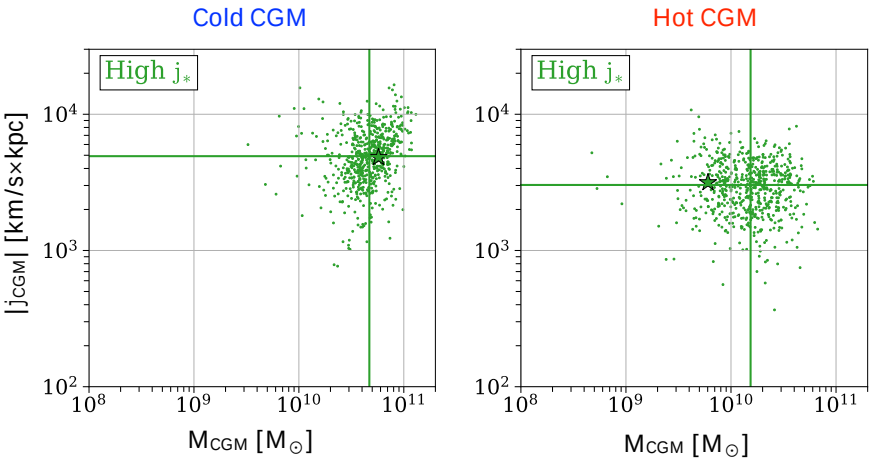

Figure 1. *Left*: Specific angular momentum of the cold phase of the CGM vs. mass of the cold phase. Vertical and horizontal green lines show the medians of the x and y-axis distributions respectively. The outlined star corresponds to a galaxy shown in 3D during the talk summarized by this proceeding, which can be found at http://gam18.icrar.org/talks/. *Right*: Same as left, but for the hot phase of the CGM.

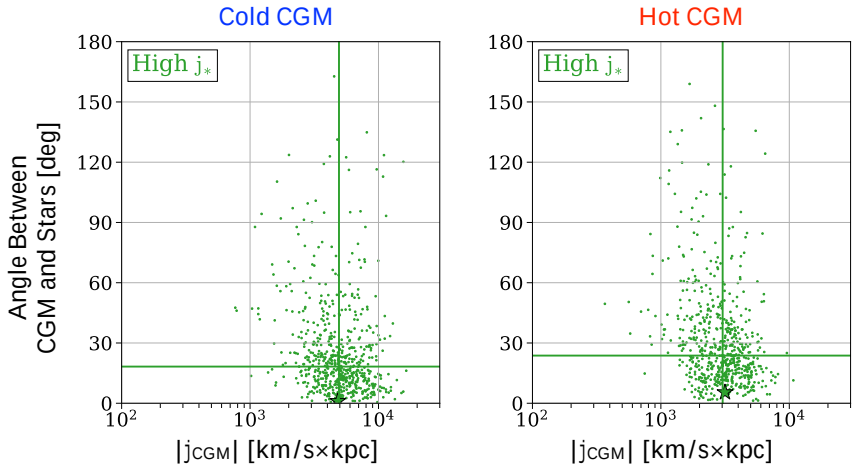

Figure 2. *Left*: Alignment angle of the cold CGM angular momentum vector with respect to the the stellar angular momentum vector vs. magnitude of the cold CGM angular momentum vector. *Right*: Same as left, but for the hot phase of the CGM.

(median $\approx 60°$). These alignment distributions may explain why high-j_* and low-j_* galaxies end up as such: high-j_* galaxies accrete CGM gas that is already mostly aligned to the galaxy, so stars that form out of that gas add to the angular momentum already present, while low-j_* galaxies accrete gas that can be totally misaligned, meaning stars that form may not add to the angular momentum. Additionally, all points are clustered around the 1-1 line (with some scatter), meaning that irrespective of their alignment to the stars, the hot and cold phases of the CGM always coherently rotate with each other.

4. Summary

We selected galaxies from the IllustrisTNG simulation that are in $\sim 10^{12}\mathrm{M}_\odot$ halos at $z = 0$ and examined the angular momentum content of their CGM. We divided the CGM into hot and cold phases to understand what the effect of temperature is. We find

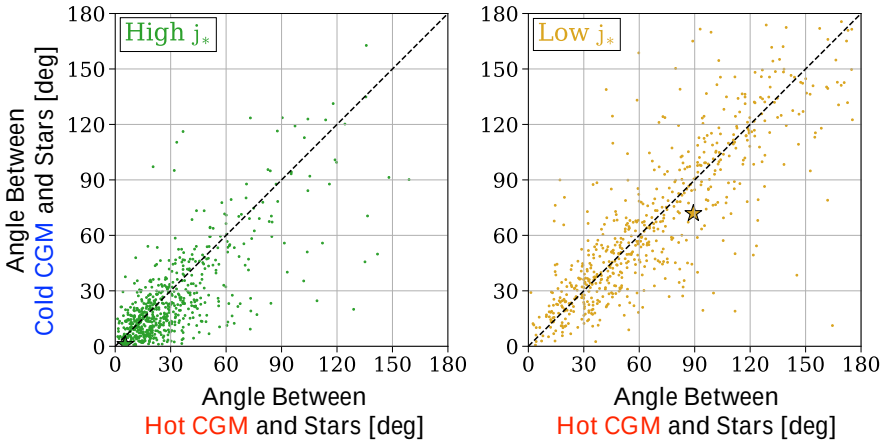

Figure 3. *Left*: Alignment angle between cold gas angular momentum vector and stellar angular momentum vector vs alignment angle between hot gas angular momentum vector and stellar angular momentum vector for high-j_* galaxies. The dotted line is the 1-1 line. *Right*: Same as left but for low-j_* galaxies.

that for galaxies with the highest stellar specific angular momentum, the cold CGM gas contains more mass and more specific angular momentum than the hot CGM gas, but both phases are well aligned to the angular momentum vector of the stars to nearly the same degree. The CGM of low-j_* galaxies is notably not well aligned to the stars, but like the high-j_* galaxies, the hot and cold CGM gas coherently rotate with each other.

All of these $z = 0$ properties suggest particular formation histories, such as hot/cold phase mixing and coherent/non-coherent accretion that may help explain angular momentum growth in the galaxy and the surrounding CGM, which will be investigated as this work continues.

References

Christensen C. R., et al. 2016, *ApJ*, 824, 57
DeFelippis D., Genel S., Bryan G. L., Fall S. M. 2017, *ApJ*, 841, 16
Fall S. M., Efstathiou G. 1980, *MNRAS*, 193, 189
Fall S. M. 1983, *IAU Symp. 100*, 391
Fall S. M., Romanowsky A. J. 2013, *ApJ*, 769, L26
Genel S., et al. 2014, *MNRAS*, 445, 175
Genel S., et al. 2015, *ApJ*, 804, L40
Marinacci F., et al. 2018, *MNRAS*, 480, 5113
Mo H. J., Mao S., White S. D. M. 1998, *MNRAS*, 295, 319
Naiman J. P., et al. 2018, *MNRAS*, 477, 1206
Nelson D., et al. 2018, *MNRAS*, 475, 624
Pillepich A., et al. 2018, *MNRAS*, 473, 4077
Pillepich A., et al. 2018, *MNRAS*, 475, 648
Springel V. 2010, *MNRAS*, 401, 791
Springel V., et al. 2018, *MNRAS*, 475, 676
Stevens A. R. H., et al. 2017, *MNRAS*, 467, 2066
Turner M. L., et al. 2017, *MNRAS*, 471, 690
Vogelsberger M., et al. 2014, *Natur*, 509, 177
Vogelsberger M., et al. 2014, *MNRAS*, 444, 1518
Weinberger R., et al. 2017, *MNRAS*, 465, 3291
Zavala J., et al. 2016, *MNRAS*, 460, 4466

XXXth IAU General Assembly, August 2018
Claude Carignan & Danail Obreschkow, ed.
DOI: 10.5281/zenodo.1481567

The Interplay between Galactic Angular Momentum and Morphology

Kareem El-Badry[1]

[1]Department of Astronomy and Theoretical Astrophysics Center, University of California Berkeley, Berkeley, CA 94720
email: kelbadry@berkeley.edu

Abstract. In both observed galaxies and in galaxy formation simulations, the degree of rotation vs. dispersion support declines with increasing mass, at least up to $L \sim L_\star$. While most isolated Milky-Way mass galaxies have thin, centrifugally supported gas disks, many lower-mass galaxies are puffy and irregular, supported by a mix of thermal pressure and feedback-driven turbulence. Cosmological simulations show that many of the halos whose galaxies fail to form disks harbor high angular momentum gas in their circumgalactic medium. The ratio of the specific angular momentum of gas in the central galaxy to that of the dark-matter halo increases significantly with galaxy mass, from $j_{\rm galaxy}/j_{\rm halo} \sim 0.1$ at $M_{\rm star} = 10^{6-7}{\rm M}_\odot$ to $j_{\rm galaxy}/j_{\rm halo} \sim 2$ at $M_{\rm star} = 10^{10-11}\,M_\odot$. Such a decrease in the angular momentum retention factor is also required to reproduce the observed $j_{\rm galaxy} - M_{\rm vir}$ relation at low masses. In simulations, the reduced rotational support in the lowest-mass galaxies is a result of (a) stellar feedback and the UV background suppressing the accretion of high-angular momentum gas at late times, and (b) stellar feedback driving large non-circular gas motions.

Keywords. galaxies: kinematics and dynamics – galaxies: irregular – galaxies: dwarf

1. Overview

Cosmological simulations of galaxy formation have only recently become capable of producing galaxies with structural parameters in broad agreement with observations. While many aspects of the galaxy formation process remain imperfectly understood, high-resolution zoom-in simulations make it possible to begin to resolve galaxies' multiphase ISM, star formation in dense gas, and the effects of feedback in driving galactic outflows.

In simulated galaxies from the FIRE project, the degree of rotational support decreases strongly below $M_{\rm star} \sim 10^9 M_\odot$ (El-Badry et al. 2018). Gas in most dwarf galaxies in the simulations is supported primarily by pressure, not rotation, and the galaxies do not form thin disks. In mock-IFU observations of the simulations, it is clear that the gas is in a state of disequilibrium, perpetually perturbed and disrupted by stellar feedback. Below $M_{\rm star} \sim 10^9 M_\odot$, galaxies also have lower specific angular momentum than naively expected from the Fall (1983) relation. As a consequence, the ratio between the specific angular momentum of the galaxy and that of the dark matter halo, $f_j \equiv j_{\rm galaxy}/j_{\rm halo}$, must decrease by more than an order of magnitude from MW-mass galaxies to the dwarf scale. Recently, it has been pointed out by Posti et al. (2018) that given the shape of the $M_{\rm star}/M_{\rm halo}$ relation, a decrease in f_j at low masses is inevitable if the $j_{\rm galaxy} - M_{\rm vir}$ relation remains a constant power law.

While this decrease in f_j is also found in simulations, there it is possible to assess its origin more physically. The specific angular momentum of MW-mass galaxies increases steadily with cosmic time, such that gas accreted at $z = 0$ has an order of magnitude higher specific angular momentum than gas accreted at $z = 2$. Low-mass galaxies accrete

almost all of their baryons before $z = 2$; at later times, the combination of heating from the UV background and stellar feedback-driven outflows that entrain gas in the CGM prevents new baryons from being accreted. Thus most of the baryons that end up in low-mass galaxies at late times were accreted at early times, before high-angular momentum gas was available. In the FIRE simulations, this leads directly to reduced rotational support and more irregular morphology (El-Badry et al. 2018b). Angular momentum content is also connected to the "burstiness" of galaxies' star formation histories: coherent bursts of star formation occur when large amounts of gas fall into the galactic center and accumulate at high density, and this cannot occur if gas is angular-momentum supported and settles into a disk.

References

El-Badry, K., Quataert, E., Wetzel, A., Hopkins, P. F., Weisz, D. R., Chan, T. K., Fitts, A., Boylan-Kolchin, M., Kereš, D., Faucher-Giguère, C.-A., Garrison-Kimmel, S. 2018, MNRAS, 473, 1930.

El-Badry, K., Bradford, J., Quataert, E., Geha, M., Boylan-Kolchin, M., Weisz, D. R., Wetzel, A., Hopkins, P. F., Chan, T. K., Fitts, A., Kereš, D., Faucher-Giguère, C.-A. 2018, MNRAS, 477, 1536.

Fall, S. M. 1983, in IAU Symp. 100, Internal Kinematics and Dynamics of Galaxies, ed. E. Athanassoula (Cambridge: Cambridge Univ. Press), 391

Posti, L., Pezzulli, G., Fraternali, F., & Di Teodoro, E. M. 2018b, MNRAS, 475, 232

XXXth IAU General Assembly, August 2018
Chanda Jog & Danail Obreschkow, ed.
DOI: 10.5281/zenodo.1481598

A Lagrangian View on the Relation between Galaxy and Halo Angular Momentum

Shy Genel[1,2]

[1]Center for Computational Astrophysics, Flatiron Institute,
162 Fifth Avenue, New York, NY 10010, USA
email: sgenel@flatironinstitute.org

[2]Columbia Astrophysics Laboratory, Columbia University,
550 West 120th Street, New York, NY 10027, USA

Abstract. Observations combined with basic theoretical considerations suggest that disk galaxies have approximately the same specific angular momentum (sAM) as a typical dark matter halo with the corresponding host mass. The most simplistic interpretation of this newly established result is that the baryons that make up the disks have retained the sAM they obtained from cosmological tidal torques throughout their evolution from the intergalactic medium down to the present-day stars within the galaxy. There is evidence, however, that reality may be substantially more complex than this simplistic picture. Here is a theoretical discussion of the sAM of such baryons through various stages in their evolution. It is argued that the sAM evolution during many of these stages is still not well known, is expected to be substantial, and is probably interrelated despite the diversity of scales and physical processes involved. A strong interplay is necessary to obtain a result that mimics the simplistic 'retention' picture.

Keywords. methods: numerical, galaxies: evolution, galaxies: formation, galaxies: fundamental parameters, galaxies: kinematics and dynamics, galaxies: spiral, galaxies: structure

1. Introduction

Increasingly accurate measurements of the angular momentum content of galaxies have led in recent years to a picture of the scaling relation between galaxy mass, type, and specific angular momentum (sAM) that is generally accepted, even if some important details are still debated. When this picture is extended using simple yet robust theoretical relations between galaxy mass and host dark matter halo mass, the observed angular momenta of galaxies can be directly related to theories of the emergence of angular momentum by cosmological tidal torques. It is then found that the sAM magnitudes of late-type galaxies (and more generally, galactic disks) are approximately equal to the typical sAM magnitudes of dark matter halos that have the assumed host masses. This is often loosely referred to as galactic angular momentum 'retention' or 'conservation', to be contrasted with the galactic angular momentum 'catastrophe' in early cosmological simulations, whereby the sAM magnitudes of galaxies were substantially smaller than those of their halos. This empirical approximate equality demands an explanation.

2. The Lagrangian bookkeeping of angular momentum

The Lagrangian approach adopted here traces the changes over time of the sAM of the individual baryonic particles that eventually constitute disk galaxies. The angular momentum of these particles, with respect to the center of the galaxy in which they eventually end up, changes under the influence of torques, generally both before and after they are incorporated into the galaxy, and both at early times when they are part of the gas phase and at late times when they are already locked into stars.

The quantity of focus here is the ratio between the sAM $\langle j_* \rangle$ of the stars in a typical disk galaxy of a certain mass and the sAM $\langle j_{\rm DM-halo} \rangle$ of a typical halo that has the mass of these galaxies' typical host halo mass. This ratio, Equation (2.1*a*), is estimated empirically to be very close to unity (e.g. Fall & Romanowsky 2013; see Section 1). This ratio is expanded in two steps, starting with Equation (2.1):

$$\langle j_* \rangle / \langle j_{\rm DM-halo} \rangle = [\tag{2.1a}$$
$$f_{\rm in-situ-stars} \times$$
$$j_{\rm in-situ-stars}$$
$$+ \tag{2.1b}$$
$$f_{\rm ex-situ-stars} \times$$
$$j_{\rm ex-situ-stars}$$
$$] / \langle j_{\rm DM-halo,disks} \rangle \times \tag{2.1c}$$
$$(\langle j_{\rm DM-halo,disks} \rangle / \langle j_{\rm DM-halo} \rangle). \tag{2.1d}$$

This equation describes two distinct ideas. First, the sAM of the stars is broken in Equation (2.1*b*) down to a mass-weighted average of that of the stars formed in-situ (in the main progenitor of the galaxy) and that of the stars formed ex-situ (in galaxies that will later merge onto the main progenitor). Second, the factor $\langle j_{\rm DM-halo,disks} \rangle$ is added both in the denominator (Equation (2.1*c*)) and the numerator (Equation (2.1*d*)). This factor represents the typical sAM of dark matter halos that are the actual hosts of disk galaxies (in contrast to $\langle j_{\rm DM-halo} \rangle$ that is the sAM of a typical halo of that same mass). Therefore, Equation (2.1*d*) represents the ratio between the typical spin of dark matter halos that host disk galaxies and the typical spin of all dark matter halos of the same mass. If disk galaxies reside preferentially in dark matter halos with higher spins, as suggested by some simulations (Rodriguez-Gomez et al. 2017), this ratio is larger than unity, possibly on a similar scale to the scatter in the halo spin parameter, ≈ 0.2 dex.

The ratio $\langle j_* \rangle / \langle j_{\rm DM-halo} \rangle$ is expanded further in Equation (2.2) by adding to Equation (2.1) several steps of division and multiplication by identical factors, which result in ratios that represent specific stages in the Lagrangian evolution of baryonic particles.

Equation (2.2*b*) introduces the factor $j_{\rm in-situ-stars@form}$, which is the sAM of in-situ stars at their birth time. The ratio $(j_{\rm in-situ-stars} / j_{\rm in-situ-stars@form})$ then represents the ratio between the final angular momentum content of the in-situ stars (e.g. at $z = 0$) and that at the time of their formation.

Equation (2.2*c*) introduces the factor $j_{\rm in-situ-gas@gal-acc,last}$, which is the sAM of the baryons that will eventually turn to in-situ stars, but at the last time that they are accreted onto the galaxy, still in the form of gas (what exactly constitutes the 'galaxy' for this purpose is left here unspecified). A similar factor, $j_{\rm in-situ-gas@gal-acc,1st}$, which is introduced in Equation (2.2*d*), is the sAM of those same baryons, but at the *first* time that they are accreted onto the galaxy. Any given gas parcel may accrete onto the galaxy and then be ejected from it, e.g. under the influence of some sort of feedback, only to then re-accrete onto the galaxy. This can happen several times, and the ratio $(j_{\rm in-situ-gas@gal-acc,last} / j_{\rm in-situ-gas@gal-acc,1st})$ in Equation (2.2*d*) represents the angular momentum change between the last and first accretion events, namely during the 'galaxy/halo fountain' (e.g. Oppenheimer et al. 2010). Several independent numerical studies of galactic winds indicate that this is likely to be a gain rather than a loss, perhaps by ~ 0.2 dex (e.g. Brook et al. 2012; Übler et al. 2014; DeFelippis et al. 2017). The

factor ($j_{\mathrm{in-situ-stars@form}}/j_{\mathrm{in-situ-gas@gal-acc,last}}$) in Equation (2.2*c*), on the other hand, represents the sAM change of the gas phase within the disk before star-formation.

$$
\begin{aligned}
\langle j_* \rangle / \langle\, j_{\mathrm{DM-halo}} \,\rangle = [& && (2.2a)\\
& f_{\mathrm{in-situ-stars}} \times && \\
& (j_{\mathrm{in-situ-stars}}/j_{\mathrm{in-situ-stars@form}}) \times && (2.2b)\\
& (j_{\mathrm{in-situ-stars@form}}/j_{\mathrm{in-situ-gas@gal-acc,last}}) \times && (2.2c)\\
& (j_{\mathrm{in-situ-gas@gal-acc,last}}/j_{\mathrm{in-situ-gas@gal-acc,1st}}) \times && (2.2d)\\
& (j_{\mathrm{in-situ-gas@gal-acc,1st}}/j_{\mathrm{in-situ-gas@halo-acc}}) \times && (2.2e)\\
& (j_{\mathrm{in-situ-gas@halo-acc}}/j_{\mathrm{in-situ-DM@halo-acc}}) \times && (2.2f)\\
& (j_{\mathrm{in-situ-DM@halo-acc}}/j_{\mathrm{allDM@halo-acc}}) && (2.2g)\\
& + && \\
& f_{\mathrm{ex-situ-stars}} \times && \\
& (j_{\mathrm{ex-situ-stars}}/j_{\mathrm{ex-situ-stars@gal-acc}}) \times && (2.2h)\\
& (j_{\mathrm{ex-situ-stars@gal-acc}}/j_{\mathrm{ex-situ-stars@halo-acc}}) \times && (2.2i)\\
& (j_{\mathrm{ex-situ-stars@halo-acc}}/j_{\mathrm{ex-situ-DM@halo-acc}}) \times && (2.2j)\\
& (j_{\mathrm{ex-situ-DM@halo-acc}}/j_{\mathrm{allDM@halo-acc}}) && (2.2k)\\
& \qquad] \times (j_{\mathrm{allDM@halo-acc}}/\langle j_{\mathrm{DM-halo,disks}} \rangle) \times && (2.2l)\\
& \qquad\quad (\langle j_{\mathrm{DM-halo,disks}} \rangle / \langle j_{\mathrm{DM-halo}} \rangle) && (2.2m)
\end{aligned}
$$

Further, Equation (2.2*e*) introduces $j_{\mathrm{in-situ-gas@halo-acc}}$, the sAM of those same baryons (that eventually form in-situ stars) but at the time of their accretion onto the host halo. Hence, the ratio ($j_{\mathrm{in-situ-gas@gal-acc,1st}}/j_{\mathrm{in-situ-gas@halo-acc}}$) in Equation (2.2*e*) represents the angular momentum change that occurs during the first infall phase from the halo boundary to the galaxy boundary. DeFelippis et al. (2017) found this phase to involve a significant loss of sAM in Illustris, ≈ 0.4 dex for Milky-Way-mass galaxies.

Equation (2.2*f*) and Equation (2.2*g*) do not represent evolutionary stages like the ones discussed so far, but rather contrast the sAM of different components, all at the time of accretion onto the halo. First, Equation (2.2*f*) introduces $j_{\mathrm{in-situ-DM@halo-acc}}$, which is the sAM of the dark matter that originates in the same Lagrangian region (at very high redshift) as the gas that will eventually become in-situ stars, at the time of its accretion onto the halo. Hence, the ratio ($j_{\mathrm{in-situ-gas@halo-acc}}/j_{\mathrm{in-situ-DM@halo-acc}}$) in Equation (2.2*f*) represents the ratio between the sAM values (at halo accretion time) of the gas (that will become in-situ stars) and its associated dark matter. In the standard picture, this ratio is unity as both are subject to the same large-scale tidal field, but recent work suggests otherwise due to the larger quadrupole moment of the gas, resulting is a ratio that is larger than unity, possibly ≈ 0.2 dex (Danovich et al. 2015).

Second, Equation (2.2*g*) represents the ratio between the sAM (at halo accretion time) of the dark matter component that is associated with the 'in-situ gas' and that of the total dark matter that accreted onto the halo. This ratio is different from unity if the baryons that eventually form in-situ stars are 'special' in a way that the dark matter associated with them in the Lagrangian sense does not fairly sample the sAM of the entirety of the accreted dark matter. This could be the case due to preferential wind ejection of low angular momentum gas (Brook et al. 2011) or due to preferential accretion from an inside-out cooling flow (Kassin et al. 2012) or from gas filaments (Stewart et al. 2013).

The ex-situ component has a few analogs with the in-situ component: Equation (2.2k) with Equation (2.2g), Equation (2.2j) with Equation (2.2f) and Equation (2.2i) with Equation (2.2e). It is worth noting that DeFelippis et al. (2017) found that in the Illustris simulation the product of Equations (2.2k) and (2.2j) is ≈ 0.5 dex larger than the product of the analogous Equations (2.2g) and (2.2f). Further, since no star-formation or ejections are involved, Equation (2.2h) consolidates the few steps analogous to those in Equations (2.2b) through (2.2d), and represents the ratio between the sAM of the ex-situ stars in the final galaxy and the sAM those stars had at the time they were accreted (or merged) into the galaxy. Clearly, merger dynamics can drive this ratio away from unity. Finally, Equation (2.2l) could deviate from unity due to merger dynamics of dark matter halos.

3. Discussion

From a Lagrangian point of view, the stellar sAM of a galaxy can be described as the product of some 'initial' sAM of the baryonic particles locked up in the galaxy's stars and a series of changes in their sAM over time. This is described by Equation (2.2), where the 'initial' sAM for each particle is chosen as that at the time of its accretion onto the main progenitor halo of the final galaxy. In addition to these differences between the sAM at different times, a few factors in Equation (2.2) describe relations that connect the sAM of these baryons at accretion to the typical sAM of relevant dark matter halos.

When applied to $z = 0$ disk galaxies, these combined factors relate the stellar sAM of a typical disk galaxy to that of a typical dark matter halo of the appropriate mass, which are constrained empirically to be very similar to one another (Fall & Romanowsky 2013). A ratio so close to unity immediately suggests a simple picture where stars are made of baryons that acquired the same sAM as dark matter before accreting into the halo, that are representative in sAM space to the entirety of baryons that ever accreted onto the halo, and that do not experience angular momentum gains or losses during their evolution inside the halo. This simple, popular picture of 'angular momentum retention' essentially implies that all of the factors in Equation (2.2) are very close to unity.

There is, however, substantial evidence from a diverse set of numerical work that this is not the case. Instead, simulations suggest that many of the ratios in Equation (2.2) are of order $0.1 - 0.5$ dex, as briefly mentioned throughout Section 2. These ratios operate on a large range of scales and under the influence of a diverse set of physical processes. If they were largely independent as might be a expected as a result of this diversity, they would result in a large scatter of $j_*/\langle j_{\rm DM-halo}\rangle$, contrary to empirical results. Explaining the proximity of their overall product to unity would constitute an even bigger challenge.

The conclusion therefore is that the dozen different ratios in Equations (2.2b) through (2.2m) must be tightly interrelated. Studying the interplay between the diversity of scales and processes contributing to the evolution of baryonic angular momentum is a promising avenue towards understanding the origin of disk galaxies in our Universe.

References

Brook, C. B., Stinson, G., Gibson, B. K., et al. 2012, MNRAS, 419, 771
Brook, C. B., Governato, F., Roškar, R., et al. 2011, MNRAS, 415, 1051
Danovich, M., Dekel, A., Hahn, O., Ceverino, D., & Primack, J. 2015, MNRAS, 449, 2087
DeFelippis, D., Genel, S., Bryan, G. L., & Fall, S. M. 2017, ApJ, 841, 16
Fall, S. M., & Romanowsky, A. J. 2013, ApJL, 769, L26
Kassin, S. A., Devriendt, J., Fall, S. M., et al. 2012, MNRAS, 424, 502
Oppenheimer, B. D., Davé, R., Kereš, D., et al. 2010, MNRAS, 406, 2325
Rodriguez-Gomez, V., Sales, L. V., Genel, S., et al. 2017, MNRAS, 467, 3083
Stewart, K. R., Brooks, A. M., Bullock, J. S., et al. 2013, ApJ, 769, 74
Übler, H., Naab, T., Oser, L., et al. 2014, MNRAS, 443, 2092

XXXth IAU General Assembly, August 2018
Claude Carignan & Danail Obreschkow, ed.
DOI: 10.5281/zenodo.1481548

Does Angular Momentum Regulate the Atomic Gas Content in HI-deficient Spirals?

Chandrashekar Murugeshan,[1] Virginia Kilborn,[1] Danail Obreschkow,[2] Karl Glazebrook,[1] Katharina Lutz,[3,1] Robert Džudžar,[1] Helga Dénes[4,5,6]

[1] Centre for Astrophysics and Supercomputing, Swinburne University of Technology, Hawthorn, Victoria 3122, Australia
email: cmurugeshan@swin.edu.au
[2]International Centre for Radio Astronomy Research (ICRAR), M468, University of Western Australia, WA 6009, Australia
[3]Observatoire Astronomique de Strasbourg, Université de Strasbourg, CNRS, UMR 7550, 67000 Strasbourg, France
[4]Australia Telescope National Facility, CSIRO Astronomy and Space Science, P.O. Box 76, Epping, NSW 1710, Australia
[5]Research School of Astronomy and Astrophysics, Australian National University, Canberra, ACT 2611, Australia
[6]ASTRON, The Netherlands Institute for Radio Astronomy, Postbus 2, NL-7990 AA Dwingeloo, the Netherlands

Abstract. The neutral atomic hydrogen (H I) content of spiral galaxies has been observed to vary with environment, with spirals residing in high-density environments being more H I-deficient. This can been explained by environmental effects such as ram pressure stripping and tidal interactions, which remove H I from the discs of galaxies. However, some spirals in low-density environments have also been observed to have relatively low H I mass fractions. The low densities of the Intra Galactic Medium and lack of nearby galaxies in such environments make ram pressure stripping and tidal interactions unlikely candidates of gas removal. What then could be making these spirals H I deficient? In this work, we show that for a sample of H I-deficient spirals from low-density environments, their specific angular momentum influences their H I gas content through its ability to regulate global star formation in their discs. We find that our sample of H I-deficient galaxies consistently follow the model predicted by Obreschkow et al., where the atomic gas fraction (f_{atm}), in a symmetric equilibrium disc is a function of the global atomic stability parameter (q), which depends on specific angular momentum.

Keywords. galaxies: evolution, galaxies: fundamental parameters , galaxies: ISM, galaxies: kinematics and dynamics

1. Introduction

H I scaling relations of late type galaxies, such as the $M_{\rm H\,I}$ − M_R relation (Dénes et al. 2014) as in Fig. 1 show a large scatter, with some galaxies appearing to be H I-excess, and others appearing to be H I-deficient for the same R-band magnitude. The origin of this scatter could be associated with both the influence of the environment on the galaxies' H I content as well as internal parameters that maybe regulating their H I gas. It is well known that the atomic gas fraction in spiral galaxies residing in denser environments is on average less compared to galaxies of similar type and stellar mass, residing in the field (Davies & Lewis 1973; Giovanelli & Haynes 1985; Solanes et al. 2001). This can be associated with gas removing mechanisms in dense environments, such as ram pressure and tidal stripping, which remove H I gas from galaxies, making them H I-deficient (Gunn & Gott 1972; Fasano et al. 2000; Bekki et al. 2011).

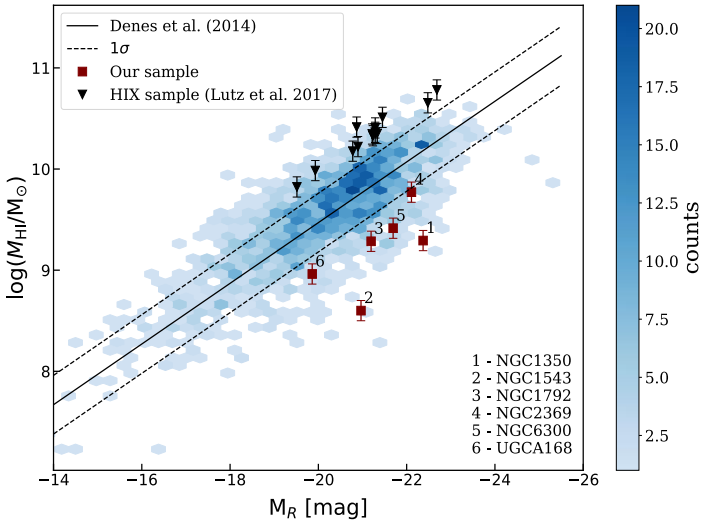

Figure 1: The $M_{\rm H\,I} - {\rm M}_R$ scaling relation from Dénes et al. (2014) for over 1700 HIPASS galaxies from the HOPCAT catalogue. The colourbar shows the number density of galaxies within each hexagon in the plot. The maroon squares represent the current sample of H I-deficient galaxies, which have at least 3 times less H I as is expected for their R-band magnitudes. In contrast, also shown in black (inverted triangles) are the H IX sample of H I-excess galaxies from Lutz et al. (2017).

However, a few studies, notably Kilborn et al. (2005), Sengupta & Balasubramanyam (2006) and Hess & Wilcots (2013) have shown that some galaxies in lower density environments such as loose groups are also HI-deficient. The low densities of the Intra Group and Intra Galactic Medium (IGM) in such environments make ram pressure and tidal stripping unlikely candidates for gas removal. What then could be making these galaxies H I-deficient? This suggests that some other internal physics maybe driving their H I gas content.

Angular momentum is regarded as one of the fundamental properties of galaxies. Many previous works have linked stellar angular momentum to other fundamental properties of a galaxy, such as its stellar mass and bulge-to-total ratio (Fall 1983; Romanowsky & Fall 2012). Recently, a relation between specific angular momentum and atomic gas fraction in late-type galaxies has been established. Obreschkow et al. (2016)[hereafter O16] introduced a parameter-free quantitative model connecting the neutral atomic mass fractions of isolated disc galaxies to their specific angular momentum. A strong test for this model are disc galaxies that are particularly gas-excess or gas-deficient for their stellar content. Lutz et al. (2017) studied a sample of 13 H I-excess galaxies (with a median $\log M_{\rm H\,I}[{\rm M}_\odot] \sim 10.4$) from the H I eXtreme (H IX) survey and find that the H IX galaxies have a low star forming efficiency owing to their large angular momenta.

In this study we examine if this effect is also observed among H I-deficient spirals and test if their deficiency is driven by their specific angular momentum. We select six H I-deficient spirals from the $M_{\rm H\,I} - {\rm M}_R$ relation (Fig. 1), with the condition that they have an isophotal diameter $D_{25} > 210''$, so that we maybe able to perform 3D kinematic fits to the data to derive their rotation curves and other kinematic parameters. They have also been sampled from low-density environments with no close neighbours so as to minimize the effects of the environment on their H I gas. The H I observations have been made using the Australia Telescope Compact Array (ATCA), with a typical synthesized beam resolution of $\sim 30''$.

2. The $f_{atm} - q$ relation

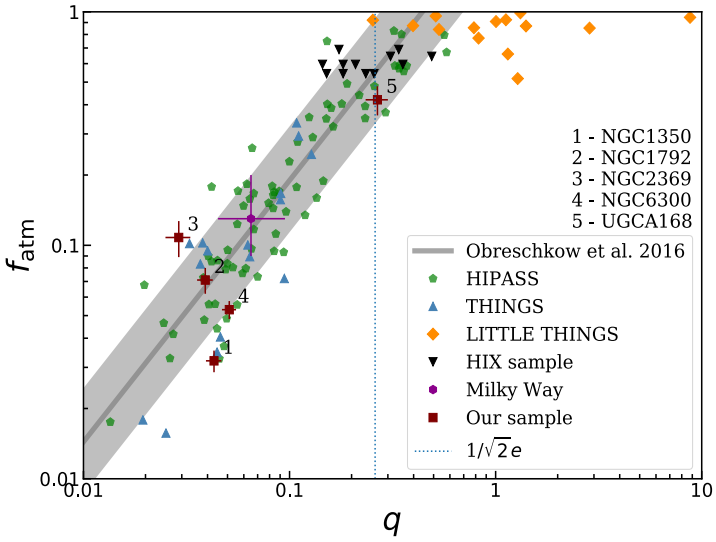

Figure 2: The $f_{atm} - q$ relation. The galaxies in our sample are represented by the maroon squares. The dark gray line is the analytical model for f_{atm} from O16. The shaded gray region shows the 40% scatter about the model. Also shown are galaxies from THINGS, LITTLE THINGS, HIPASS and the H I X surveys. The vertical dotted line represents $q = 1/\sqrt{2}e$, the threshold beyond which axially symmetric exponential disks of constant velocity can remain entirely atomic.

O16 find a tight relation between the atomic mass fraction $f_{atm} = \frac{1.35 M_{\rm H\,I}}{M}$ and the stability parameter $q = \frac{j\sigma}{GM}$, where $M = M_\star + 1.35(M_{\rm H\,I} + M_{\rm H_2})$ is the total baryonic mass and $M_{\rm H\,I}$, $M_\star$ and $M_{\rm H_2}$ are the H I, stellar and molecular hydrogen mass respectively. The factor 1.35 accounts for the 26% He in the local universe. σ is the dispersion velocity of the Warm Neutral Medium (WNM), and G is the universal gravitational constant. The authors describe the stability parameter as a global analog to the local Toomre stability parameter of a hypothetical single-component WNM disc. We test this model for our H I-deficient sample. We fit 3D tilted ring models to the data to derive the rotation velocities and the inclination and position angles for the rings. The 3D tilted rings are then projected onto the 2D intensity maps to compute the H I and stellar mass within each ring. To calculate the H I mass we use the moment 0 (integrated flux) maps and to calculate the stellar mass, we use the 2MASS (Skrutskie et al. 2006) background subtracted images. The H I and stellar mass is calculated within each tilted ring and summed up across all rings to get the total mass. Finally we compute the neutral atomic gas mass fractions (f_{atm}), specific angular momentum (j) and the q values for the sample galaxies. We note that we have assumed a constant velocity dispersion (σ) of 10 km s^{-1}for all galaxies in our sample. Fig. 2 shows the scaling relation between f_{atm} and q for a sample of local disc galaxies. We find that the galaxies in our sample follow the relation fairly consistently but with some scatter. This result comes in support of the idea that angular momentum plays an important role in regulating the H I gas content in disc galaxies, particularly those from low-density environments. Galaxies with lower specific angular momentum have lower q values which directly sets instabilities in the disc leading to increased star formation. This tends to deplete their H I gas reservoir. On the contrary, galaxies with higher specific angular momenta will support a more stable disc leading to a reduced star formation efficiency. These systems will appear to have excess H I for their

given R-band magnitudes (or stellar mass). Angular momentum by virtue of its cosmic variance, will play an important role in controlling the evolution of galaxies, with galaxies having higher specific baryonic AM retaining a larger fraction of their gas and appearing H I-excess and those with lower specific AM depleting gas more efficiently and appearing gas-depleted. This effect will naturally contribute to the scatter that is observed in the various scaling relations. This result solidifies the role of specific angular momentum in controlling the H I gas fraction in disc galaxies and consequently their evolution.

References

K. Bekki and W. J. Couch. Transformation from spirals into S0s with bulge growth in groups of galaxies. *MNRAS*, 415:1783–1796, August 2011. .

R. D. Davies and B. M. Lewis. Neutral hydrogen in Virgo cluster galaxies. *MNRAS*, 165: 231–244, 1973. .

H. Dénes, V. A. Kilborn, and B. S. Koribalski. New H I scaling relations to probe the H I content of galaxies via global H I-deficiency maps. *MNRAS*, 444:667–681, October 2014. .

S. M. Fall. Galaxy formation - Some comparisons between theory and observation. In E. Athanassoula, editor, *Internal Kinematics and Dynamics of Galaxies*, volume 100 of *IAU Symposium*, pages 391–398, 1983.

G. Fasano, B. M. Poggianti, W. J. Couch, D. Bettoni, P. Kjærgaard, and M. Moles. The Evolution of the Galactic Morphological Types in Clusters. *ApJ*, 542:673–683, October 2000. .

R. Giovanelli and M. P. Haynes. Gas deficiency in cluster galaxies - A comparison of nine clusters. *ApJ*, 292:404–425, May 1985. .

J. E. Gunn and J. R. Gott, III. On the Infall of Matter Into Clusters of Galaxies and Some Effects on Their Evolution. *ApJ*, 176:1, August 1972. .

K. M. Hess and E. M. Wilcots. Evolution in the H I Gas Content of Galaxy Groups: Pre-processing and Mass Assembly in the Current Epoch. *AJ*, 146:124, November 2013. .

V. A. Kilborn, B. S. Koribalski, D. A. Forbes, D. G. Barnes, and R. C. Musgrave. A wide-field HI study of the NGC 1566 group. *MNRAS*, 356:77–88, January 2005. .

K. A. Lutz, V. A. Kilborn, B. Catinella, B. S. Koribalski, T. H. Brown, L. Cortese, H. Dénes, G. I. G. Józsa, and O. I. Wong. The HIX galaxy survey I: Study of the most gas rich galaxies from HIPASS. *MNRAS*, 467:1083–1097, May 2017. .

D. Obreschkow, K. Glazebrook, V. Kilborn, and K. Lutz. Angular Momentum Regulates Atomic Gas Fractions of Galactic Disks. *ApJL*, 824:L26, June 2016. .

A. J. Romanowsky and S. M. Fall. Angular Momentum and Galaxy Formation Revisited. *ApJSS*, 203:17, December 2012. .

C. Sengupta and R. Balasubramanyam. HI content in galaxies in loose groups. *MNRAS*, 369: 360–368, June 2006. .

M. F. Skrutskie, R. M. Cutri, R. Stiening, M. D. Weinberg, S. Schneider, J. M. Carpenter, C. Beichman, R. Capps, T. Chester, J. Elias, J. Huchra, J. Liebert, C. Lonsdale, D. G. Monet, S. Price, P. Seitzer, T. Jarrett, J. D. Kirkpatrick, J. E. Gizis, E. Howard, T. Evans, J. Fowler, L. Fullmer, R. Hurt, R. Light, E. L. Kopan, K. A. Marsh, H. L. McCallon, R. Tam, S. Van Dyk, and S. Wheelock. The Two Micron All Sky Survey (2MASS). *AJ*, 131:1163–1183, February 2006. .

J. M. Solanes, A. Manrique, C. Garcia-Gomez, G. González-Casado, R. Giovanelli, and M. P. Haynes. The H I Content of Spirals. II. Gas Deficiency in Cluster Galaxies. *ApJ*, 548: 97–113, February 2001. .

XXXth IAU General Assembly, August 2018
Patricia Tissera & Danail Obreschkow, ed.
DOI: 10.5281/zenodo.1481545

Galaxy Simulations after the Angular Momentum Catastrophe

Aura Obreja[1,2], Andrea Macciò[2,3], Benjamin Moster[1], Aaron Dutton[2], Tobias Buck[3] and Liang Wang[4]

[1]University Observatory Munich,
Scheinerstraße 1, D-81679 Munich, Germany

[2]New York University Abu Dhabi,
PO Box 129188, Saadiyat Island, Abu Dhabi, United Arab Emirates

[3]Max-Planck-Institut für Astronomie,
Königstuhl 17, 69117 Heidelberg, Germany

[4]International Centre for Radio Astronomy Research (ICRAR), M468,
University of Western Australia, WA 6009, Australia

Abstract. Current simulations have enough resolution to study in detail the evolution of galactic angular momentum by looking separately at the various stellar dynamical components. The comparison of this kind of simulation results with observations is non trivial given all the caveats for estimating angular momentum in the latter. Therefore, mock observations of high resolution zoom-in simulations are a necessary step for a more meaningful comparison with observations.

Keywords. galaxies: structure, galaxies: kinematics and dynamics, methods: numerical

---

The current state of zoom-in cosmological simulations

Analytical models of galaxy formation have a long history of reproducing observed galaxy properties (e.g. Dalcanton, Spergel & Summers 1997). Simulations, on the other side, have only recently reached enough realism. For almost two decades simulations produced galaxies with too small sizes (Navarro & Benz 1991), a problem known as "the angular momentum catastrophe". Solutions to the problem of catastrophic gas cooling and angular momentum loss in simulations have been proposed in the early 2000s, the most effective ones including: accurate force symmetrization in Smoothed Hydrodynamical simulations (e.g. Serna et al. 2003) increasing the resolution (e.g. Governato et al. 2004), and modeling in greater detail the impact of star formation on the gas (e.g. Okamoto et al. 2005, Stinson et al. 2006).

Nowadays, various groups using different kind of numerical codes that implement these solutions are able to simulate realistic galaxies in a cosmological context (e.g. Brook et al. (2011), Stinson et al. 2013, Roškar et al. 2014, Marinacci et al. 2014, Wang et al. 2015, Grand et al. 2017, Hopkins et al. 2018, Buck et al. 2018). In particular, Brook et al. 2011 were the first to show that supernova feedback is effective in removing low angular momentum (AM) gas from the inner galaxy, and that some of this gas is subsequently re-accreted at larger radii, thus driving the formation of extended disks.

High resolution zoom-in cosmological simulations are extremely demanding in terms of computational time, and for this reason most efforts are being spent on simulating one type of galaxy. The NIHAO project (Numerical Investigation of a Hundred Astrophysical Objects) of Wang et al. (2015) has adopted a different approach by providing cosmological zoom-in simulations of galaxies spanning nearly four orders of magnitude in mass, from dwarfs to MWs, with $\sim 10^6$ (dark matter) particles per halo at all masses. The NIHAO

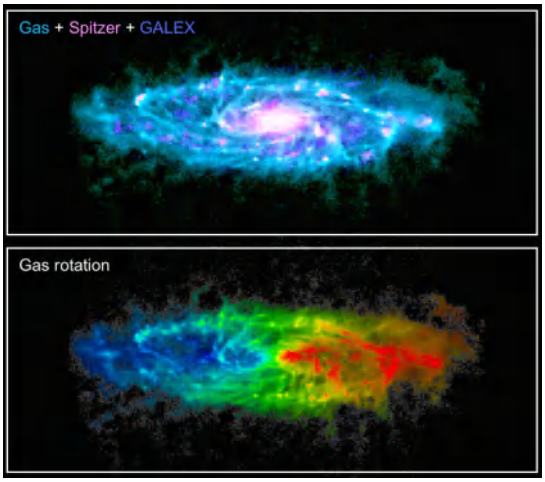

Figure 1. Composite image of the high resolution NIHAO galaxy g8.26e11.

project has been run with the N-body SPH code Gasoline2.1, last described by Wadsley et al. (2017). Star formation follows a Kennicutt-Schmidt relation. The implementation of metal line cooling is described in Shen et al. (2010). The star formation feedback includes two different effects: blastwave from SNe II (Stinson et al. 2006) and gas pre-heating by the massive stellar progenitors of SNe II ("early stellar feedback"; Stinson et al. 2013). These two types of feedback are crucial for the simulated galaxies to respect the multi-epoch abundance matching (e.g. Moster et al. 2013).

One NIHAO galaxy very similar to the Milky Way in terms of total stellar mass and disk structure, g8.26e11, is part of a project to re-simulate at higher resolution ($\sim 10^7$ particles/halo) some of the most massive galaxies in the original sample (Buck et al. 2018). This galaxy is shown in Fig. 1 as a composite image of HI gas, Spitzer MIPS 70μm and GALEX FUV on the top panel, while the bottom panel shows the HI column density map color coded by the HI velocity. The Spitzer and GALEX images have been obtained with the radiative transfer code GRASIL-3D (Domínguez-Tenreiro et al. 2014).

Stellar angular momentum in observations and simulations

The level of detail in recent simulations opened the possibility to study the evolution of galactic AM. It is important though to keep in mind that while galactic AM in simulations can be directly computed, observationally it can only be inferred from (biased) tracers of the true rotational velocities and mass distributions. Also, given that stellar orbits keep at least partial memory of the way in which galaxies assemble, it is particularly interesting to study separately the different dynamical components of simulated galaxies and compare the results with observations. For this purpose, we used a sub-sample of 25 NIHAO galaxies to first look for ways of identifying the dynamical stellar structures like (thin/thick) disks, bulges, spheroids, halos and inner disks in simulations (Obreja et al. 2018b). Our method of choice is Gaussian Mixture Models (GMM) on a 3D parameter space of normalized angular momentum projections and binding energy (Obreja et al. 2018a), extending previuos work by Doménech-Moral et al. (2012).

The stellar particles of the least massive galaxies in this 25 NIHAO galaxy sample can be meaningfully separated using GMM into a disk and a spheroid, while the more massive objects host up to five different components. In particular, the MW analogue g8.26e11 has a thin and a thick disk, a classical and a pseudo- bulge, and a stellar halo (Obreja et al. 2018a). Fig. 2 shows the stellar surface mass density profiles (left), and the various velocity measures (right) of g8.26e11 dynamical components. This galaxy is a good example of how biased the assumptions made in observations can sometimes be.

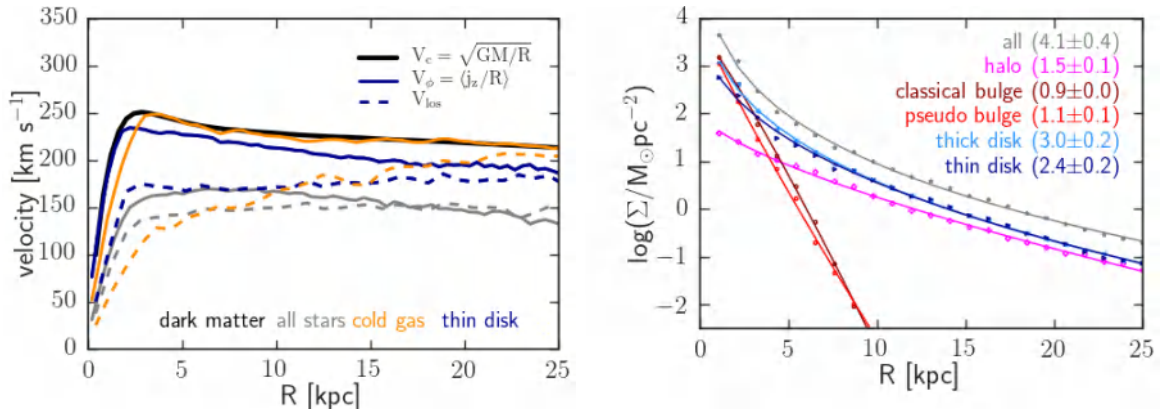

Figure 2. Edge-on line-of-sight velocities V_{los} (colored dashed) vs rotational velocities V_ϕ (colored solid) vs total circular velocity V_c (black thick solid), and edge-on stellar surface mass density profiles (with Sérsic indices in parenthesis) for the various dynamical components of g8.26e11.

One particularly important assumption in observations is that all the stars on circular orbits (the dynamical disks) are well described by a purely exponential surface mass density profile, extending all the way to the centre of the galaxy (the exponential disk). However, the thin stellar disk of g8.26e11 is better described by a Sérsic profile with $n = 2.4 \pm 0.2$. While this occurrence might seem unexpected, recent dynamical modeling of a large sample of galaxies shows that in some cases the stellar material on circular orbits can have $n > 1$ (Zhu et al. 2018). Regarding the velocity factor when computing the stellar AM, the left panel of Fig. 2 shows that the true rotational velocity V_ϕ of the (thin) stellar disk (solid navy) of g8.26e11 coincides with the edge-on line-of-sight (los) velocity V_{los} (dashed navy) only at very large radii, the former being larger than the latter by up to ∼50 km/s at small radii. Large differences can be seen also between the cold (or HI) gas velocities V_ϕ and V_{los}. Moreover the stellar disk rotation is not the same as the HI rotation. Thus, the left panel of Fig. 2 shows the case of a galaxy for which it seems highly unlikely that an accurate AM value can be computed without a proper dynamical modeling of the complete stellar surface brightness and velocity maps.

While keeping in mind all the caveats previously discussed, it is still interesting to compare the simulations and observations in terms of AM. Therefore, Fig. 3 shows the (thin) disks of the 25 NIHAO galaxies in the M_*-J_* plane (Fall 1983). The NIHAO disks follow a very tight power law with an exponent close to the value of 5/3 predicted

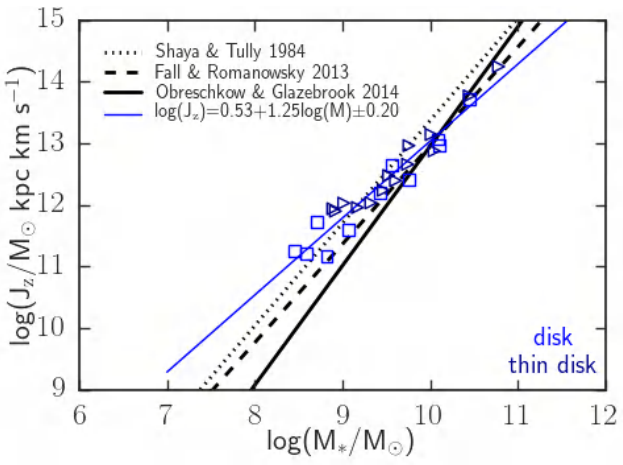

Figure 3. M_*-J_* relation for disks.

analytically by Shaya & Tully (1984). A very similar relation is followed by the disks disentangled from observations by Romanowsky & Fall (2012) and Fall & Romanowsky (2013), who assume exponential mass profiles and use ionized gas to trace the rotational velocity of the stellar disk components. On the other hand, the observational study of Obreschkow & Glazebrook (2014) who use the complete HI velocity field to trace the rotation of the stellar disks results in a larger exponent for the power law. These two observational studies use not only different velocity tracers, but also different methods to estimate the total disk AM, and therefore it is not totally unexpected they result in different M_*-J_* power laws. Given the assumptions behind the observational values and the analytical predictions, it is actually a wonder that all four data sets overlap to such a large degree.

Summary

Simulations are now reaching the resolution to study galaxy stellar structures such as (thin/thick) disks, bulges and stellar halos. Thus, in the context of galactic AM, zoom-in cosmological simulations can provide invaluable information for interpreting observations.

We use a sub-sample of NIHAO to show that: projection corrected LOS velocities are only approximating the rotation, HI is not a good tracer for stellar rotation, and not all dynamical disks are well represented by exponentials. In this light, simulation efforts have to be dedicated to produce mock observations, while accurate galactic AM measurements in observations require dynamical modeling of IFU data extended to large radii.

References

Brook, C. B. et al. 2011 *MNRAS*, 415, 1051
Buck, T. et al. 2018 *eprint*, arXiv:1804.04667
Dalcanton, J. J., Spergel, D. N. & Summers, F. J. 1997 *ApJ*, 482, 659
Doménech-Moral et al. 2012 *MNRAS*, 421, 2510
Domínguez-Tenreiro, R. et al. 2014 *MNRAS*, 439, 3868
Fall, S. M. 1983 *Internal Kinematics and Dynamics of Galaxies*, 100, 391
Fall, S. M. & Romanowsky, A. J. 2013 *ApJ* (Letters), 769, L26
Governato, F. et al. 2004 *ApJ*, 607, 688
Grand, R. J. J. et al. 2017 *MNRAS*, 467, 179
Hopkins, P. F. et al. 2018 *MNRAS*, 480, 800
Marinacci, F., Pakmor, R. & Springel, V. 2014 *MNRAS*, 437, 1750
Moster, B. P., Naab, T. & White, S. D. M. 2013 *MNRAS*, 428, 3121
Navarro, J. F. & Benz, W. 1991 *ApJ*, 380, 320
Obreja, A. et al. 2018a *MNRAS*, 477, 4915
Obreja, A. et al. 2018b *eprint*, arXiv:1804.06635
Obreschkow, D. and Glazebrook, K. 2014 *ApJ*, 784, 26
Okamoto, T. et al. 2005 *MNRAS*, 363, 1299
Romanowsky, A. J. & Fall, S. M. 2012 *ApJ*, 203, 17
Roškar, R. et al. 2014 *MNRAS*, 444, 2837
Serna, A., Domínguez-Tenreiro, R. & Sáiz, A. 2003 *ApJ*, 597, 878
Shaya, E. J. & Tully, R. B. 1984 *ApJ*, 281, 56
Shen, S., Wadsley, J. & Stinson, G. 2010 *MNRAS*, 407, 1581
Stinson, G. et al. 2006 *MNRAS*, 373, 1074
Stinson, G. S. et al. 2013 *MNRAS*, 428, 129
Wadsley, J. W., Keller, B. W. & Quinn, T. R. 2017 *MNRAS*, 471, 2357
Wang, L. et al. 2015 *MNRAS*, 454, 83
Zhu, L. et al. 2018 *MNRAS*, 479, 945

XXXth IAU General Assembly, August 2018
Claude Carignan & Danail Obreschkow, ed.
DOI: 10.5281/zenodo.1481552

The extended Planetary Nebula Spectrograph (ePN.S) Early Type Galaxy Survey: the Kinematic Diversity of Stellar Halos

Claudia Pulsoni[1,2], Ortwin Gerhard[1], Magda Arnaboldi[3], Lodovico Coccato[3], & PN.S Consortium

[1]Max-Planck-Institut für extraterrestrische Physik, Giessenbachstraße, 85748 Garching, Germany

[2] Excellence Cluster Universe, Boltzmannstraße 2, 85748, Garching, Germany

[3] European Southern Observatory, Karl-Schwarzschild-Straße 2, 85748 Garching, Germany
email: cpulsoni@mpe.mpg.de

Abstract.
In this contribution we report on a kinematic study for 33 early type galaxies (ETGs) into their outer halos (average 6 effective radii, R_e). We use planetary nebulae (PNe) as tracers of the main stellar population at large radii, where absorption line spectroscopy is no longer feasible. The ePN.S survey is the largest survey to-date of ETG kinematics with PNe, based on data from the Planetary Nebula Spectrograph (PN.S), counter-dispersed imaging, and high-resolution PN spectroscopy. We find that ETGs typically show a kinematic transition between inner regions and halos. Slow rotators have increased rotational support at large radii. Most of the ePN.S fast rotators show a decrease in rotation, due to the fading of the stellar disk in the outer, more slowly rotating spheroid. 30% of these fast rotators are dominated by rotation also at large radii, 40% show kinematic twists or misalignments, indicating a transition from oblate to triaxial in the halo. Despite this variety of kinematic behaviors, the ePN.S ETG halos have similar angular momentum content, independently of fast/slow rotation of the central regions. Estimated kinematic transition radii in units of R_e are $\sim 1-3$ R_e and anti-correlate with stellar mass. These results are consistent with cosmological simulations and support a two-phase formation scenario for ETGs.

Keywords. galaxies: elliptical and lenticular, cD; evolution; formation; halos; kinematics and dynamics; ISM: planetary nebulae: general

1. Introduction

Our understanding of the nature of early type galaxies (ETGs) has progressed remarkably in the last decade with the advent of the integral field spectroscopy (IFS). In the ATLAS3S survey (Cappellari et al. 2011) ETGs have been found to divide among fast (FR) and slow rotators (SR) according to the angular momentum of their central regions (Emsellem et al. 2011). The two classes have been interpreted as the result of different gas-rich or gas-poor merger processes that compete in the formation and evolution of these objects, while shaping their morphology and kinematics (Naab et al. 2014, Penoyre et al. 2017, Smethurst et al. 2018). Current surveys (MANGA, Bundy et al. 2015, CALIFA, Sánchez et al. 2012, SAMI, Bryant et al. 2015, and MASSIVE, Ma et al. 2014) are working to increase the sample size of the IFS mapped objects, and extend the study to a wider range of environments and masses, but they are all focused to the central 1-2 effective radii (R_e). This limitation is naturally imposed by the low surface brightness

in the outskirts of galaxies, which hampers spectroscopic measurements at larger radii. On the other hand the study of the kinematics in the outer regions is important since they contain half of the galaxies' stars and most of their dynamical mass. In addition, simulations suggest that the halos are mostly made of accreted material (Cooper et al. 2013, Rodriguez-Gomez et al. 2016, Pillepich et al. 2018), hence the study of the halos implies exploring a different phase of the galaxies.

The study of the kinematics at large radii requires alternative tracers that overcome the limit of low surface brightness in the outskirts. Planetary nebulae (PNe) are the optimal probes for the halo stellar kinematics. They are bright [OIII] emitters, which makes them easily detectable in narrow-band images over the faint halo. Because they are drawn from the main stellar population of the galaxy, their number density is proportional to the surface brightness, and their kinematics agrees with that from integrated light in the radial range of overlap: PNe follow light. This makes them reliable tracers for the kinematics of stars in the halos.

2. ETG halo kinematics traced by PNe

The extended Planetary Nebula Spectrograph (ePN.S) survey of ETGs is based on data from the custom built Planetary Nebula Spectrograph at the William Hershel Telescope in La Palma, supplemented with catalogs of PN radial velocities from high-resolution spectroscopy and counter-dispersed imaging. With a total of 8636 PNe, the ePN.S survey is the largest kinematic survey to-date of extragalactic PNe in the outer halos of ETGs. The sample of galaxies is magnitude limited, and contains 33 objects spanning a wide range of structural parameters, such as luminosity, ellipticity, central velocity dispersion (Arnaboldi et al. in prep.). In this sample, 24 galaxies are FR and 9 are SR.

In Pulsoni et al. (2018) we reconstructed halo velocity and velocity dispersion fields from the measured PN velocities using an adaptive kernel smoothing technique as in Coccato et al. 2009. This procedure is calibrated with simulations and finds the best compromise between spatial resolution and statistical noise smoothing. From the smoothed velocity fields we measured rotation velocity $V_{\rm rot}$(R), kinematic position angle $PA_{\rm kin}$(R), and velocity dispersion $\sigma(R)$ profiles. The PNe extend the kinematic information out to a maximum radius of $[3-13]$ R_e, with a median of 5.6 R_e (average of $6R_e$). The complement with absorption line data from the literature delivers a complete description of the kinematics from the central regions to the halos.

We found that the halos of the ePN.S ETGs show a larger variety of kinematic behaviors in the halos than they do in the central regions. Most of the FR have a drop in $V_{\rm rot}$ in the halo. This property was already been observed by Coccato et al. (2009), with PNe on a smaller sample of galaxies, and by Arnold et al. (2014), using slitlets kinematics from the SLUGGS survey, who interpreted it as the fading of a rotating disk-like component into a more dispersion dominated spheroidal halo. In our sample we observed it in 70% of the FR. While the central $PA_{\rm kin}$ of the ePN.S FR is well aligned with the photometric major axis (Krajnović et al. 2008, 2011, Foster et al. 2016), showing that the central regions are mostly axisymmetric, the measurement of the $PA_{\rm kin}$ at large radii reveals that the halo component might be triaxial for 40% of these galaxies. The sample of SR shows increased rotation at large radii, and $PA_{\rm kin}$ generally twisting with radius or misaligned with the photometric position angle ($PA_{\rm phot}$). This is, again, signature of a triaxial halo. Most ePN.S galaxies have flat or slightly falling $\sigma(R)$ profiles, but 15% of the sample have steeply falling profiles.

3. Angular momentum at large radii

Figure 1 (left panel) compares the V/σ ratio at $1R_e$ and in the halo. The ePN.S SR crowd below the one-to-one line, showing the increased rotation in the halo. Most of the ePN.S FR are still fast rotating in the halo, but have a lower V/σ at large radii than in the central regions, comparable to the SR V/σ(halo). This uniformity in angular momentum content suggests the idea that the halos of these galaxies might actually be structurally similar, despite the differences in the central regions. A smaller group of ePN.S FR, representing 30% of the sample, stands out for having particularly high V/σ. These galaxies do not show any decrease in the $\mathrm{V_{rot}}$, and the high rotation may be due either to an extended disk-like component (NGC 7457), or to a rapidly rotating spheroid (NGC 2768). The ePN.S FR showing kinematic signatures of a triaxial halo at the survey resolution span all values of V/σ(halo). The distribution of the V/σ(halo) values is reflected in the $\lambda_R(R)$ profiles in Coccato et al. in prep.

4. Kinematic transition and dependence on stellar mass

The variation of the kinematics from the central regions to the halos can be parametrized by defining a transition radius ($\mathrm{R_T}$), marking the radial range where the kinematics change significantly. In Pulsoni et al. (2018) we defined it using one of the following criteria:

- in case of declining $\mathrm{V_{rot}(R)}$, $\mathrm{R_T}$ is the average of the radial interval between the maximum rotation $\mathrm{V_{rot}^{max}}$ and $\mathrm{V_{rot}^{max} - 50}$ km/s;
- in case of growing $\mathrm{V_{rot}(R)}$, $\mathrm{R_T}$ is the average of the radial interval between $\mathrm{V_{rot} = 0}$ km/s and $\mathrm{V_{rot} = 50}$ km/s;
- in case of kinematic twist, $\mathrm{R_T}$ is the average of the radial range in which $\mathrm{PA_{kin}(R)}$ changes significantly.

Figure 1 (right panel) shows that $\mathrm{R_T}/R_e$ anti-correlate with stellar mass M_*, so that most massive galaxies have the transition in the kinematics at smaller fractions of R_e. A natural interpretation for the different kinematics of the halos with respect to the central regions is that halos have a different origin. The two phase formation scenario (e.

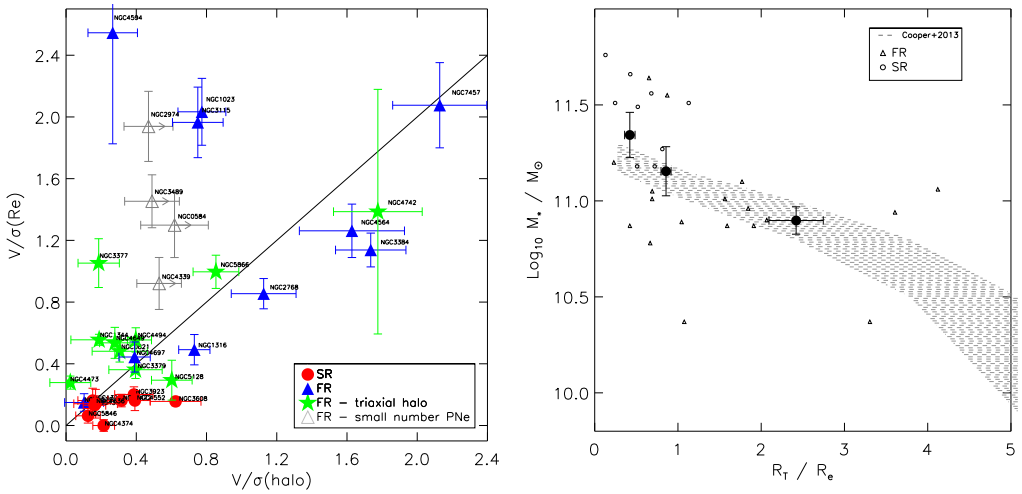

Figure 1. Left panel: $\mathrm{V}/\sigma(1\mathrm{R_e})$ from absorption line data compared with V/σ(halo) from PN data. Different symbols show SRs, FRs, FRs with triaxial halos, and FRs with small numbers of PNe; for the latter V/σ(halo) is a lower limit estimate. Right panel: transition radius R_T in units of R_e as a function of stellar mass M_*. The shaded area shows the corresponding quantities from the simulations of Cooper et al. (2013). Credit: Pulsoni et al., A&A, 618, A94, 2018, reproduced with permission ©ESO.

g Trujillo et al. 2006 and Oser et al. 2010) implies that galaxies are layered structures, in which the central regions are mostly formed by primordial (in-situ) stars and the halos are mainly made of accreted (ex-situ) stars (Cooper et al. 2013, Rodriguez-Gomez et al. 2016). More massive galaxies built up their mass by hierarchically accreting more satellites, and their ex-situ component dominates over the in-situ down to smaller radii. By comparison, lower mass galaxies have a lower accreted fraction, which is mainly deposited in the outskirts (Pillepich et al. 2018). The shaded regions in Fig.1 report the transition radius between in-situ to ex-situ dominated regions as a function of M_* from the particle tagging simulations of Cooper et al. (2013). The agreement between the trend from the simulations and that from the observed kinematics supports the interpretation of R_T as marking the transition between in-situ central regions and accreted halos. Hence the fact that the halos of the SRs and of the massive FRs in the ePN.S sample have similar angular momentum content can be explained by a common, ex-situ, nature.

5. Summary

PNe are reliable tracers for the kinematics of stars, hence they can be used to probe the outer regions of ETGs, which are too faint for absorption line measurements. In the ePN.S survey PNe extend the kinematic information out to $6R_e$ on average. In the ePN.S sample ETGs show a larger diversity of kinematic properties in the halos than in their central regions. A small group of FRs, representing $\sim 30\%$ of the FR sample stands out for having particularly high V/σ ratio in the halo. On the other hand most of the galaxies show similar halo angular momentum, independently from their FR or SR status of their central regions. The fraction of high V/σ(halo) FRs might vary for samples of galaxies with different luminosity. We defined a transition radius to describe the variation of the kinematics from the central regions to the halos, and found that this quantity anti-correlates with mass. This is consistent with cosmological simulations and supports a common ex-situ origin for the halos of these galaxies.

References

Arnold, J. A., Romanowsky, A. J., Brodie, J. P., et al. 2014, *ApJ*, 791, 80
Bryant, J. J., Owers, M. S., Robotham, A. S. G., et al. 2015, *MNRAS*, 447, 2857
Bundy, K., Bershady, M. A., Law, D. R., et al. 2015, *ApJ*, 798, 7
Cappellari, M., Emsellem, E., Krajnović, D., et al. 2011, *MNRAS*, 413, 813
Coccato, L., Gerhard, O., Arnaboldi, M., et al. 2009, *MNRAS*, 394, 1249
Cooper, A. P., D'Souza, R., Kauffmann, G., et al. 2013, *MNRAS*, 434, 3348
Emsellem, E., Cappellari, M., Peletier, R. F., et al. 2004, *MNRAS*, 352, 721
Foster, C., Arnold, J. A., Forbes, D. A., et al. 2013, *MNRAS*, 435, 3587
Krajnović, D., Bacon, R., Cappellari, M., et al. 2008, *MNRAS*, 390, 93
Krajnović, D., Emsellem, E., Cappellari, M., et al. 2011, *MNRAS*, 414, 2923
Ma, C.-P., Greene, J. E., McConnell, N., et al. 2014, *ApJ*, 795, 158
Naab, T., Oser, L., Emsellem, E., et al. 2014, *MNRAS*, 444, 3357
Oser, L., Ostriker, J. P., Naab, T., Johansson, P. H., & Burkert, A. 2010, *ApJ*, 725, 2312
Penoyre, Z., Moster, B. P., Sijacki, D., & Genel, S. 2017, *MNRAS*, 468, 3883
Pillepich et al. 2018, *MNRAS*, 475, 648
Pulsoni C., Gerhard, O., Arnaboldi, M. et al. 2018, *A&A*, in press, 2017arXiv171205833P
Rodriguez-Gomez, V., Pillepich, A., Sales, L. V., et al. 2016, *MNRAS*, 458, 2371
Sánchez, S. F., Kennicutt, R. C., Gil de Paz, A. an d van de Ven, G., et al. 2012, *A&A*, 538, A8
Smethurst, R. J., Masters, K. L., Lintott, C. J., et al. 2018, *MNRAS*, 473, 2679
Trujillo, I., Conselice, C. J., Bundy, K., et al. 2007, *MNRAS*, 382, 109

XXXth IAU General Assembly, August 2018
Chanda Jog & Danail Obreschkow, ed.
DOI: 10.5281/zenodo.1481579

Connecting Angular Momentum, Mass, and Morphology: Insights from the Magneticum Simulations

Rhea-Silvia Remus[1], Adelheid F. Teklu[1,2], Felix Schulze[1,3], and Klaus Dolag[1,4]

[1]Universitäts-Sternwarte München, Scheinerstr. 1, D-81679 München, Germany
[2]Excellence Cluster Universe, Boltzmannstr. 2, D-85748 Garching, Germany
[3]MPI for Extraterrestrial Physics, P.O. Box 1312, D-85748 Garching, Germany
[4]MPI for Astrophysics, Karl-Schwarzschild Strasse 1, D-85748 Garching, Germany
email: rhea@usm.lmu.de

Abstract. Understanding the connection between the angular momentum properties of a galaxy and its formation history and thus its morphological properties is one of the most intriguing quests in extragalactic astrophysics. State-of-the-art hydrodynamical cosmological simulations of large volumes with sufficient resolution to trace the properties of an entire population of galaxies with a large range of masses are essential to disentangle the different processes in galaxy formation that lead to the huge variety in morphological and kinematical properties observed in present-day galaxies, but such simulations only recently became available. One such set of simulations is Magneticum Pathfinder. We present insights obtained from these simulations with regard to the close connection between the angular momentum, the stellar mass, and the morphology of galaxies. Here, we demonstrate that the position of a galaxy in the M_*–j_* plane, described by the so-called b-value (see Teklu et al. 2015), is an excellent tracer for the morphology of a galaxy, visible also in the mass–size relation, the λ_R–ϵ plane, and other galaxy properties. This clearly highlights the importance of observational measurements of the angular momentum of galaxies, even though they are difficult to obtain. We conclude that using the b-value to classify galaxies is an extremely powerful tool for both simulations and observations.

Keywords. galaxies: kinematics and dynamics – galaxies: elliptical – galaxies: spiral – methods: numerical

1. The Magneticum Pathfinder Simulations

The *Mageticum Pathfinder* simulation suite (**www.magneticum.org**, Dolag et al., in prep., see also Hirschmann et al. 2014; Steinborn et al. 2015 for more details) consists of several hydrodynamical cosmological boxes with volumes ranging from $(2688\ h^{-1}\mathrm{Mpc})^3$ to $(18\ h^{-1}\mathrm{Mpc})^3$ with different resolutions. They were performed with a modified version of GADGET (Springel 2005), including radiative cooling, star formation, and kinetic winds (Springel & Hernquist 2003), stellar evolution and metal enrichment (Tornatore et al. 2007), and black hole feedback (Springel et al. 2005; Hirschmann et al. 2014). Furthermore, special treatment of artificial viscosity to resolve turbulent motion (Dolag et al. 2005) and thermal conduction (Dolag et al. 2004) are included. For all simulations, a WMAP7 (Komatsu et al. 2011) ΛCDM cosmology with $h = 0.704$, $\Omega_m = 0.272$, and $\Lambda = 0.728$ was adopted. Galaxies within the simulations are identified with the baryonic SUBFIND version (Springel et al. 2001; Dolag et al. 2009).

To study galaxies in detail, we use a medium-sized box (Box4, $(48\ h^{-1}\mathrm{Mpc})^3$) with a resolution of $M_{\mathrm{DM}} = 3.6 \times 10^7\, h^{-1} M_\odot$ and $M_{\mathrm{Gas}} = 7.3 \times 10^6\, h^{-1} M_\odot$. Each gas particle spawns up to four star particles, and the softening for the stars is $\epsilon_* = 0.7\, h^{-1}\mathrm{kpc}$. The

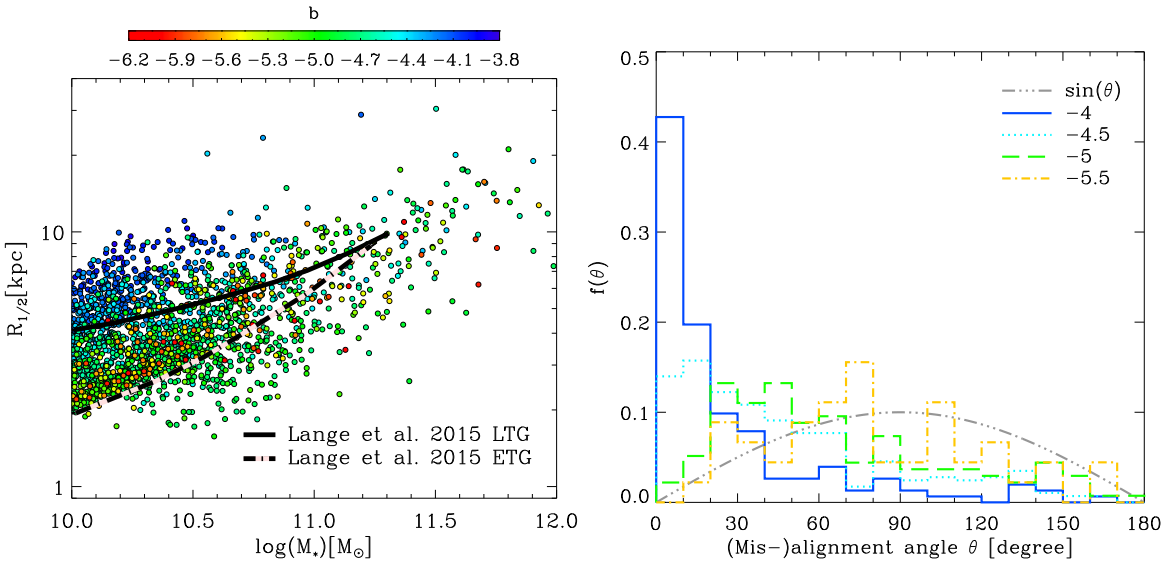

Figure 1. *Left panel:* The mass–size relation for all galaxies from Magneticum Box4, colored according to their b-value calculated as in Eq. 2.1, at $z = 0$. Black lines show the observed relations for late- (solid line) and early-type (dashed line) galaxies derived by Lange et al. (2015) from the GAMA survey. *Right panel:* Histograms of the angle between the angular momentum axes of the stellar and cold gas components of the galaxies from Magneticum Box4, for different b-value bins. The blue solid line shows the histogram for galaxies classified as disks according to their b-value, and the orange dash-dotted line shows the histogram for galaxies classified as spheroidals. The gray dash-dot-dot-dotted line marks a random distribution of the angles.

properties of the galaxies from this box have been shown to excellently reproduce the observed galaxy properties of both disk and spheroidal galaxies (e.g., Teklu et al. 2015; Remus et al. 2015; Teklu et al. 2016, 2017; Remus et al. 2017; Schulze et al. 2018).

2. Morphological Classification with the M_*–j_* Plane

As demonstrated by Teklu et al. (2015), the Magneticum galaxies successfully reproduce the observed distribution of galaxies in the M_*–j_* plane (Fall & Romanowsky 2013). The position of a galaxy in this plane can be described by the b-value:

$$b = \log_{10}\left(\frac{j_*}{\text{kpc km s}^{-1}}\right) - \frac{2}{3}\log_{10}\left(\frac{M_*}{M_\odot}\right), \tag{2.1}$$

the y-intercept of a linear function with slope 2/3 in the $\log_{10}(M_*)$–$\log_{10}(j_*)$ plane. At $z = 0$, galaxies with $b \approx -4$ resemble disk galaxies, and with decreasing b-value the galaxies gradually become more spheroidal, until they clearly resemble elliptical galaxies for $b \leqslant -5$. Therefore, the b-value describes a fundamental connection between three critical parameters in galaxy formation scenarios: the stellar angular momentum j_*, the stellar mass M_*, and the morphology.

This morphological split-up in the M_*–j_* plane is already present at $z = 2$ (Teklu et al. 2016), but shifted towards lower b-values as galaxies generally have a lower stellar specific angular momentum at redshifts higher than $z = 0$. This shift is in good agreement with theoretical predictions of $j_*|_{M_*} \propto \sqrt{z+1}^{-1}$ by Obreschkow et al. (2015). Thus, shifted accordingly, the b-value can be used to classify galaxies up to $z = 2$.

2.1. *Mass–Size Relation*

The left panel of Fig. 1 shows the stellar mass–size plane, color-coded according to the b-value, while the solid and dashed lines mark the observationally found relations for

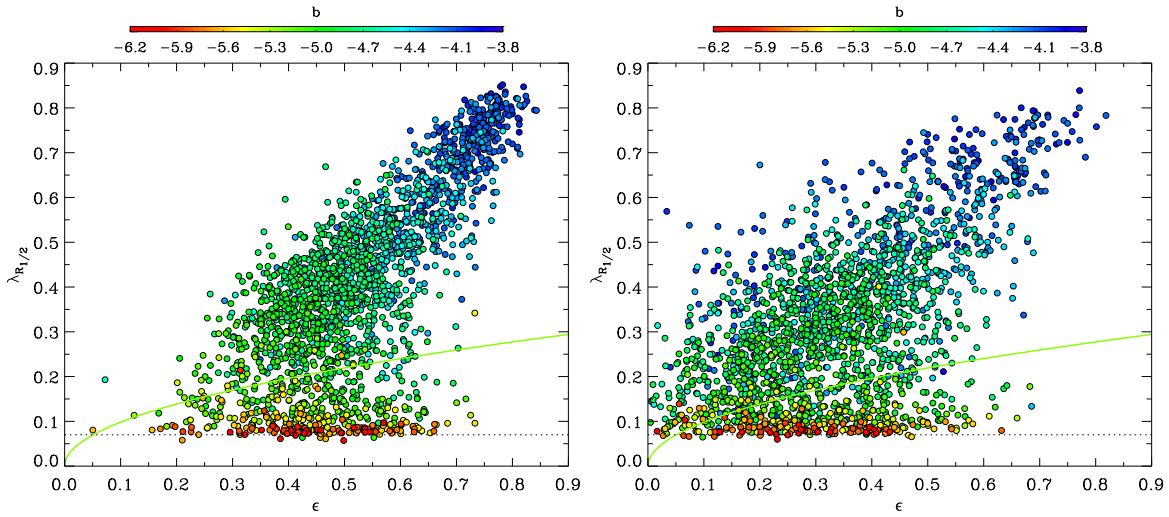

Figure 2. λ_R–ϵ plane for all galaxies from Magneticum Box4, with colors indicating the b-values of the galaxies calculated as in Eq. 2.1, at $z = 0$. The green solid line marks the threshold between slow and fast rotators as defined by Emsellem et al. (2011). *Left panel:* Both λ_R and ϵ are measured for the edge-on projection of each galaxy. *Right panel:* Same as left panel but for random projections.

late-type and early-type galaxies, respectively (Lange et al. 2015). Although Magneticum produces on average slightly larger half-mass radii than found by Lange et al. (2015), we find, for a given stellar mass, a continuous transition from high (disk-like) to low (spheroidal-like) b-values when going from larger to smaller half-mass radii. This confirms that the b-value is an excellent tracer of morphology also in the mass–size plane.

2.2. *Angle between Stellar and Gas Disk Angular Momentum Axes*

The right panel of Fig. 1 shows the distributions of the alignment angles between the angular momentum of the stellar and the gas component, for different b-value bins. While the axes of the galaxies with high b-value (disk-like, blue solid line) are clearly well aligned, the alignment distribution becomes increasingly more random for decreasing b-values, and shows a completely random distribution for spheroidal-like b-values (orange dash-dotted line). This clearly shows that the classification according to the b-value also captures the fact that the stellar and gaseous components of disk galaxies are always aligned, while their orientation can be completely random for spheroidal galaxies (see Teklu et al. 2015 for more details).

2.3. *Kinematical Properties*

Fig. 2 displays the widely used $\lambda_{R_{1/2}}$–ϵ plane (Emsellem et al. 2007), with $\lambda_{R_{1/2}}$ describing the amount of ordered versus random motion and ϵ the ellipticity of a galaxy, for the edge-on projection (left panel) and a random projection (right panel), color-coded according to the b-value. The green solid line marks the fast/slow rotator threshold introduced by Emsellem et al. (2011). In both panels there is a clear trend for the b-value to increase with rising $\lambda_{R_{1/2}}$ and ϵ, although the effect is more pronounced in the edge-on projection. The color gradient evolves continuously along an almost linear relation, indicating a transition from more elliptical-like galaxies towards disk-like morphologies with increasing $\lambda_{R_{1/2}}$ and ϵ, in agreement with observations. Therefore, the b-value also captures the fundamental fast/slow rotator classification (see Schulze et al. 2018 for more details, also with regard to other kinematical properties correlated with the b-value).

3. Conclusions

The Magneticum pathfinder simulations successfully reproduce a large variety of observed galaxy properties, especially the observed distribution of disks and spheroidals in the M_*–j_* plane (e.g., Teklu et al. 2015, 2016). The position of a galaxy in the M_*–j_* plane, characterized by the b-value, is found to be an excellent tracer of morphology. This becomes evident not only in the mass–size plane (see also Dolag et al., in prep.), but also in the distribution of the angles between the angular momentum axes of the gaseous and stellar components of galaxies (see Teklu et al. 2015 for more details). Thus, using the b-value to classify galaxies is an extremely powerful tool for both simulations and observations of galaxies. Furthermore, the b-value is closely correlated to the kinematical λ_R parameter (see Schulze et al. 2018 for more details), clearly demonstrating that those galaxies with the lowest b-values are always slow rotators.

We conclude that the connection between the stellar angular momentum j_* and the stellar mass M_* of a galaxy is a clear indicator for its morphology and thus there exists a clear connection between both quantities and other properties that strongly depend on morphology. Understanding the details of these connections will be a key component in deciphering the formation history of individual galaxies and needs to be studied in more detail in the future.

Acknowledgements

The Magneticum team was supported by the DFG Excellence Cluster "Universe", the Computational Center C^{2}PAP, and the Leibniz-Rechenzentrum (project pr86re).

References

Dolag, K., Borgani, S., Murante, G., & Springel, V. 2009, *MNRAS*, 399, 497
Dolag, K., Vazza, F., Brunetti, G., & Tormen, G. 2005, *MNRAS*, 364, 753
Dolag, K., Jubelgas, M., Springel, V., *et al.* 2004, *ApJL*, 606, L97
Emsellem, E., Cappellari, M., Krajnović, D., *et al.* 2011, *MNRAS*, 414, 888
Emsellem, E., Cappellari, M., Krajnović, D., *et al.* 2007, *MNRAS*, 379, 401
Fall, S. M., & Romanowsky, A. J. 2013, *ApJL*, 769, L26
Hirschmann, M., Dolag, K., Saro, A., *et al.* 2014, *MNRAS*, 442, 2304
Komatsu, E., *et al.* 2011, *ApJS*, 192, 18
Lange, R., Driver, S. P., Robotham, A. S. G., *et al.* 2015, *MNRAS*, 447, 2603
Obreschkow, D., Glazebrook, K., Bassett, R., *et al.* 2015, *ApJ*, 815, 97
Peebles, P. J. E. 1971, *A&A*, 11, 377
Remus, R.-S., Dolag, K., Naab, T., *et al.* 2017, *MNRAS*, 464, 3742
Remus, R.-S., *et al.* 2015, *Galaxies in 3D across the Universe*, 309, 145
Schulze, F., Remus, R.-S., Dolag, K., *et al.* 2018, *MNRAS*, 480, 4636
Springel, V. 2005, *MNRAS*, 364, 1105
Springel, V., Di Matteo, T., & Hernquist, L. 2005, *MNRAS*, 361, 776
Springel, V. & Hernquist, L. 2003, *MNRAS*, 339, 289
Springel, V., White, S. D. M., Tormen, G., & Kauffmann, G. 2001, *MNRAS*, 328, 726
Steinborn, L. K., Dolag, K., Hirschmann, M., *et al.* 2015, *MNRAS*, 448, 1504
Teklu, A. F., Remus, R.-S., Dolag, K., & Burkert, A. 2017, *MNRAS*, 472, 4769
Teklu, A. F., Remus, R.-S., & Dolag, K. 2016, *The Interplay between Local and Global Processes in Galaxies*, 41
Teklu, A. F., Remus, R.-S., Dolag, K., *et al.* 2015, *ApJ*, 812, 29
Tornatore, L., Borgani, S., Dolag, K., & Matteucci, F. 2007, *MNRAS*, 382, 1050

XXXth IAU General Assembly, August 2018
Claude Carignan & Danail Obreschkow, ed.
DOI: 10.5281/zenodo.1481556

S0 Galaxies Are Faded Spirals: Clues from their Angular Momentum Content

Francesca Rizzo[1]

[1]Max Planck Institute for Astrophysics, Karl-Schwarzschild-Strasse 1, 85740, Garching, Germany
email: frizzo@MPA-Garching.MPG.DE

Abstract. We study the stellar specific angular momentum of the disc components for a sample of ten field/group unbarred lenticular (S0) galaxies from the CALIFA survey. The location of these discs in the $j_\star$-$M_\star$ plane allows us to obtain clues on the physical processes that lead to the formation of S0s from spirals. We found that eight of our S0 discs have a distribution in the $j_\star$-$M_\star$ plane that is fully compatible with that of spiral discs, while only two have values of $j_\star$ lower than the spirals. These two outliers show signs of recent merging. Our results suggest that merger and interaction processes are not the dominant mechanisms in S0 formation in low-density environments. Instead, S0s appear to be the result of secular processes and the fading of spiral galaxies after the shutdown of star formation.

Keywords. galaxies: elliptical and lenticular, cD, galaxies: evolution, galaxies: formation, galaxies: fundamental parameters (classification, colors, luminosities, masses, radii, etc.), galaxies: kinematics and dynamics

1. Introduction

S0 galaxies are characterized by properties that encompass multiple distinct classes of galaxies (Kormendy & Bender 2012). Their main features are that they have a bulge and a disc, like spiral galaxies, but lack cold gas and, as a consequence, star formation. The formation of S0 galaxies in clusters is well understood (e.g. Gunn & Gott 1972, Larson, Tinsley, & Caldwell C. N. 1980). There is not, instead, a general consensus on the physical mechanisms that lead to the formation of S0s in galaxy groups and in the field. This is the main motivation that prompted us to study group and field S0s. In low density environments, the numerous S0 formation mechanisms belong to two main categories: passive, in which the cold gas of the progenitor disc galaxy is slowly removed because of star formation (e.g. Armillotta, Fraternali, & Marinacci 2016, Bellstedt, *et al.* 2017), or violent, in which, as a result of mergers (Querejeta *et al.* 2015) or tidal interactions (Bekki & Couch 2011), the galaxy cold gas is rapidly consumed. These two scenarios cause distinctive changes to the properties of a spiral galaxy, in addition to quenching its star formation. Therefore, some of the structural properties that characterize S0 galaxies could provide a record of the physical mechanisms that have triggered their evolution.
Most previous work has focused on structural and morphological properties of S0s (Laurikainen *et al.* 2010; Head *et al.* 2014). In our analysis, we focused on the distribution of the S0 discs in the plane of specific angular momentum ($j_\star$) versus stellar mass ($M_\star$). Observations obtained with a number of techniques and instruments (e.g. Fall 1983; Romanowsky & Fall 2012, RF12 hereafter; Posti *et al.* 2018) show that different morphological types follow different relations between their $j_\star$ and $M_\star$. This allowed us to compare the distribution of our S0 discs in the $j_\star$-$M_\star$ plane with the relations and distributions that characterize spiral discs and ellipticals. This comparison gives important

Table 1. For each galaxy in our sample (column 1) we report the morphological types taken from visual classification by the CALIFA group (Walcher *et al.* 2014) (column 2) and the environment indication taken from NED (column 3). In column 4 we show the values of the angular momentum estimator, $j_{\star,\mathrm{RF}}$, as defined by RF12, while in column 5 we show the values of disc stellar masses, calculated under the assumptions of RF12.

Galaxy	Type	Environment	$j_{\star,\mathrm{RF}}$	$\log(M_{\star\mathrm{d,RF}}/M_{\odot})$
NGC 7671	S0	Pair	1359^{+120}_{-140}	10.91±0.05
NGC 7683	S0	Isolated	2048^{+186}_{-183}	10.81±0.03
NGC 5784	S0	Group	1408^{+283}_{-283}	11.22±0.02
IC 1652	S0a	Group	1003^{+81}_{-95}	10.63±0.10
NGC 7025	S0a	Isolated	3824^{+304}_{-512}	11.30±0.08
NGC 6081	S0a	Field	1979^{+113}_{-188}	11.03±0.02
NGC 0528	S0	Group	1470^{+166}_{-100}	10.78±0.07
UGC 08234	S0	Field	1833^{+167}_{-149}	10.97±0.27
UGC 10905	S0a	Field	3284^{+346}_{-378}	11.18±0.26
NGC 0774	S0	Field	535^{+101}_{-92}	10.92±0.02

clues to the formation of S0s, since the position of a galaxy in this plane is subject to a characteristic change with respect to its progenitors depending on the physical mechanisms associated to the two formation scenarios (passive or violent). A violent scenario should result in a distribution of S0s similar to that of ellipticals, while a passive scenario (consumption of cold gas) should give a distribution similar to that of spirals.

2. Sample and data

The sample of galaxies studied in this work is drawn from the CALIFA (Calar Alto Legacy Integral Field Area) Survey (Sanchez *et al.* 2012). We selected all the unbarred S0 or S0a galaxies from the CALIFA Second Public Data Release (Garcia-Benito *et al.* 2015). We selected only unbarred galaxies because both the photometric and spectroscopic decomposition are easier if only two components, bulge and disc, are included in the analysis. However, since the barred galaxies studied in RF12 do not show any systematic difference in the $j_{\star}$-$M_{\star}$ plane from the unbarred ones, we do not expect that an analysis of barred S0s results in significant deviations from the results found in this work. In Table 1, for each galaxy (column 1) we report the indication of the galaxy environment (column 3), taken from NED.

3. Bulge-disc decomposition

The estimation of the stellar angular momentum can be obtained from observations by measuring two quantities: the surface brightness and the rotation velocity.
Photometric bulge-disc decomposition. The galaxy decomposition in bulge and disc components is performed using the 2D fitting routine GALFIT (version 3.0.5, Peng *et al.* 2010). The surface-brightness distribution of each galaxy of the sample is modelled using a Sersic function for the bulge and an exponential function for the disc. Beside the parameters that define these two components, this decomposition method provides an estimate for the bulge-to-disc luminosity ratio, B/D, in each spatial pixel.
Kinematic bulge-disc decomposition. To derive the kinematics of bulge and disc components of our galaxy sample separately we devised a method that fits the galaxy spectrum at each location using a Markov Chain Monte Carlo routine (Rizzo, Fraternali & Iorio 2018). The main assumption of our fitting method is that the observed line-of-sight velocity distribution (LOSVD) is produced by the contribution of bulge and disc components

that are, in principle, characterized by different kinematics. In order to describe these different kinematics, we model the LOSVD at each point of the galaxy with two Gaussians that have amplitudes fixed by the B/D given by our photometric decomposition and different means ($V_{\rm b}$, $V_{\rm d}$) and dispersions ($\sigma_{\rm b}$, $\sigma_{\rm d}$). The disc velocity fields, resulting from the application of our kinematic-decomposition software, are then analysed using the tilted-ring model (Begeman 1987), that allows to obtain the rotation curves for each of the disc of our sample.

4. Specific angular momentum and stellar masses

In order to compare the distribution of our S0 discs in the $j_\star$-$M_\star$ plane to the relations found by RF12 for all morphological types, we have estimated the values of $j_\star$ using their angular momentum estimator ($j_{\star,\rm RF}$), and their assumptions on the derivation of the stellar masses for the disc components ($M_{\star\,\rm d,RF}$).

5. Results and discussion

The derivation of $j_{\star,\rm RF}$ and of disc stellar masses $M_{\star\,\rm d,RF}$ allows us to compare the distribution of our S0 discs with the relation between these two quantities derived by RF12 for different morphological types. In Fig. 1 we show the best-fit found by these authors for different subtype spiral discs, S0 and elliptical galaxies. The relation shown for spirals (blue line) in Fig. 1 refers to their disc components, while the dashed black and

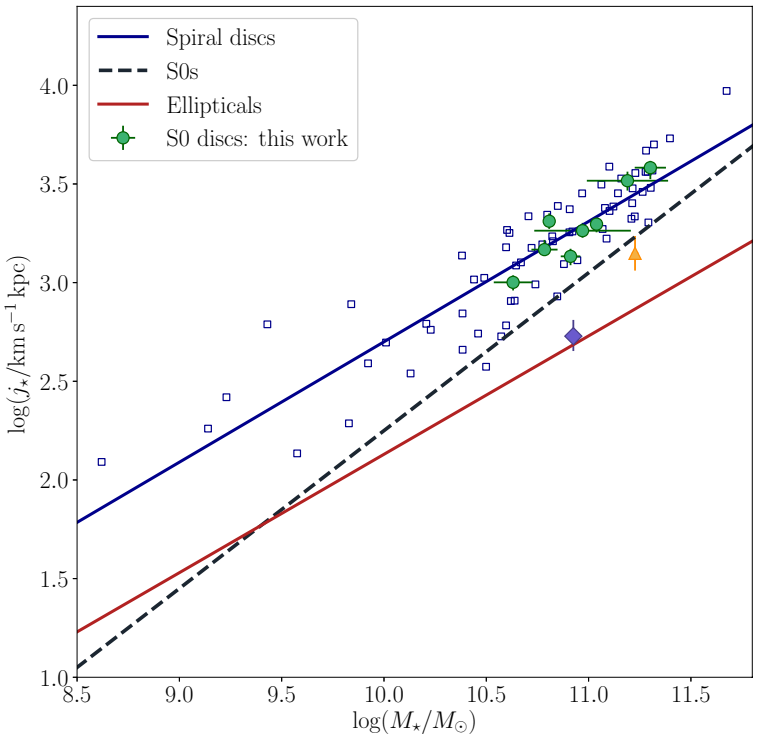

Figure 1. Distribution of the ten S0 discs of our sample in the $j_\star$-$M_\star$ log-space. Eight of our galaxies are represented by green circles, while for the two problematic cases we use an orange triangle (NGC 5784) and a violet diamond (NGC 0774). The lines represent the best-fit relation for $j_\star$-$M_\star$ found by RF12. The blue line, with a slope of ~ 0.6, refers to all spiral discs (Sa, Sb, Sc, Sd, Sm); the black dashed line, with a slope of ~ 0.8, was found for S0s (without separation of their bulge and disc components), while the red line, with a slope of ~ 0.6, is the best-fit for elliptical galaxies. The blue empty squares represent the spiral discs from RF12.

red lines for S0s and ellipticals refer to the best-fits for total $j_\star$-$M_\star$, without taking into account the decomposition in disc and bulge. From Fig. 1 we can see that eight of our ten S0 discs have a distribution in the $j_\star$-$M_\star$ plane that is in full agreement with those of spiral discs. Furthermore, their scatter is fully compatible with the intrinsic scatter $\sigma_{\log j_\star} = 0.17$ found by RF12, as showed also by the blue squares in Fig. 1 that represent the spiral discs in RF12. This result implies that spiral and S0 discs are dynamically similar, differing more in their morphological features mostly related to the presence or absence of star formation activity. The absence of a systematic shift towards lower values of $j_\star$, that would be caused by tidal interactions or mergers, suggests that the violent processes are not the dominant mechanisms that transform spirals into S0s. The position of our S0 discs in $j_\star$-$M_\star$ diagram, indeed, is fully compatible with the kinematic properties of the discs of spiral galaxies. Eight of our ten S0s can be considered as faded spirals, namely as a result of the quenching of their star formation and of the consecutive fading of the spiral arms. This passive fading appears as the most likely mechanism that does not change the disc $j_\star$ and $M_\star$ values. Only two galaxies, NGC 5784 and NGC 0774, are located systematically below the others. These two outliers are the only two galaxies that show signs of interaction/merger (see Rizzo, Fraternali & Iorio 2018 for further details). Our results on the position of S0 discs in $j_\star$-$M_\star$ diagram suggest that a passive scenario for the transformation from spiral galaxies to S0s is the most plausible. In this passive evolutionary scenario a spiral galaxy is transformed into an S0 because of the consumption of the cold gas reservoir. The exhaustion of the fuel for sustaining the star formation causes the fading and reddening of the disc, as well as the disappearance of its spiral arms. As a result, this quenched spiral galaxy is classified as an S0 and ends up on the red sequence.

References

Armillotta, L., Fraternali, F., Marinacci, F. 2016, *MNRAS*, 462, 4157

Begeman, K. G. 1987, *PhD thesis*, Groningen University

Bekki, K., & Couch, W. J. 2011, *MNRAS*, 415, 1783

Bellstedt, S., Forbes, D. A., Foster, C., Romanowsky, A. J., Brodie, J. P., Pastorello, N. , Alabi, A., & Villaume, A. 2011, *MNRAS*, 467, 4540

Fall, S. M. 1983, *Internal kinematics and dynamics of galaxies*, Proc. IAU Symposium No. 100 (Besancon, France), p. 391

Garcia-Benito, R. 2015, *A&A*, 576A, 135

Gunn J. E., & Gott J. R. I. 1972, *ApJ*, 176, 1

Head, J., Lucey, J. R., Hudson, M. J., &Smith, R. J. 2014 *MNRAS*, 440, 1690

Kormendy, J., & Bender, R. 2012, *ApJ*, 198, 2

Larson, R. B., Tinsley, B. M., & Caldwell C. N. 1980, *ApJ*, 237, 692

Laurikainen, E., Salo, H., Buta, R., & Knapen, J. H. 2010, *MNRAS*, 405, 1089

Peng, C. Y., Ho, L. C., Impey, C. D., & Rix H. W. 2010 *AJ*, 139, 2097

Posti, L. , Fraternali, F., Di Teodoro, E. M., & Pezzulli, G. 2018 *A&A*, 612, 6

Querejeta, M., Eliche-Moral, M. C., Tapia, T., Borla, A., van de Ven, G., Lyubenova, M., Martig, M., & Falcon-Barroso, J. 2015, *A&A*, 579, 2

Romanowsky, A. J., & Fall S. 2012, *ApJS*, 203, 17

Rizzo, F., Fraternali, F., & Iorio, G. 2018 *MNRAS*, 476, 2137

Sanchez, S. F. 2012 *A&A*, 538A, 8

Walcher,C.J., *et al.* 2014 *A&A*, 569, 1

XXXth IAU General Assembly, August 2018
Chanda Jog & Danail Obreschkow, ed.
DOI: 10.5281/zenodo.1481565

Angular Momentum Transport in Lopsided Galaxies

Kanak Saha[1]

[1]Inter-University Centre for Astronomy and Astrophysics,
Post Bag 4, Ganeshkhind, Pune - 411007, India
email: kanak@iucaa.in

Abstract. About 30% of spiral galaxies in the local universe are lopsided (e.g., the well-known M101). In a typical lopsided galaxy, the spatial distribution of stars and gas are elongated in one direction than the other and the asymmetry is often prominent in the out-skirts of the disk. Such a lopsided asymmetry is also evident in the kinematics. However, despite being common and a large-scale asymmetry, its role in the angular momentum (AM) transfer remained unexplored. Recently, Saha & Jog (2014) showed that like bars and spirals, lopsidedness also takes part in the outward AM transport in a galaxy, provided *it is leading in nature*. It was shown that a combination of trailing spiral and leading lopsidedness is necessary for a galaxy to transport AM outward - facilitating smooth in-flow of cold gas along the galactic plane from cosmic filaments. Using N-body simulations of off-centered disk and dark matter halo, we first generate lopsidedness in the outer part of the disk and demonstrate that indeed lopsidedness is leading in nature.

Keywords. galaxies: structure, galaxies: evolution, galaxies: kinematics and dynamics

1. Introduction

An important physical process that drives evolution of spiral galaxies, especially in the secular evolution phase, is the transport of angular momentum within various components in the disk and between the disk and its surrounding dark matter halo. Strong non-axisymmetric features such as a bar, and spiral arms that are abundant in local disk galaxies, are also the two commonly recognized drivers of this process as shown theoretically and via numerical simulations (Lynden-Bell & Kalnajs 1972; Tremaine & Weinberg 1984; Weinberg & Katz 2002; Athanassoula & Misiriotis 2002; Sellwood & Debattista 2006; Dubinski et al. 2009; Saha & Naab 2013). As a result of this physical process, the disk tends to reach a state of minimum energy configuration and may continue to do so. Concurrently, the disk grows central concentration or form a pseudo-bulge in the central region (Combes & Sanders 1981; Pfenniger & Norman 1990; Raha et al. 1991; Kormendy & Kennicutt 2004; Saha et al. 2010). The process of outward AM transport is also intimately linked to the accretion of gas along the cosmic filaments (Kereš et al. 2005; Dekel et al. 2009; Combes et al. 2014). In an isolated disk galaxy, gas can flow inward due to positive torque exerted by the bars and spirals that dominate the optical disk. However, to bring gas from cosmic filaments to the central region of a stellar disk along the galactic plane, removal of angular momentum is a must and direction of angular momentum flow must be outward. Lopsided asymmetry (Baldwin et al. 1980) which is often prominent in the outer disk (Fig.1a shows the classic example of M101 in which lopsidedness is prominent in the outer parts as can be seen from far-UV to optical to 21 cm observation) is shown to bridge the gap between the filaments and the inner optical disk (see Saha & Jog 2014). In addition, it is shown that lopsidedness has to be leading in order to transport angular momentum outward (as shown by Saha & Jog

2014) whereas spirals need to be trailing (shown by Lynden-Bell & Kalnajs 1972). Using N-body simulations (as presented below), we show that lopsidedness is indeed leading in nature (Saha, Combes and Jog, in prep).

2. AM transport

In a pioneering work, Lynden-Bell & Kalnajs (1972) showed that spiral structure can transport angular momentum outward provided it is trailing. Redistribution of this angular momentum is associated with the build up of central concentration and gas inflow along the galactic plane. This transport of angular momentum is primarily due to the gravity torque exerted by the spiral structure. However, there is another physical process that adds to the angular momentum transport known as the Lorry transport or advective transport (see appendix of Lynden-Bell & Kalnajs (1972)). In general, the lorry transport may add on to the effect of gravity torque or oppose it, and this depends on a number of parameters such as the physical properties of the non-axisymmetric perturbation, the underlying mass distribution etc.. So the net sign of the angular momentum flow (gravity torque plus advective torque) is not clear a priori in a galactic disk. Saha

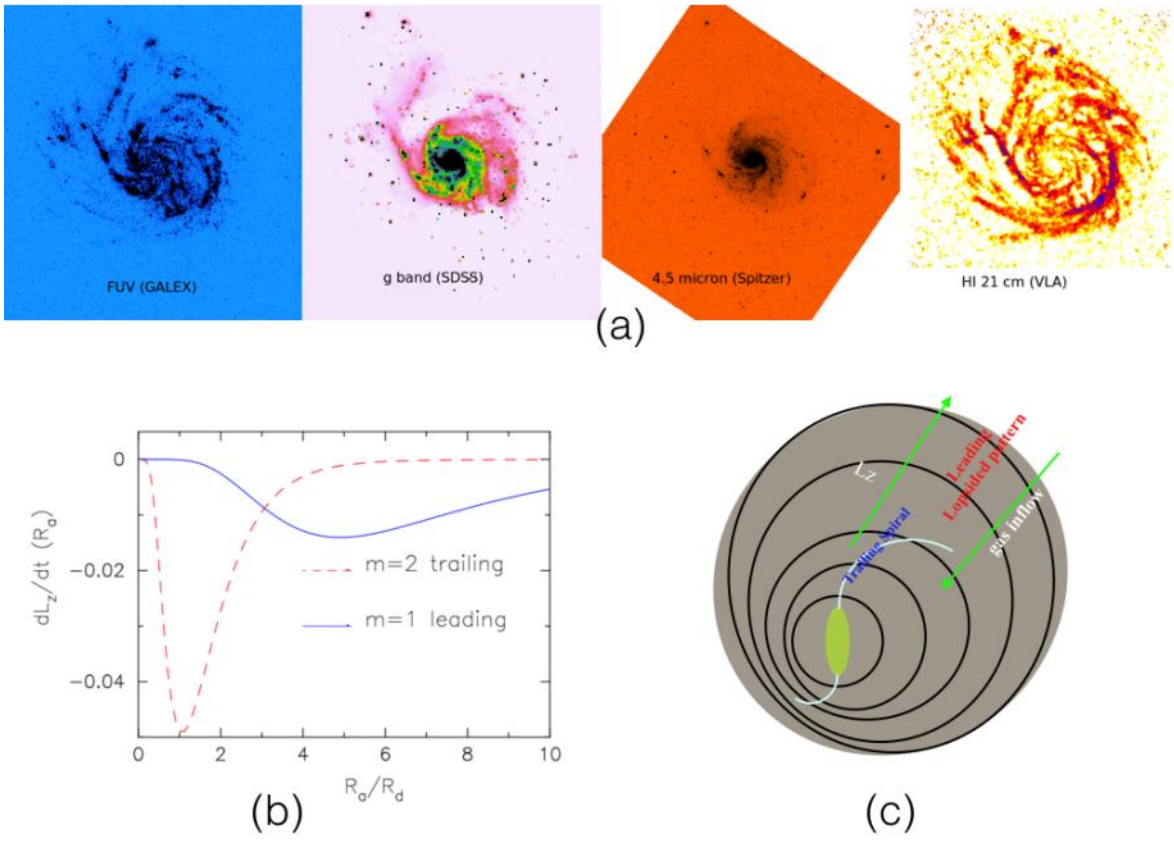

Figure 1. Lopsidedness and gravitational torque: Figure (a)- shows that prevalence of lopsidedness across the electro-magnetic spectrum starting far-ultraviolet (from GALEX) to optical (SDSS), IR (from Spitzer) and 21cm (VLA). The Figure (b) (from Saha & Jog 2014) shows that the rate of change of angular momentum within a given radius is negative when the $m = 2$ spiral is trailing and $m = 1$ lopsidedness is leading in nature and this combination allows the disk to transfer angular momentum outward. The Figure (c) shows a cartoon of net outward flow of AM in the galaxy and inflow of gas - in which leading lopsidedness and trailing spirals are shown to work in tandem.

& Jog (2014) have shown that lopsidedness which is predominantly seen in the outer part of a galactic disk (Zaritsky et al. 2013) can take part in the angular momentum transfer and the angular momentum flow is outward if lopsidedness is leading in nature. Since the presence of lopsidedness is positively correlated with spiral structure (Reichard et al. 2008; Jog & Combes 2009), the net outward flow of angular momentum demands that a combination of trailing spiral structure and leading lopsidedness be present in a lopsided spiral galaxy (see Fig. 1b). Such a combination of spiral and lopsidedness may be at work in accreting cold gas (see Zaritsky & Rix 1997) along the galactic plane from cosmic filaments (schematic diagram in Fig. 1c). However, we lack observational evidence in favour of leading lopsidedness; in fact, observationally it is not clear whether lopsidedness is leading or trailing. In Fig. (2), we show a time sequence of simulated surface density maps which show clear lopsidedness in the outer stellar disk. Such lopsidedness has been created by off-centered dark matter halo (details will be presented in forthcoming paper by Saha, Combes and Jog (2018) in prep). The bulk of the stars in the disk rotates anti-clockwise. The time sequence starting from 200 Myr to 480 Myr, reveals that lopsidedness is a slowly rotating pattern and is leading in nature. However, this is one of the several ways to generate lopsidedness (see review by Jog & Combes 2009) in a galactic disk and it remains to be verified whether lopsidedness is leading in every case.

3. Discussion

In a typical lopsided spiral galaxy, while the inner optical disk is dominated by $m = 2$ modes such as a bar and/or spiral structure, the outer part is dominated by $m = 1$ lopsidedness. It is intriguing why a spiral galaxy would prefer such an arrangement. Of course, following Lindblad's original kinematic argument it can be said that in a typical disk galaxy with flat rotation curve, the free precession frequency of an $m = 2$ mode i.e., $\Omega - \kappa/2$ varies slowly or even remains constant (depending on the mass model) in the inner part - making it susceptible for the m=2 mode. On the other hand, $\Omega - \kappa$ for an $m = 1$ mode has a steep gradient in the inner part compared to the outer - implying strong differential precession and hence harder for an $m = 1$ mode to survive there. Such an arrangement of modes become advantageous for regulating the flow of

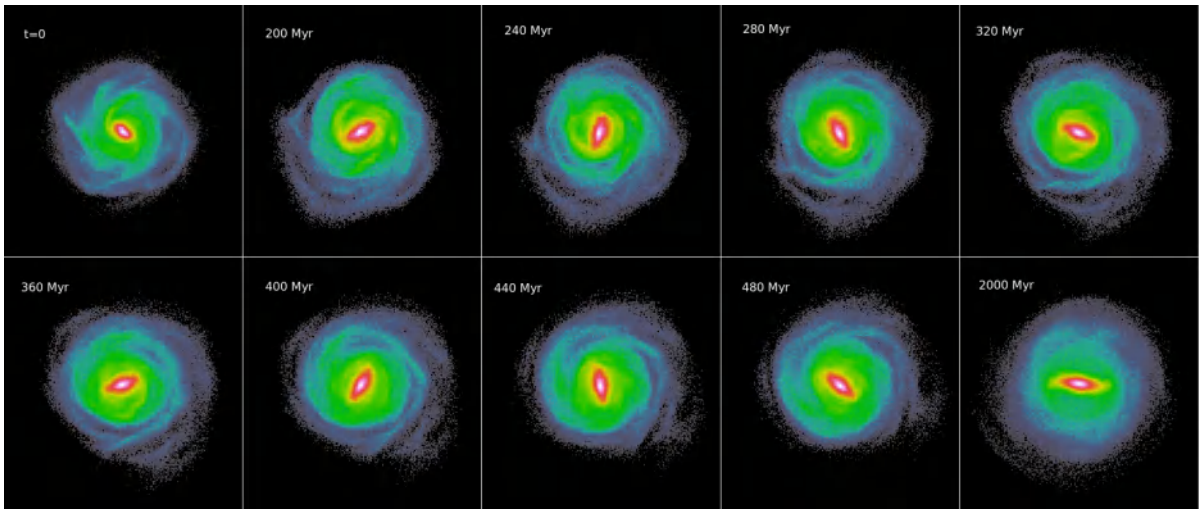

Figure 2. N-body simulations of an off-centred disk and dark matter halo system: the time sequence from $t = 200$ Myr to $t = 480$ Myr reveals that the outer lopsidedness is leading in nature (details will appear in a forthcoming paper by Saha, Combes and Jog, in prep). Note that the rotation of the stars in the galaxy is anti-clockwise.

angular momentum in the galaxy - as shown by Saha & Jog (2014), that a combination of trailing spiral plus leading lopsidedness is required for the net angular momentum flow to be outward. Being a large-scale perturbation, lopsidedness can effectively link the inner optical disk to outer cosmic filaments and let the cold gas flow (Bournaud et al. 2005) inward along the galactic plane. However, the other possibility in which lopsidedness could be trailing, would make the angular momentum flow inward and perhaps outflows of gas from the disk. The author acknowledges Anvar Shukurov (who was present in this meeting) for pointing out this possibility and enlightening discussion. The author thanks Chanda Jog for a careful reading of the manuscript.

References

Athanassoula E., Misiriotis A., 2002, MNRAS, 330, 35
Baldwin J. E., Lynden-Bell D., Sancisi R., 1980, MNRAS, 193, 313
Bournaud F., Combes F., Jog C. J., Puerari I., 2005, A&A, 438, 507
F. Combes et al. 2014, A&A, 565, A97
Combes, F., & Sanders, R. H. 1981, A&A, 96, 164
A. Dekel et al., 2009, Nature, 457, 451
Dubinski J., Berentzen I., Shlosman I., 2009, ApJ, 697, 293
Jog C. J., Combes F., 2009, Physics Reports, 471, 75
Kereš D., Katz N., Weinberg D. H., Davé R., 2005, MNRAS, 363, 2
Kormendy, J., & Kennicutt, Jr., R. C. 2004, ARA&A, 42, 603
Lynden-Bell D., Kalnajs A. J., 1972, MNRAS, 157, 1
Pfenniger, D., & Norman, C. 1990, ApJ, 363, 391
Raha, N., Sellwood, J. A., James, R. A., & Kahn, F. D. 1991, Nature, 352, 411
T. A. Reichard et al., 2008, ApJ, 677, 186
Saha, K., & Jog, C. J. 2014, MNRAS, 444, 352
Saha K., Naab T., 2013, MNRAS, 434, 1287
Saha, K., Tseng, Y., & Taam, R. E. 2010, ApJ, 721, 1878
Sellwood J. A., Debattista V. P., 2006, ApJ, 639, 868
Tremaine S., Weinberg M. D., 1984, MNRAS, 209, 729
Weinberg M. D., Katz N., 2002, ApJ, 580, 627
D. Zaritsky et al., 2013, ApJ, 772, 135
Zaritsky D., Rix H.-W., 1997, ApJ, 477, 118

XXXth IAU General Assembly, August 2018
Chanda Jog & Danail Obreschkow, ed.
DOI: 10.5281/zenodo.1481585

Spatially Resolved Galaxy Angular Momentum

Sarah M. Sweet[1], Deanne B. Fisher[1], Karl Glazebrook[1], Danail Obreschkow[2], Claudia D. P. Lagos[2], and Liang Wang[2]

[1]Centre for Astrophysics and Supercomputing, Swinburne University of Technology, PO Box 218, Hawthorn, VIC 3122, Australia
email: sarah@sarahsweet.com.au

[2]International Centre for Radio Astronomy Research, University of Western Australia, 7 Fairway, Crawley, WA 6009, Australia

Abstract. The total specific angular momentum j of a galaxy disk is matched with that of its dark matter halo, but the distributions are different, in that there is a lack of both low- and high-j baryons with respect to the CDM predictions. We illustrate how PDF(j/j_{mean}) can inform us of a galaxy's morphology and evolutionary history with a spanning set of examples from present-day galaxies and a galaxy at $z \sim 1.5$. The shape of PDF(j/j_{mean}) is correlated with photometric morphology, with disk-dominated galaxies having more symmetric PDF(j/j_{mean}) and bulge-dominated galaxies having a strongly-skewed PDF(j/j_{mean}). Galaxies with bigger bulges have more strongly-tailed PDF(j/j_{mean}), but disks of all sizes have a similar PDF(j/j_{mean}). In future, PDF(j/j_{mean}) will be useful as a kinematic decomposition tool.

Keywords. galaxies: bulges — galaxies: evolution — galaxies: fundamental parameters — galaxies: high-redshift — galaxies: kinematics and dynamics — galaxies: spiral

1. Introduction

Angular momentum (AM) is a fundamental parameter in the evolution of galaxies. In a much simplified picture, a dark matter (DM) halo spinning up in the early universe is subject to the same tidal torques as the baryons at its centre, so the total AM of both components is linked, and the specific AM, $j = J/M$ of the baryons is well matched to j of the DM, (e.g Catalan & Theuns 1996). j is connected to photometric morphology via the stellar mass – specific AM – morphology plane, first shown by Fall 1983, such that galaxies with higher M_* have higher j, modulo morphology, with the relation for earlier type galaxies offset to lower j. This has since also been shown by Romanowsky & Fall (2012), Obreschkow & Glazebrook (2014), Cortese et al. (2016), Posti et al. (2018), and Sweet et al. (2018).

Although the total j for baryons and DM is linked, further physical processes affect the distribution of j for baryons. van den Bosch et al. (2001) studied the probability density function of j normalised to the mean of the galaxy, PDF(j/j_{mean}), and found that dwarf galaxies had a deficit of high-j and of low-j material with respect to the prediction for a DM halo. They attributed this to tidal stripping of the outer, rapidly-rotating material and feedback ejecting the inner, dispersion-dominated material respectively. Sharma & Steinmetz (2005) then predicted the PDF(j/j_{mean}) for baryonic components (see Fig. 1), where bulges, which are dominated by random motions, exhibit a peak at $j = 0$, and disks have a PDF(j/j_{mean}) of the form $x\exp(-kx)$ due to their well-ordered rotation. Also see our updated predictions using the NIHAO simulations (Wang et al., in prep)).

The PDF(j/j_{mean}) encodes more physical information than photometry alone, so in

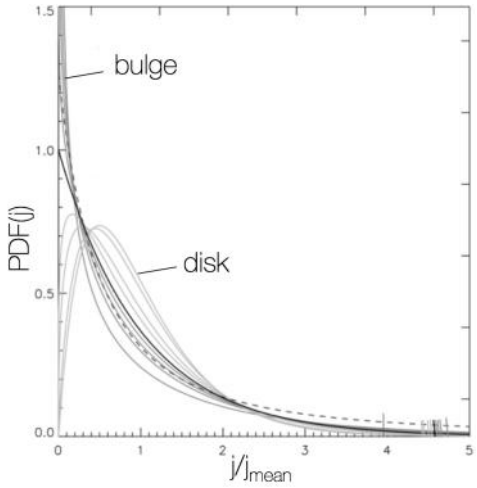

Figure 1. Predictions from Sharma & Steinmetz 2005 for baryonic galaxy components. The PDF(j/j_{mean}) for bulge peaks at $j = 0$, while disk components have an exponential profile.

this work we are investigating the utility of PDF(j/j_{mean}) as a kinematic tracer of morphology and kinematic decomposition tool.

2. PDF(j/j_{mean})

We have constructed PDF(j/j_{mean}) for a subset of the Calar Alto Legacy Integral Field Area survey (CALIFA, Sanchez et al. 2012), using observations of 25 galaxies where the stellar kinematics reach to three times the effective radius. We calculate $j_i = r_i \times v_i$ in every spaxel i, where the velocity $v_i = sqrt(v_{i,circ}^2 + v_{i,disp}^2)$ includes the circular velocity $v_{i,circ}$ and dispersion $v_{i,disp}$ added in quadrature. The map of j is then weighted by stellar surface density, as a proxy for mass, and the histogram plotted as the PDF(j/j_{mean}).

A spanning set of local examples is shown in Fig. 2. The colour represents radial distance, with lighter colours indicating material nearer the centre. NGC 6063 is a late-type spiral galaxy with low bulge-to-total light ratio B/T = 0.04. Its PDF(j/j_{mean}) is broad and symmetric, and peaks near 1, reminiscent of the predictions by Sharma & Steinmetz (2005) for pure disks. NGC 2592 is an early type galaxy with large B/T = 0.54; its PDF(j/j_{mean}) is strongly-skewed and peaks near $j = 0$ like the spheroidal components in Sharma & Steinmetz (2005). Intermediate between these two extremes, the PDF(j/j_{mean}) for NGC 7653 (B/T = 0.33) has characteristics of both disk and bulge. Unfortunately the spatial resolution, which dictates the number of bins, is not sufficient to resolve separate components in the PDF(j/j_{mean}).

We also show a clumpy disk galaxy at $z \sim 1.5$, using a combination of OSIRIS adaptive optics integral field spectroscopy to mitigate the effects of beam smearing in the centre of the galaxy, with deeper KMOS seeing-limited data to trace the velocity field out to higher multiples of the effective radius, using a method described in Sweet et al. (in prep.). The shape is intermediate between the pure disk and bulge-dominated local examples, likely due to the typical high-z morphology of dispersion-dominated clumps embedded in a strongly-rotating disk.

There is an apparent trend whereby PDF(j/j_{mean})that are more skewed and peak nearer $j = 0$ correspond to galaxies that are earlier in type and have bigger bulges. This is quantified in the correlation between shape of PDF(j/j_{mean}) (traced by skewness or kurtosis) and morphology (traced by Hubble type and B/T ratio). For instance, Fig. 3 illustrates the relation between skewness and Hubble type. Much of the scatter in this

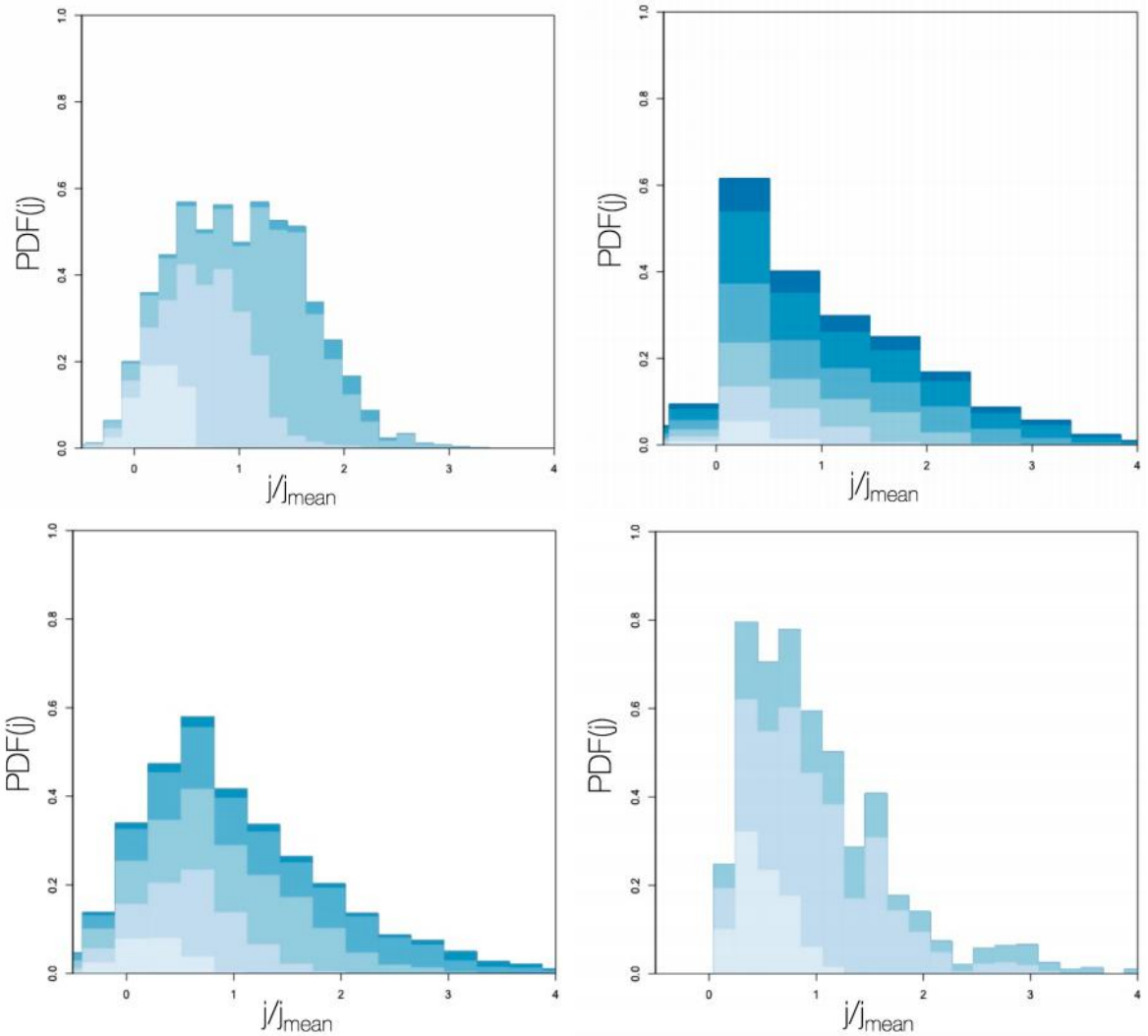

Figure 2. Example PDF(j/j_{mean}) for local galaxies in the CALIFA sample and one disk at $z \sim 1.5$. Top left: late-type spiral NGC 6063 with low B/T ratio has a broad, symmetric PDF(j/j_{mean}) which peaks near 1. Top right: early type NGC 2592 with high B/T ratio has a strongly-skewed PDF(j/j_{mean}) which peaks nearer 0. Bottom left: NGC 7653 with moderate B/T ratio has a PDF(j/j_{mean}) which is intermediate between the two extremes. Bottom right: $z \sim 1.5$ clumpy disk galaxy COSMOS 127977 also has an intermediate PDF(j/j_{mean}).

correlation arises from the difficulties inherent in photometric classification of Hubble type and quantifying bulge-to-total ratio. Arguably, PDF(j/j_{mean}) as a kinematic quantity encodes more physical information than photometry alone, so may be a more robust tracer of morphology.

We also see that the bulge is linked with PDF(j/j_{mean}). Fig. 4 demonstrates that the shape of PDF(j/j_{mean}) is moderately correlated with the surface brightness of the bulge, such that galaxies with bigger bulges have more strongly-tailed PDF(j/j_{mean}). On the other hand, the PDF(j/j_{mean}) shape is not at all correlated with the central surface brightness of the disk. This indicates that the size of the bulge is related to the distribution of j within a galaxy, but disks of all sizes have similar PDF(j/j_{mean}).

3. Conclusion: Utility of PDF(j)

The PDF(j/j_{mean}) traces kinematic morphology of a galaxy. It encodes more physical information than photometry alone, and is a product of the evolutionary history of the

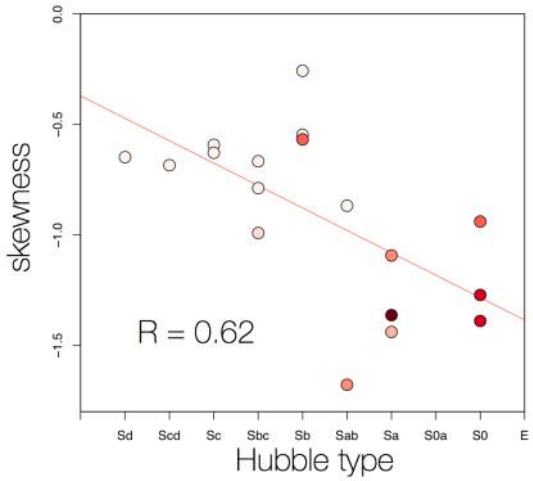

Figure 3. Correlation between morphology and shape of PDF(j/j_{mean}). Galaxies with earlier Hubble type are more strongly negatively skewed.

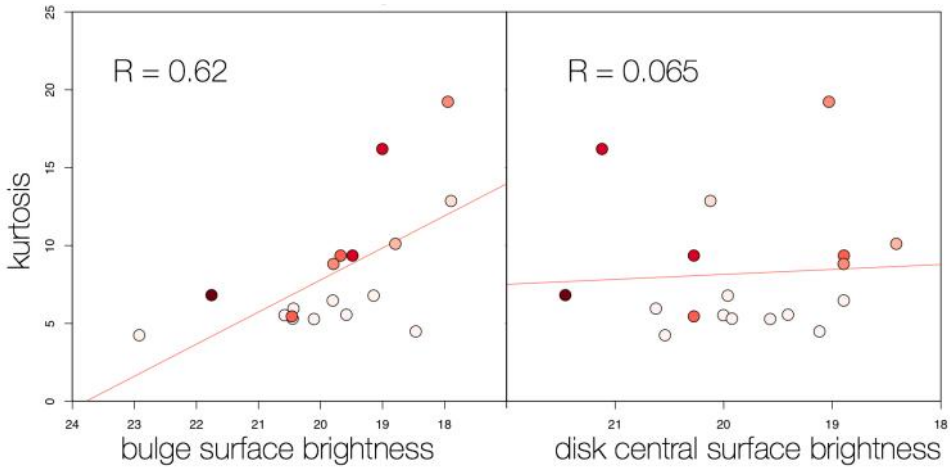

Figure 4. Correlation between galaxy components and shape of PDF(j/j_{mean}). Galaxies with bigger bulges have more strongly-tailed PDF(j/j_{mean}), but the shape of PDF(j/j_{mean}) is the same for disks of all sizes.

galaxy. In the future, as spatial resolution increases, we predict that PDF(j/j_{mean}) will be useful to separate out kinematic components: thin disk from thick disk and bulge, clumps from bulges, and pseudo-bulges from classical bulges.

References

Catalan, P., & Theuns, T., 1996, *MNRAS*, 282, 455
Cortese L., et al., 2016, *MNRAS*, 463, 170
Fall S. M., 1983, Athanassoula E., ed., in *IAU Symposium*, 100, 391
Obreschkow D., Glazebrook K., 2014, *ApJ*, 784, 26
Posti L., Fraternali F., Di Teodoro E. M., Pezzulli G., 2018, *A&A*, 612, L6
Romanowsky A. J., Fall S. M., 2012, *ApJS*, 203, 17
Sanchez, S. F., et al., 2005, *A&A*, 538, A8
Sharma, S., Steinmetz, M., 2005, *ApJ*, 628, 21
Sweet S. M., Fisher D., Glazebrook K., Obreschkow D., Lagos C., Wang L., 2018, *ApJ*, 860, 37
van den Bosch, F. C., Burkert A., Swaters, R. A., 2001, *MNRAS*, 326, 1205

XXXth IAU General Assembly, August 2018
Danail Obreschkow, ed.
DOI: 10.5281/zenodo.1481550

Stellar Kinematics in the Cosmic Web: Lessons from the SAMI Survey and the Horizon-AGN Simulation

Charlotte Welker[1,2,3]

[1] International Centre for Radio Astronomy Research (ICRAR), M468, University of Western Australia, WA 6009, Australia
[2] CNRS and UPMC Univ. Paris 06, UMR 7095, Institut d'Astrophysique de Paris, 98 bis Boulevard Arago, F-75014 Paris, France
[3] ASTRO 3D , ARC Centre of Excellence for Astrophysics in 3 Dimensions
email: charlotte.welker@uwa.edu.au

Abstract. We reconstruct the 3D network of cosmic filaments on Mpc scales across GAMA fields and assign SAMI field galaxies to their nearest filament to estimate the degree of alignment between SAMI galaxies' kinematic axes and their nearest filament in projection. We present the first detection of differential galactic spin alignment trends with local cosmic filaments using IFS kinematics. Low-mass galaxies show a tendency to align their spin with their nearest filament while higher mass counterparts are more likely to display an orthogonal orientation. The stellar transition mass is confidently bracketed between $10^{10.1}\,M_\odot$ and $10^{10.7}\,M_\odot$. In addition, we find that on average, v/σ peaks at a physical distance $d_{\rm fil} = 2.4 + -0.5$ Mpc from the centre of the filaments. A similar trend is recovered in the Horizon-AGN simulation. We also find this trend to be consistent with the build-up of galaxies in rich vorticity quadrants dispatched around filaments identified in the Horizon-AGN simulation.

Keywords. cosmic web, galaxy evolution, integral field spectroscopy, numerical simulations

1. Introduction

In standard cosmology, the anisotropic distribution of matter on largest scales, referred to as the cosmic web, naturally arises from the anisotropic gravitational collapse of an initially gaussian random field of density perturbations. Haloes form and reside within the overdensities of the cosmic web, accreting smooth material and smaller haloes via filaments they contributed to form in between them (see Bond *et al.* (1996) for details and references). Knots at the intersection of several of the most contrasted filaments house clusters, the largest virialized objects in the universe. On such scales, the filamentary pattern of the cosmic web is apparent in all large-scale galaxy surveys (de Lapparent *et al.* (1986) and Doroshkevich *et al.* (2004), Colless *et al.* (2003), Alpaslan *et al.* (2014)), traced by the galaxy distribution.

This structure conditions the geometry and dynamics of gas and galaxy flows from early times onwards. Simulations predict that gas trapped in collapsed dark matter halos is funnelled through cold filamentary streams shaped by the cosmic filaments and advected towards the centre of forming galaxies to which it transfers angular momentum (see Pichon *et al.* (2011) and Danovich *et al.* (2012) for references). An important prediction from simulations is that low-mass galaxies tend to align their spin with their nearby filament while their more massive counterparts are more likely to display an orthogonal orientation Aragon *et al.* (2007), Hahn *et al.* (2007), Paz *et al.* (2008), Bett *et al.* (2012), Codis *et al.* (2012), Dubois *et al.* (2014), Codis *et al.* (2018). Hints of such a transition have been identified in the SDSS using morphology as a proxy for spin by Tempel *et al.*

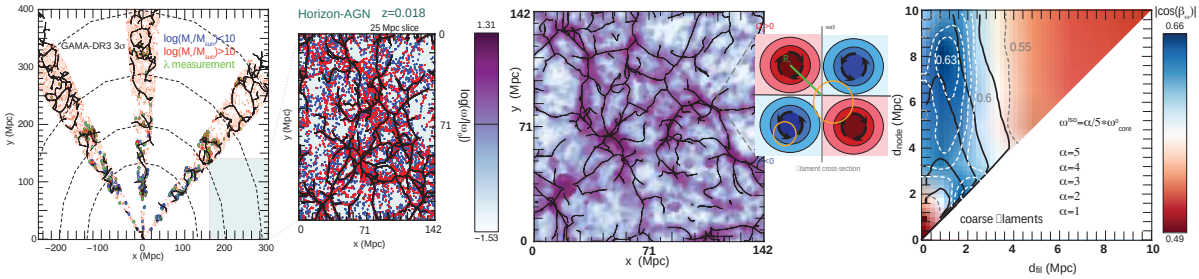

Figure 1. *Left panel:* Network of cosmic filaments across the three GAMA fields that host SAMI galaxies (solid black lines). SAMI galaxies with $M_* > 10^{10}\,M_\odot$ are indicated as red circles, those with $M_* < 10^{10}\,M_\odot$ as blue circles, green filling indicate available v/σ measurements. Pink dots indicate the initial GAMA population. Dashed hemicircles indicate the redshift tiers of the SAMI survey. The right inset shows the galaxy population and filaments extracted in a 25 Mpc thick slice from the Horizon-AGN simulation. *Intermediate panel:* Amplitude of the vorticity field in Horizon-AGN and sketch of the cosmic filament cross-section. *Right panel:* vorticity-filament angle (cosine) in the $d_{\rm fil} - d_{\rm node}$ plane: colours and dashed contours for $|\cos(\beta_\omega)|$ and black contours for amplitude of the vorticity.

(2013) but with limited significance. Overall, this faint signal has therefore remained elusive in observations.

In recent years, a number of galactic properties have been found to correlate with cosmic web features in spectroscopic and photometric surveys Laigle *et al.* (2018), Malavasi *et al.* (2017), Kraljic *et al.* (2018). Among all tracers of this interplay, spin orientations are expected to be independent of purely mass or density driven effects but are harder to obtain. The SAMI Integral Field Spectroscopy (IFS) survey Croom *et al.* (2012) provide high quality $z = 0$ stellar kinematics within one effective radius across a wide range of environments with near kiloparsec resolution and therefore offers an unprecedented opportunity to detect such signals directly on the kinematics of galaxies. Hereafter we present the first detection of spin alignments in the SAMI IFS survey and explore galaxies connection to their large-scale anisotropic environment.

2. Reconstructing the cosmic web: how and why?

We focus on the 761 galaxies of the SAMI DR1 data release Croom *et al.* (2012) found across the G09, G12 and G15 sub-fields of the deep spectroscopic survey GAMA Driver *et al.* (2011). For this sample, precise kinematics measurements of the stellar intrinsic angular momentum, kinematic position angle and v/σ within one effective radius and within elliptical aperture are available. Their computation is extensively described in van de Sande *et al.* (2017), van de Sande *et al.* (2018).

To reconstruct cosmic nodes and filaments on mega-parsec scale, an accurate tracer of the underlying density field over a large volume is required. We use the GAMA survey containing 300 000 galaxies with most stellar masses comprised between 10^8 and $10^{12}\,M_\odot$. The density field is reconstructed directly real space from the distribution of galaxies (weighted by their mass) using a Delaunay tessellation. The tessellated density field is then used as an input for the topology extractor DisPerSe Sousbie *et al.* (2011), which identifies the ridge lines of the density field to produce a contiguous network of segments that trace the spine of the cosmic web, i.e. the cosmic filaments. Filaments are directly trimmed by DisPerSe according to a signal-to-noise criterium expressed as a number of standard deviations σ, here set to 3σ. The projected $3\,\sigma$ network of filaments across GAMA is presented on the left panel of Fig. 1. The left inset illustrates a similar reconstruction across the Horizon-AGN hydrodynamic simulation (Dubois *et al.* (2014)).

Such filaments are crucial to understand galaxy evolution as they inform cosmic flows around them, and therefore the geometry of accretion onto galaxies in their vicinity. It is indeed predicted that the anisotropic collapse of matter onto a filament gives rise to regions of high vorticity (i.e curl of the velocity field $\omega = \nabla \times \mathbf{v}$). The middle panel of Fig. 1 shows the amplitude of the gas vorticity field in Horizon-AGN in shades of purple, with overlaid cosmic filaments. One can notice that vorticity is confined in the immediate vicinity of filaments. Moreover, it is typically aligned with the filament, dispatched in four quadrants of opposite polarity, i.e.whirling in opposite direction, as sketched on the intermediate inset which displays the idealised cross-section of a filament (Pichon *et al.* (2011), Laigle *et al.* (2015), Codis *et al.* (2015)).

The typical scale across which these quadrants are found depends on the scales of extracted filaments and that on which the vorticity is computed. Focusing on our specific filaments and on scales of vorticity which constitute the immediate environment of galaxies (smoothed over $1Mpc$), the right panel of Fig. 1 displays $|\cos(\beta_\omega)|$, the average cosine of the angle between the local vorticity and the nearby cosmic filament in the $d_{\rm fil} - d_{\rm node}$ plane in Horizon-AGN, with $d_{\rm fil}$ the distance of the object (here gas cells) to the nearest filament and $d_{\rm node}$ the distance to the nearest node. Blue areas show regions where an alignment trend is detected, i.e. with $|\cos(\beta_\omega)| > 0.5$. We find that the vorticity is typically aligned with filaments within 2 to 3 Mpc from their spine, with the exception of the immediate proximity of clusters ($d_{\rm node} < 2$Mpc). Interestingly, the peak of alignment is found offset from the spine of the filament, consistently with the existence of quadrants.

In simulations, galaxies growing in such regions are therefore expected to accrete coherently from their surrounding quadrant, hence building their angular momentum parallel to filaments. At later cosmic times, they migrate towards the spine of the filament, overlap quadrants and drift along the filament as they grow in mass. This steady supply of angular momentum is lost and mergers along the filament become the dominant process driving spin evolution, on average flipping the stellar spins orthogonal to the filament (Codis *et al.* (2012), Laigle *et al.* (2015)). The kinematics of galaxies and their distribution therefore bear great promises as tracers of the geometry of cosmic flows. In the following section we look for the signal of this interplay in the kinematics of SAMI galaxies.

3. Evolution of stellar spins in the cosmic web

We assign every SAMI galaxy to its nearest cosmic filament in real space. We then project filaments on the sphere and estimate for each of them a filament position angle. We then compute the angle $\theta^{\rm 2D}_{\rm kin}$ between the kinematic spin axis of each SAMI galaxy (derived from its kinematic axis) and its filament position angle. To detect the spin transition, we split the SAMI sample into two sub-samples according to a given stellar mass threshold $M_{\rm thresh}$. Fig. 2, left panel, shows $\langle\theta_{\rm high}\rangle$, the average spin-filament angle in the higher mass sub-sample, versus $\langle\theta_{\rm low}\rangle$, that in the lower mass sub-sample for $M_{\rm thresh} = 10^{10.4}\,M_\odot$ which gives the highest signal-to-noise ratio. As expected, we find $\langle\theta_{\rm high}\rangle > 45^{\rm o}$ while $\langle\theta_{\rm low}\rangle < 45^{\rm o}$ ($45^{\rm o}$ = uniformly distributed angles). This signal is recovered with a particularly high confidence ($> 2\sigma$) given the extremely low statistics.

The left intermediate panel shows the evolution of $\langle\theta\rangle = \langle\theta^{2D}_{\rm kin}\rangle$ versus median mass, for irregular bins of increasing median mass. This shows a steady increase of the average spin-filament angle with stellar mass, confirming the tendency of stellar spins to flip from parallel to filaments at low-mass to orthogonal to them at high mass. The typical transition mass is bracketed between $10^{10.1}$ and $10^{10.7}$, consistently with numerical studies (Codis *et al.* (2012), Dubois *et al.* (2014), Codis *et al.* (2018)).

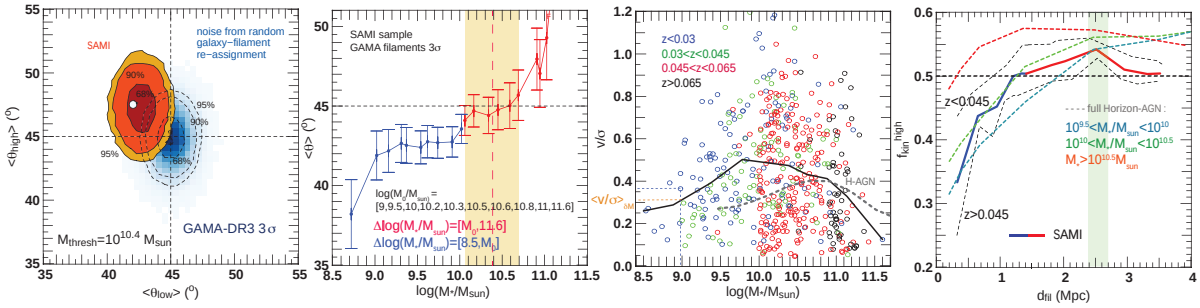

Figure 2. *Left panel:* Average spin-filament angle $\theta_{\rm kin}^{\rm 2D}$ for SAMI galaxies with $M_* < 10^{10.4}\,M_\odot$ versus average angle for galaxies with $M_* > 10^{10.4}\,M_\odot$. Shades of blue and dashed contours indicate the distribution of the expected noise, from random re-pairing of galaxies and filaments. Straight black dashed lines show the expectation for uniformly distributed angles (45°).*Middle left panel:* Evolution of $\theta_{\rm kin}^{\rm 2D}$ with median stellar mass in SAMI for overlapping bins of increasing median mass. The transition mass in found in the orange shaded area. *Middle right panel*: SAMI population in the $v/\sigma - \log(\mathrm{M_*/M_\odot})$ plane, with the average evolution overlaid as a black solid line. Evolution in Horizon-AGN is overlaid as a grey dashed line. *Right panel*: Evolution of $f_{\rm kin}$ in three different mass bins in Horizon-AGN (dashed coloured curves) and in SAMI (solid lines and dashed black lines). Regular bins in distance are used for Horizon-AGN and overlapping bins for SAMI.

To investigate the possible connection with vortical flows, we then follow the evolution of v/σ with respect to $d_{\rm fil}$. To correct from mass driven evolution, we study $f_{\rm kin}^{\rm high} = N_{\rm bin}(\mathrm{gal}|\,\mathrm{v}/\sigma > \langle \mathrm{v}/\sigma \rangle)/\mathrm{N_{bin}^{tot}}$, the fraction of "higher than average rotators" i.e. the fraction (in each distance bin) of galaxies with a v/σ parameter higher than the median for their mass (medians are computed from the SAMI sample as illustrated on the right intermediate panel). The resulting evolution with $d_{\rm fil}$ is displayed on the right panel, for both the SAMI population and the Horizon-AGN population. It is easily notice that $f_{\rm kin}^{\rm high}$ sharply increases away from the filaments until it plateaus or peaks between 2 and 3 Mpc from the spine of the filament. Removing galaxies within 2 Mpc from the nodes of the cosmic web does not qualitatively change the signal. This distribution of fast rotators peaking offset from filaments is consistent with the existence of underlying vorticity quadrants as those found in Horizon-AGN.

4. Conclusion

Reconstructing cosmic filaments from the GAMA survey and correlating them to the kinematics of 761 SAMI galaxies, we find the first kinematic evidence of galaxy spin flips: low-mass galaxies tend to align their angular momentum to their nearby filaments while their higher mass counterparts are more likely to display an orthogonal orientation. The transition mass is estimated between $10^{10.1}$ and $10^{10.7}\,M_\odot$. This is most often interpreted as an effect of mass accretion in vorticity rich regions in the vicinity of filaments, followed by merger activity along the filaments as galaxies grow in mass. Regions of high vorticity, aligned with filaments ate detected in the Horizon-AGN simulation. Following the evolution of galaxies with higher v/σ than what is predicted for their stellar mass with distance to the nearest filament, we find that the fraction of such galaxies increases sharply with $d_{\rm fil}$ before it reaches a peak 2 to 3 Mpc it. Such offset fast rotators are consistent with the existence of vorticity quadrants feeding them with coherent angular momentum but better statistics will be required to explore the effect of environments of various density on the signal and extend this study to the full $d_{\rm fil} - d_{\rm node}$ plane.

References

Codis, S., Pichon, C., Devriendt, J. et al. 2012, *MNRAS*, 427, 3320-3336
Codis, S., Pichon, C. & Pogosyan, D. 2015, *MNRAS*, 452, 3369-3393
Codis, S., Jindal, A., Chisari, N. E. et al. 2018, *MNRAS*, 481, 4753-4774
Dubois, Y., Pichon, C., Welker, C. et al. 2014, *MNRAS*, 444, 1453-1468
Codis, S., Pichon, C., Arnouts, S. & McCracken, H. J. 2018, *MNRAS*, 474, 5437-5458
Driver, S. P., Hill, D. T., Kelvin, L. S. *et al.* (2011) 2011, *MNRAS*, 413, 971-995
Kraljic, K., Arnouts, S., Pichon, C. & Laigle, C. 2018, *MNRAS*, 474, 547-571
Malavasi, N., Arnouts, S., Vibert, D. & de la Torre, S. et al. 2017, *MNRAS*, 465, 3817-3822
Laigle, C., Pichon, C., Codis, S. et al. 2015, *MNRAS*, 446, 2744-2759
Croom, S. M., Lawrence, J. S., Bland Hawthorn, J. et al. 2012, *MNRAS*, 421, 872-893
Sousbie, T. 2011, *MNRAS*, 414, 350-383
van de Sande,J., Bland Hawthorn,J., Fogarty,L. M. R. et al. 2017, *ApJ*, 835, 104
van de Sande,J., Lagos,C., Welker,C. et al. 2018, *submitted to MNRAS*, 1810.10542
de Lapparent, V., Geller, M. J. & Huchra,J . P. 1986, *ApJ*, 302,L1-L5
Bond, J. R., Kofman, L. & Pogosyan,D. 1996, *Nature*, 380,603-606
Colless, M. 2003, *Mercury*, 32,30
Alpaslan, M., Robotham, A. S. G., & Driver, S. 2014, *MNRAS*, 438,177-194
Doroshkevich, A., Tucker, D. L., Allam, S. et al. 2004, *AAP*, 603, 7-11
Pichon, C., Pogosyan, D., Kimm, T. et al. 2011, *MNRAS*, 418,2493-2507
Danovich, M., Dekel, A., Hahn, O. et al. 2012, *MNRAS*, 422, 1732-1749
Aragon-Calvo, M. A, van de Weygaert, R., Jones, B. J. T et al. 2007, *ApJ*, 655, L5-L8
Bett, P. E. & Frenk, C. S. 2012, *MNRAS*, 420, 3324-3333
Hahn, O., Carollo, C. M., Porciani,C. et al. 2007, *MNRAS*,381,41-51
Paz, D. J., Stasyszyn, F. & Padilla, N. D. 2008, *MNRAS*, 389, 1127-1136
Tempel, E., Stoica, R. S. & Saar, E. 2013, *MNRAS*, 428, 1827-1836